Title
New pathways for producing fermentation acids during glucose fermentation in bacteria

Author
Zhang, Bo

Publication Date
2022

Peer reviewed|Thesis/dissertation

New pathways for producing fermentation acids during glucose fermentation in bacteria

By

BO ZHANG
DISSERTATION

Submitted in partial satisfaction of the requirements for the degree of

DOCTOR OF PHILOSOPHY

in

Animal Biology

in the

OFFICE OF GRADUATE STUDIES

of the

UNIVERSITY OF CALIFORNIA

DAVIS

Approved:

Timothy Hackmann, Chair

Matthias Hess

Payam Vahmani

Committee in Charge

2022

Acknowledgements

This dissertation contains work I performed from 2018 to 2022. I could not have finished it without the support from my mentors and colleagues. First, I want to give my warmest thanks to Dr. Timothy Hackmann for offering this opportunity, an excellent lab environment, academic advice, technical training, encouragement, guidance, and persistent support. I am grateful to Dr. Matthias Hess, who served as a member of my mentoring committee, qualifying committee and dissertation committee, and for spending time on my training and providing valuable suggestions on my projects. I would also like to thank Dr. Payam Vahmani for offering professional insight into my dissertation and timely encouragement. I am thankful to Dr. Ermias Kebreab, Dr. Rebecca Parales, and Dr. Douglas Nelson for their comments on my projects. I want to thank Dr. James Fadel and Dr. James Murray for their mentoring. I appreciate all the efforts Dr. Russ Hovey did to promote my growth, such as training my teaching skills and offering professional advice.

I am very grateful to Christopher Lingga, Hannah De Groot, Lynn Wolfe, Courtney Bowman, Halima Sultana, and other members of Hackmann lab for their accompany and helping with my lab work. I would like to thank Barbara Jean Nitta, Janelle Belanger-Sandoval, and Gabriela Grigorean for offering technical assistance. I want to thank Jennie Buse, Leslie Oberholtzer, and other staffs and colleagues of the Department of Animal Science, without whom I could not have finished my work. I would like to thank Dr. Peter Hansen, Dr. José Eduardo P. Santos, Dr. Albert De Vries, Renee Parks-James, and friends from the Department of Animal Sciences at the University of Florida for their help during the first year of my PhD training.

Finally, I must express my gratitude to my parents, siblings, and friends for supporting and caring me throughout these years.

Table of Contents

List of Tables

List of Figures

Abstract

Fermentation is a major type of metabolism, which is carried out by both prokaryotes and eukaryotes. Organisms carrying out this metabolism live in many habitats, including the rumen of cows, gastrointestinal tracts of other animals, aquatic environments, and anaerobic digesters. These organisms ferment organic compounds and produce small molecular metabolites. Three important metabolites formed during fermentation are acetate, propionate, and butyrate. The production of these short-chain fatty acids during fermentation has broad importance for foods, agriculture, industry, and human health. For example, up to 70% of energy metabolized in a cow is from fermentation products formed in the rumen.

Despite the importance of fermentation acids, we still lack a full understanding of how microbes form these fermentation acids. While explanations of fermentation acid formation have existed in textbooks for decades, genomic studies suggested that some bacteria lack pathways described in textbooks and instead they may possess unrecognized alternate pathways. For example, some bacteria lack genes for enzymes that form acetate. Instead, they have genes for a previously unrecognized pathway involving the enzymes succinyl-CoA:acetate CoA-transferase (SCACT) and succinyl-CoA synthetase (SCS). Bacteria may use the SCACT/SCS pathway to form acetate. Likewise, some bacteria lack a step for forming propionate; however, they have genes for Rnf (Rhodobacter nitrogen fixation), an enzyme that is able to fill the missing step. Though the genomic evidence for these pathways is strong, biochemical evidence is still needed.

The first aim was to test if bacteria can use the SCACT/SCS pathway to form acetate. We found that the bacterium *Cutibacterium granulosum* formed acetate during fermentation of glucose. Using genomics, proteomics, and enzymatic assays, we demonstrated this bacterium used the

SCACT/SCS pathway, rather than the typical pathway found in nearly all acetate-forming bacteria. Among nearly 600 genomes of bacteria known to form acetate, we found 36 genomes of bacteria encoded homologs with SCACT and SCS activity. These species belong to 5 different phyla, suggesting the SCACT/SCS pathway is important for acetate formation in many branches of the tree of life.

The second aim was to test if the enzyme Rnf fills in a missing step to complete the pathway for forming propionate during fermentation in bacteria. This missing step is for reducing oxidized NAD and oxidizing reduced ferredoxin, which are both redox cofactors. We confirmed that two rumen bacteria (*Prevotella ruminicola* and *Prevotella brevis*) formed propionate (or its precursor, succinate) during fermentation of glucose. Genes for Rnf were identified and their expression in the cell were confirmed with shotgun proteomics. Enzyme assays confirmed these bacteria had the ferredoxin:NAD^+ oxidoreductase activity characteristic of Rnf. Other redox related enzymes were identified using the same methods. We searched for Rnf genes in the genomes of bacteria that form propionate/succinate, and found 44 type strains from many habitats encode it. This suggests that Rnf is important to propionate/succinate formation in bacteria from many habitats.

In sum, our work identified the SCACT/SCS pathway for forming acetate and also identified an ion pump Rnf involved in forming propionate during fermentation in bacteria. These pathways can be used by bacteria living in various environments. Our work not only filled the knowledge gap in understanding biochemical pathways for forming fermentation acids in bacteria, but also provide insights for modifying fermentation. Enzymes in these pathways could be targets for modifying acetate and propionate production during fermentation, such as fermentation in ruminants.

Chapter 1. Literature review

Definition and major products of fermentation

Definition of fermentation

The definition for fermentation varies by context. In many contexts, fermentation refers to the breakdown of sugar into alcohol found in beer, wine, and other liquor. In industry, any process producing chemicals on a massive scale with microbes is called fermentation. In biochemistry and this dissertation, fermentation is narrowly defined as a type of metabolism where the final electron acceptor is an organic molecule rather than O_2.

O_2 is the final electron acceptor during aerobic aspiration. When glucose is broken down, electrons are released and transferred to an immediate acceptor, NAD, which then transfers electrons to the final acceptor O_2. By contrast, O_2 is not used as final electron acceptor during fermentation. NAD still function as electron carrier, but it transfers electrons to an organic molecule instead.

Major products of fermentation

The end products of fermentation are varied. If the electron acceptor is pyruvate, lactate or ethanol can be formed. Other end products of fermentation include acetate, acetone, propionate, isopropanol, butyrate, n-butanol, 2,3-butanediol, and succinate (Shuler and Kargi 2002). A byproduct of fermentation is gas, such as CO_2 and H_2. These are waste products to the organism that forms them, but they are useful to others—such as animals hosting fermentative microbes in their gut.

Microbial fermentation in the gut

Microbial fermentation occurs in the gastrointestinal tract of animals, aquatic environments, and anaerobic digesters. Common features of these environments are that organic compounds are available, and the oxygen levels are very low. Here, microbial fermentation that occurs in the forestomach (rumen) of ruminants is first discussed, followed by fermentation in the gastrointestinal tract of other animals, as well as in other habitats.

Ruminants and rumen

Ruminants are capable of converting plant carbohydrates to high-value milk and meat. This unique ability to digest fibrous feedstuff is due to microbes living in the forestomach of ruminants. Ruminal microbes break down the carbohydrates, proteins, and lipids stored in feedstuff, and convert them into volatile fatty acids (VFA), ammonia, CO_2, and other products (e.g., saturated fatty acids) (Owens 2016). The VFA include mainly acetate, propionate, and butyrate. Together, these products account for up to 70% of the energy metabolized by the host (Bergman 1990). By cooperating with microbes living in the rumen, ruminants are able to digest plant carbohydrates and provide human with valuable products, such as milk and meat.

The rumen maintains ideal conditions for microbial fermentation such as temperature that is usually maintained within the range of 38 to 41°C (Hobson 1997). The pH is about 5.5 to 7 (Owens 2016). One strategy used to sustain homeostasis in the rumen is its ability to absorb VFA including mainly acetate, propionate, and butyrate. These are formed by microbial fermentation and help maintain stable pH in the rumen (Owens 2016). Ingested feedstuff is mixed with saliva and directed into the rumen on a regular and frequent basis. Ruminal contents are well mixed and reduced in particle size by regular rumination. Trace amounts of oxygen mixed in the feedstuff are

consumed by facultative anaerobic microbes. The oxygen levels in the rumen are so low that they are undetectable after the feeding of animals (Scott et al 1983).

Rumen microbes - rumen microbiota members and their roles in microbial fermentation

The microbial community of the rumen consists of 5 groups: bacteria, fungi, protozoa, methanogen, and viruses (Owens et al 1988). Bacteria are the most abundant microbes in the rumen. There are about 10^9 bacterial cells per milliliter of rumen fluid. They also account for over 50% of biomass in the rumen (Dehority 2003). Rumen bacteria are diverse and involved in many steps of degradation of nutrients stored in a feedstuff. They can be divided into several functional groups based on their specialties in degrading feedstuff, such as cellulose-degrading bacteria, hemicellulose and pectin-degrading bacteria, starch-degrading bacteria, sugar-degrading bacteria, protein-degrading bacteria, amino acid-degrading bacteria, and shot-chain fatty acids-utilizers. Some bacterial species only metabolize one type of substrate. For instance, *Fibrobacter succinogenes* mainly feed on cellulose while *Ruminobacter amylophilus* mainly digests starch (Hamlin and Hungate 1956, Stewart and Flint 1989). Most bacterial groups have broad substrates such as *Prevotella* species (e.g., *Prevotella ruminicola*), which can grow on starch, hemicellulose, pectin, and protein (Russell 2002, Whitman 2020). *Butyrivibrio fibrisolvens* is another example as it hydrolyzes cellulose, hemicellulose, pectin, starch, and sugars (Russell 2002). The interactions within bacterial species and interactions between bacteria and other microbes are important to their collective survival. For example, cross feeding occurs within bacterial species and also between bacteria and other microbes. Obligate amino acid fermenting bacteria do not grow with proteins, but other proteolytic species can degrade proteins and peptides into amino acids. Once the proteins are degraded into peptides and amino acids by the proteolytic species, then the obligate amino acid fermenting bacteria can utilize these amino acids as substrate. Similarly, lactate-producing bacteria

(e.g., *Streptococcus bovis*, *Lactobacillus* spp., *B. fibrisolvens*, and *Lachnospira multiparus*) forms lactic acid during fermentation of sugars (Mackenzie 1967), which promotes the surge of lactate-utilizing bacteria (e.g., *Megasphaera elsdenii*, *Veillonella gazogenes*) since these lactate-utilizer ferment lactic acid in the rumen (Mackenzie 1967).

Ruminal protozoa are eukaryotes, often ranging in size from 10 to 500 μm (Russell 2002). The cell amounts of protozoa is about one million cells per milliliter of rumen fluid. Both ciliate protozoa and flagellate protozoa can be found in the rumen. Protozoa have been traditionally expected to be about 50% of total microbial mass (Jouany 1996, Newbold et al 2015). However, the prior protozoal volume was overestimated by 25-40% (Wenner et al 2018). A more accurate expectation should be about 25% of the microbial mass being derived from protozoa (Ahvenjarvi et al 2018, Firkins et al 2020). Rumen protozoa have a role in degrading fiber, sugar, starch, and protein (Firkins et al 2020). They also can be called as ecosystem engineers, due to their ability to shape the prokaryotic community. Rumen protozoa can act as bacterial grazers likely decreasing the effects of competitive exclusion between bacteria taxa (Solomon et al 2022).

Fungi, another eukaryotic group, also inhabit the rumen. The concentration of fungi is about 10^6 per milliliter of rumen fluid. Ruminal fungi may encompass 0.5% to 8% of microbial mass (Denman and McSweeney 2006). The major role of fungi in the rumen is to break down the cell wall of plant cells. Anaerobic fungi have efficient and extensive set of enzymes for the degradation of plant structural polymers (Solomon et al 2016). Rhizoids of fungi physically penetrate plant structural barriers, which increases plant cell surface area for other microbes to colonize (Huws et al 2018).

Methanogens are archaea that are present in the rumen and are responsible for generating methane. The majority methane is produced from H_2 and CO_2. Other substrates for forming

methane are formate, acetate, and methyl-group chemicals (trimethylamine, methanol). The concentration of methanogens is about 10^9 per milliliter of rumen fluid. They may account for 1% to 2% of the total microbial mass. Methanogens serve as a sink for hydrogen. When consuming H_2 and CO_2 produced during fermentation, methanogens form methane by a process called methanogenesis. Because methane is a greenhouse gas, there has been much work done on decreasing its production (Lan and Yang 2019, McAllister and Newbold 2008, Weimer 1998).

Lytic phages are also found in the rumen fluid. These phages are able to lyse bacterial cells. This should alter the bacterial community, though more work is needed to determine their exact impact (Gilbert 2015).

Biochemical reactions to degrade feedstuff

Rumen microbes degrade nutrients in feedstuff, and this is a complex process. The major organic nutrients in feedstuff are carbohydrates, protein, and lipids. The overall process of degradation involves breaking down polymers into monomers, decomposing oligomers into monomers, and fermenting the monomers to produce VFA, ammonia, H_2 and CO_2 in the rumen (Russell 2002). Specifically, dietary carbohydrates are decomposed to oligosaccharides and then hydrolyzed to either hexose or pentose sugars. Hexose and pentose sugars are metabolized to pyruvate by either the Embden-Meyerhof-Parnas (EMP) pathway, the Entner-Doudoroff (ED) pathway, or the pentose phosphate pathway. Pyruvate is then converted to different fermentation products. Dietary proteins are hydrolyzed into peptides and amino acids by proteolytic enzymes and peptides are decomposed into amino acids by peptidases. Amino acids can be either used for microbial protein synthesis or be metabolized into fatty acids. Esterified plant lipids in diet are hydrolyzed into long-chain fatty acids and glycerol by lipase. Glycerol is usually fermented to propionate. Long-chain unsaturated fatty acids are rapidly hydrogenated by microbes to more saturated end products.

These saturated long-chain fatty acids are used for microbial phospholipids and directed into small intestine of ruminants.

Rumen microbes benefit the host

Rumen microbes provide the host with VFA, microbial proteins, and vitamin B_{12}. Rumen microbes also help to remove toxic compounds from feedstuff.

The major VFA are acetate, propionate, and butyrate. Usually, these VFA are produced in a mole ratio ranging from 75:15:10 to 40:40:20 (Bergman 1990). This mole ratio changes with the diet's composition. Acetate level decreases and propionate contents increases when the contents of nonstructural carbohydrates in the feedstuff increases. As most of the VFA produced in the rumen are absorbed in the rumen and omasum, only a small proportion of VFA enters the abomasum (Bergman 1990, Williams et al 1968). Once absorbed in the rumen in the free form, the VFA pass into the hepatic portal blood to circulate as neutralized anions at blood pH. Most of butyrate and very little acetate is metabolized by the rumen epithelium. Most of the remaining butyrate and propionate in portal blood is metabolized in the liver, while acetate is directed to other tissues. These VFA contribute up to 70% of the energy metabolized by the host (Bergman 1990).

Acetate is the major source of energy and a precursor of milk fat. Very little acetate is metabolized in the rumen and almost no acetate is metabolized in the liver. It must be converted to acetyl-CoA before being utilized by the ruminants. Acetyl-CoA synthetase catalyzes the reaction of acetate, ATP, and coenzyme A (CoA) to form acetyl-CoA and ADP. This enzyme can be found in tissues such as the heart, skeletal muscle, adipose tissue, mammary glands, kidneys and the brain, but not in the liver of ruminants (Mayfield et al 1966). Acetyl-CoA can be oxidized and used as energy source by entering the citric acid cycle. Acetyl-CoA is also used for *de novo*

fatty acid synthesis through carboxylation to malonyl-CoA in the mammary gland (Marinez et al 1976) and adipose tissue (Hanson and Ballard 1967).

Propionate is a major source of glucose for ruminants. In the ruminant 50% of the glucose is from propionate (Bergman 1990). The remaining glucose is from amino acids, lactate, and starch that escaped to the small intestine and has not been fermented. Part of propionate is metabolized in the rumen wall. Propionate is converted to phosphoenolpyruvate in the liver (Aschenbach et al 2010). Most of the phosphoenolpyruvate is used as a precursor to lactose in mammary gland and α-glycerol phosphate (Aschenbach et al 2010), while a small amount is directly metabolized in the brain and other tissues.

Butyrate serves as the energy source for the rumen wall. About 30% to 80% of butyrate is metabolized as β-hydroxybutyrate (Annison et al 1963). The remaining butyrate is oxidized in peripheral tissues or used for fatty acid synthesis in the adipose and mammary gland (Annison et al 1963, Black et al 1961).

Microbial protein that passed through the rumen is a major protein source for the ruminants. Microbial protein accounts for at least half of ruminant's protein needs (Storm et al 1983). Microbes synthesize proteins from amino acids. These amino acids can be produced from non-protein nitrogen, such as urea and ammonia, as well as carbohydrates. Furthermore, these amino acids are also derived from diet protein hydrolysis. Microbes hydrolyze dietary proteins into peptides and amino acids to meet their own nitrogen needs. Factors affecting microbial degradation of dietary proteins are rumen pH, microbial population, the type of dietary proteins, the type of feed ration, the passage rate, and interaction of dietary proteins with other nutrients (Bach et al 2005). Microbial protein synthesis depends on many factors related to diet and feed management, including sources of carbohydrates and proteins, the concentrate to forage ratio, the intake level,

and the feeding frequency (Febel and Fekete 1996). The most important factor that limits microbial protein synthesis in the rumen is the energy generated during fermentation of carbohydrates.

Vitamin B complex produced by rumen microbes have great benefits to the host. For instance, vitamin B_{12} is necessary for the activity of methylmalonyl-CoA mutase and methionine synthetase in dairy cows. Methylmalonyl-CoA mutase catalyzes the conversion of methylmalonyl-CoA to succinyl-CoA. This conversion is part of gluconeogenesis processes converting propionate to glucose in the liver of ruminants. Propionate contributes to half of the glucose needs in ruminants. Methionine synthetase is involved in generating methionine and tetrahydrofolate, two essential compounds for the synthesis of S-adenosylmethionine and nucleic acids (Mahmood 2014, Rizzo and Lagana 2020).

Rumen microbes have the ability to metabolize toxic compounds that could cause the host poisoning (Loh et al 2020). For example, leaves and seeds of plant *Leucaena lleucocephala* are rich in a toxic amino acid, mimosine. Mimosine is converted to 3,4-dihydropyran (DHP) by enzymes in rumen bacteria. DHP causes low weight gain, hair loss and even esophageal ulceration in cattle (Hegarty et al 1976). However, some cattle can tolerate leucaena. This is because a special bacterium, *Synergistes jonesii*, isolated from ruminal fluid of those cattle can degrade DHP. Inoculating this bacterium to other cattle protects them from these toxic effects (Klieve et al 2002).

Microbial fermentation in other habitats

Microbial fermentation in the gut of other animals

In addition to the rumen, microbial fermentation occurs in the gastrointestinal tract of many different animals, including vertebrates and invertebrates. The gut microbiota varies with the host species, diets, and environments. It is reported that diet and host phylogeny in mammals are the

major factors determining the structure and composition of gut microbes (Song et al 2020). The digestive systems of herbivores, omnivores, and carnivores are different and adapted towards digesting their specific diets. The size of the gastrointestinal tract as well as the transit time inside can affect the microbial composition between mammals. Despite the compositional differences between gut microbiota in the gastrointestinal tract of mammals, they commonly form short-chain fatty acids and affect host energy metabolism and immune response (Elia and Cummings 2007, Rooks and Garrett 2016).

Microbial fermentation also occurs in birds. These animals have paired caeca and this is where most fermentation occurs. The core bacteria in chickens and wild birds are composed mainly by four phyla, *Bacteroidetes*, *Firmicutes*, *Proteobacteria*, and *Actinobacteria* (Grond et al 2018). Gut microbes in the avian gut are involved in digestion of nutrients, facilitating breakdown of dietary fiber, fermenting intermediates, and detoxification of toxic compounds for the host (Rehman et al 2007). Members of *Firmicutes* (e.g., *Clostridium acidi-uridi*) produce short-chain fatty acids (e.g., acetic acid) during fermentation of non-digestible carbohydrates (Barker and Beck 1942, Mead 1989). These molecules can be directly absorbed by the gut wall as energy source by the birds (Adil and Magray 2012, Svihus et al 2013). Protein fermentation has also been reported. Caecal protein fermentation occurs when high levels of protein are present in the diet. Fermentation of proteins in the caeca produces compounds that could have negative effects on animal performance (Elling-Staats et al 2021, Qaisrani et al 2015). It is not clear how gut microbes relate to the immune function of birds (Grond et al 2018).

The gastrointestinal tract of fish is dominated by aerobes or facultative anaerobes, but some strict anaerobes have been detected (Romero and Navarrete 2006). Certain lactic acid bacteria, such as *Lactococcus lactis* and *Lactobacillus fermentum*, are identified in zebrafish (Rawls et al

2004), implying that microbial fermentation occurs in fish (Luna et al 2022, Wang et al 2018). Studies on gut microbiome of reptiles and amphibians are limited. The analysis of gastrointestinal tract microbiome of the American alligator identified high abundance of *Fusobacteria* and low abundance of *Firmicutes*, *Proteobacteria*, and *Bacteroidetes* (Keenan and Elsey 2015). *Fusobacteria* isolated from rumen samples can produce butyrate and ferment cellulose and starch (Van Gylswyk 1980), suggesting that microbial fermentation may happen in the gut of alligators; however, it needs to be verified.

Microbial colonization can be found in the gastrointestinal tract of certain invertebrates. Most insect guts contain a low abundance of microbes compared to that of mammals (Engel and Moran 2013). Some insects form a mutualistic relationship with their gut microbes. One such example can be found in the gut of termites. These microbes in the gut of termites help the host to fix nitrogen (Benemann 1973, Desai and Brune 2012, Kohler et al 2012), digest lignocellulose, and ferment the intermediates. Acetate produced by fermentation and CO_2-reductive acetogenesis are used as the main carbon source for their host (Warnecke et al 2007).

Fermentation in food industry, aquatic environment and anaerobic digesters

Microbial fermentation is important in food industry, such as in cheese and wine production. The first step of cheese production is fermenting lactose in milk to lactic acid with lactic acid bacteria. In wine production, yeast carry out fermentation, turning sugars into ethanol and CO_2. During the process of producing red wine, some lactic acid bacteria can ferment malic acid, a natural compound found in grapes, into lactic acid (Kunkee 1991). This malolactic fermentation can result in a wine with a softer mouth feel but is not easy to control (Bauer and Dicks 2004).

Fermentation can also be found in aquatic environments and anaerobic digesters. Common anaerobic environments are sediments of lakes, rivers and oceans as well as bogs, marshes, and flooded soils. Sediments of freshwater enrich both prokaryotes and organic compounds (Nealson 1997). These microbial communities play an important role in carbon and nitrogen cycling within the freshwater ecosystem. Fermentative bacteria found in these habitats can ferment organic compounds to many fermentation products, such as acetate, CO_2, and H_2. Interestingly, many fermentative bacteria are facultative anaerobic and can switch back to fermentative mode in the presence of oxygen (Nealson 1997). Microbial fermentation refers to the acidification process in the anaerobic digesters. Acidogenic bacteria ferment small molecules formed by hydrolysis to VFA, lactate, CO_2 and H_2. These acidogenic bacteria are mainly affiliated to five phyla, *Firmicutes*, *Bacteroidetes*, *Chloroflexi*, *Proteobacteria*, and *Actinobacteria* (Castellano-Hinojosa et al 2018, Xu et al 2021).

Biochemical pathways producing major fermentation products

Biochemical pathways written in textbook

Fermentation pathways have been studied for decades. The pathways that form acetate, for example, are the result of over 80 years of work (Lipmann 1939). Over time, a view has emerged about how most microbes form fermentation products (Figure 1).

In general, anaerobic bacteria employ the EMP pathway or ED pathway to convert glucose to pyruvate, while the pentose phosphate pathway enables the microbes to utilize both hexoses and pentoses (Figure 1). Typically, glycolysis in EMP pathway involves ten steps, during which one mole of glucose is converted into two moles of pyruvate (Nelson et al 2008). The redox cofactor oxidized NAD (NAD_{ox}) is reduced by enzyme glyceraldehyde-3-phosphate dehydrogenase,

forming reduced NAD (NAD_{red}). The phosphorylated metabolites (1,3-disphosphate glycerate and phosphoenolpyruvate) are hydrolyzed and drive ATP formation via substrate level phosphorylation. Overall, two moles of pyruvate, two moles of NAD_{red}, and two moles of ATP are produced from one mole of glucose. The enzyme 6-phosphofructokinase is unique to the formation of pyruvate in the EMP pathway (Nelson et al 2008). Unlike the EMP pathway, the ED pathway forms two moles of pyruvate and one mole of ATP from each mole of glucose (Stettner and Segre 2013). The key enzymes are 6-phosphogluconate dehydrogenase and 2-keto-3-deoxy-6-phosphogluconate (KDPG) aldolase (Figure 1).

Pyruvate can be metabolized into several organic compounds, such as ethanol, lactate, acetyl-CoA, formate, and oxaloacetate (Figure 1 and 2), depending on the enzyme systems in bacteria. Pyruvate decarboxylase converts pyruvate to acetaldehyde and CO_2 (Eram and Ma 2013). One mole of acetaldehyde is reduced to one mole of ethanol by alcohol dehydrogenase. Therefore, two moles of ethanol are produced from one mole of glucose during alcoholic fermentation.

Pyruvate can be reduced with NAD_{red} to form lactate by lactate dehydrogenase (Figure 1 and 2). When two moles of lactic acid are the produced from one mole of glucose during fermentation, this process is often referred as homolactic fermentation. The bacteria performing homolactic fermentation are usually lactic acid bacteria. In contrast, heterolactic fermentation leads to formation of ethanol and CO_2, in addition to lactate (Gunsalus and Gibbs 1952). Among these products, CO_2 is formed together with ribulose 5-phosphate from decarboxylation of gluconate 6-phosphate. Then ribulose 5-phosphate is epimerized and subsequently broken down into glyceraldehyde-3-phosphate and acetyl-phosphate. Glyceraldehyde-3-phosphate is converted to lactate by the same reactions as in the homolactate pathway. The acetyl-phosphate is converted

to acetyl-CoA, then reduced to acetaldehyde by acetaldehyde dehydrogenase, and finally reduced to ethanol by alcohol dehydrogenase.

Pyruvate dehydrogenase and pyruvate:ferredoxin oxidoreductase convert pyruvate and CoA to acetyl-CoA, CO_2, with the production of NAD_{red} or reduced ferredoxin (Fd_{red}), respectively (Bothe and Nolteernsting 1975). Acetyl-CoA is a precursor of acetate, ethanol, and butyrate (Figure 1). The typical pathway converting acetyl-CoA to acetate involves phosphotransacetylase and acetate kinase (Thauer et al 1977). Phosphotransacetylase converts acetyl-CoA to acetyl-phosphate, while acetate kinase converts acetyl-phosphate and ADP to acetate and ATP (Figure 2). Alternatively, acetyl-CoA can be reduced to acetaldehyde by acetaldehyde dehydrogenase, and alcohol dehydrogenase can then convert acetaldehyde to ethanol (Figure 2).

Furthermore, two moles of acetyl-CoA are converted to one mole of acetoacetyl-CoA in butyrate-producing clostridia (Hackmann and Firkins 2015), which is reduced to β-hydroxybutyryl-CoA (Figure 2). β-hydroxybutyryl-CoA dehydratase converts β-hydroxybutyryl-CoA to crotonyl-CoA. The crotonyl-CoA is reduced to butyryl-CoA with NAD_{red} by butyryl-CoA dehydrogenase. Bytyryl-CoA is converted to butyryl-phosphate by phosphotransbutyrylase and butyrate kinase catalyzes reaction of butyryl-phosphate with ADP to form butyrate and ATP (Buckel 2001). Alternatively, bytyryl-CoA:acetate CoA-transferase catalyzes reaction of butyryl-CoA with acetate to form butyrate and acetyl-CoA (Buckel 2001), and acetyl-CoA is converted to acetate using enzymes described above (Figure 2). Butyryl-CoA can also be reduced to butyraldehyde by butyraldehyde dehydrogenase (Lee et al 2008). Butanol dehydrogenase reduces butyraldehyde with NAD_{red} or reduced $NADP^+$ (NADPH, $NADP_{red}$) to form butanol.

Pyruvate formate lyase catalyzes simultaneous formation of formate and acetyl-CoA from pyruvate and CoA (KNAPPE et al 1974). Under anaerobic conditions, the pyruvate formate lyase

in *Escherichia coli* is activated by pyruvate formate lyase activating enzyme. In contrast to pyruvate dehydrogenase and pyruvate:ferredoxin oxidoreductase, the pyruvate formate lyase forms acetyl-CoA without consumption of any redox cofactors. Formate can be excreted out of cells or it is oxidized to CO_2 by formate dehydrogenases.

Pyruvate carboxylase converts pyruvate to oxaloacetate (Uy et al 1999). Alternatively, oxaloacetate is produced from phosphoenolpyruvate in a reaction catalyzed by phosphoenolpyruvate carboxykinase. Oxaloacetate is reduced to malate by malate dehydrogenase. Malate is converted to fumarate by fumarase. Fumarate is reduced to succinate by fumarate reductase or succinate dehydrogenase. Two moles of NAD_{red} are consumed during the conversion of one mole of oxaloacetate to one mole of succinate.

Propionate is another major fermentation product (Figure 1 and 2). Propionate is produced by the succinate pathway (also called randomizing pathway) and the acrylate pathway (also known as direct reductive pathway) (Reichardt et al 2014). The succinate pathway involves the formation of succinate and the conversion of succinate to propionate (Figure 2). Succinate is produced via pathways as mentioned above. The conversion of succinate to propionate involves the conversion of succinate to succinyl-CoA, and the conversion of (L)-methylmalonyl-CoA to (D)-methylmalonyl-CoA. (D)-Methylmalonyl-CoA is converted to propionyl-CoA by either methylmalonyl-CoA transcarboxylase, such as in propionibacteria (Falentin et al 2010), or by methylmalonyl-CoA decarboxylase (Na^+ pumping), such as in *Bacteroides fragilis* and *S. ruminantium* (Reichardt et al 2014). Propionyl-CoA:succinate CoA-transferase catalyzes the CoA transfer from propionyl-CoA to succinate.

The acrylate pathway is used by *M. elsdenii* (Hino and Kuroda 1993), *Clostridium propionicum* (Hetzel et al 2003), and many other organisms (Reichardt et al 2014). Propionyl-CoA

transferase converts propionyl-CoA and lactate to lactyl-CoA (also called lactoyl-CoA) and propionate, while lactyl-CoA dehydratase catalyzes the removal of the H_2O molecule from lactyl-CoA, producing acrylyl-CoA (also called acryloyl-CoA). Acrylyl-CoA reductase converts acryl-CoA to propionyl-CoA, which is converted to propionate by propionyl-CoA transferase (Figure 2).

P. ruminicola 23 was reported to produce propionate via the acrylate pathway (Joyner and Baldwin 1966). The enzymatic evidence was that *P. ruminicola* 23 possessed lactyl-CoA dehydrase, now known as dehydratase, a key enzyme in acrylate pathway (Joyner and Baldwin 1966). Using radiolabeled glucose ([2-^{14}C]-glucose), another laboratory measured labeled pattern of propionate (Wallnofer and Baldwin 1967), but found no randomization label in propionate, suggesting the succinate pathway was impossible for propionate production in *P. ruminicola* 23. The enzymatic assays confirmed activity of lactyl-CoA dehydratase and acryl-CoA dehydrogenase, but they failed to show reduction of acrylyl-CoA by NAD_{red} and cell extract (Wallnofer and Baldwin 1967). The vitamin B_{12}-dependence for propionate and succinate production matches with the possibility that the succinate pathway could be used for propionate production. *P. ruminicola* 23 produced large amount of propionate in the presence of vitamin B_{12}. The production of propionate in *P. ruminicola* 23 depends on vitamin B_{12} (Strobel 1992). The activity of methylmalonyl mutase in succinate pathways depend on vitamin B_{12} (Buckel 2021, Takahashi-Iniguez et al 2012).

New pathways for converting glucose to pyruvate

Variations are reported during the conversion of glucose to pyruvate (Taillefer and Sparling 2016). Some key enzymes employ alternative cofactors and some enzymes are bypassed by other enzymes in the pathways. The typical glucokinase in prokaryotes is ATP-dependent (Ronimus and

Morgan 2003), where the phosphoryl group donor is ATP. In some archaea, such as *Pyrococcus furiosus* and *Thermococcus,* ADP-dependent glucokinase catalyzes the phosphorylation of glucose use ADP as the phosphoryl group donor (Koga et al 2000).

Phosphofructokinase catalyzes the phosphorylation of fructose-6-phosphate into fructose-1,6-bisphosphate using ATP as phosphoryl group donor. It has been found that pyrophosphate (PP_i)-dependent phosphofructokinase converts PP_i and fructose-6-phosphate into phosphate and fructose-1,6-bisphosphate in lower eukaryotes (Siebers et al 1998) and some bacteria such as *Ruminiclostridium thermocellum* (formerly *Clostridium thermocellum*) (Mertens 1991, Zhou et al 2013). Utilization of PP_i-dependent phosphofructokinase conserves energy because PP_i is a byproduct of biosynthetic reactions and the regeneration of PP_i consumes less ATP (Bielen et al 2010).

Glyceraldehyde-3-phosphate ferredoxin oxidoreductase (GAPOR) catalyzes irreversible conversion of glyceraldehyde-3-phosphate into 3-phosphoglycerate with the electron transferred to ferredoxin. This enzyme is found in archaea *P. furiosus* (van der Oost et al 1998). Unlike the conversion of glyceraldehyde-3-phosphate to 1,3-bisphosphoglycerate by glyceraldehyde-3-phosphate dehydrogenase and the conversion of 1,3-bisphosphoglycerate to 3-phosphoglycerate by phosphoglycerate kinase, no ATP is produced but the electrons are transferred to Fd_{ox} rather than NAD_{ox}. Instead of reducing ferredoxin, *Streptococcus mutans* (Boyd et al 1995) utilizes a non-phosphorylating, NADP-dependent glyceraldehyde-3-phosphate dehydrogenase to reduce $NADP_{ox}$ and the resulting $NADP_{red}$ could be used for biosynthetic reactions.

Several pathways can bypass the pyruvate kinase to form pyruvate from phosphoenolpyruvate (PEP). These pathways include pyruvate phosphate dikinase (PPDK), combined activities of PEP carboxykinase and oxaloacetate decarboxylase, and combined

activities of PEP carboxykinase, NAD-linked malate dehydrogenase as well as NADP-linked malic enzyme (the malate shunt). One example, *R. thermocellum*, does not have the gene for pyruvate kinase. Instead, it encodes enzymes for pyruvate phosphate dikinase, GDP-linked PEP carboxylase, NAD-linked malate dehydrogenase, and NADP-linked malic enzyme (Zhou et al 2013). Enzymatic assays showed that no activity of oxaloacetate decarboxylase was observable. Isotopic labeling experiment and flux analysis revealed that the malate shunt accounted for one third of the flux to pyruvate and the PPDK was responsible for the remainder (Olson et al 2017).

New pathway for fermentative production of butyrate

An atypical pathway for butyrate formation in most butyrivibrios was proposed (Hackmann and Firkins 2015). This atypical pathway involves ion pump Rnf (Rhodobacter nitrogen fixation) and Ech (*Escherichia coli* hydrogenase-3-type, a membrane bound [NiFe]-hydrogenase) for energy conservation. Specifically, pyruvate:ferredoxin oxidoreductase and butyryl-CoA dehydrogenase reduce Fd_{ox}. Rnf oxidizes Fd_{red} and reduces NAD_{ox} and Ech oxidizes Fd_{red} and reduces H^+. Both Rnf and Ech generate ion gradient that drive ATP synthesis (Hackmann and Firkins 2015). Rnf can translocate Na^+ or H^+ across membrane while Ech can pump H^+ across membrane. Biochemical evidence verified the existence of this atypical pathway in a rumen bacterium *Pseudobutyrivibrio ruminis* (Schoelmerich et al 2020). Interestingly, *P. ruminis* possesses two different ion circuits for energy conservation which are mediated by two different ATP synthases and two ion pumps, Rnf and Ech. *In silico* analysis suggested that many different obligate anaerobes have this pathway.

New pathways for fermentative production of acetate

Many other pathways that form acetate during fermentation have been identified in organisms from all branches of the tree of life, including archaea, bacteria, and eukaryotes.

Pathway for acetate production in archaea

Archaea have not been found to use the phosphotransacetylase and acetate kinase to form acetate. The only pathway reported for fermentative acetate production in archaea is mediated by acetyl-CoA synthetase (ADP-forming). This enzyme catalyzes reversal conversion of acetyl-CoA, ADP, and phosphate to acetate, CoA, and ATP. The acetyl-CoA synthetase (ADP-forming) activity was first confirmed in both directions for the cell extract of *P. furiosus*, a hyperthermophilic archaeon (Schafer and Schonheit 1991). Two distinct isoenzymes of acetyl-CoA synthetase (ADP-forming) were purified from *P. furiosus* by two laboratories (Glasemacher et al 1997, Mai and Adams 1996). Both isoenzymes were able to catalyze acetate formation from acetyl-CoA, but they had different substrate specialties towards CoA derivatives (Glasemacher et al 1997, Mai and Adams 1996). The genes encoding the isoform I enzyme were identified and heterologously expressed in *E. coli*. Purified recombinant enzyme had similar molecular properties as the enzyme purified from *P. furiosus* (Musfeldt et al 1999). The activity of acetyl-CoA synthetase (ADP-forming) was demonstrated in many other archaea, such as *Desulfurococcus amylolyticus* and *Hyperthermus butylicus* (Schafer et al 1993, Schonheit and Schafer 1995).

New pathways for acetate production in bacteria

There are three pathways responsible for fermentative acetate production in bacteria, beyond the typical pathway mediated by phosphotransacetylase and acetate kinase. These pathways are

mediated by acetyl-CoA synthetase (ADP-forming), acetyl-CoA synthetase (AMP), and butyryl-CoA:acetate CoA-transferase.

Acetyl-CoA synthetase (ADP-forming) has also been identified in bacteria. *Chloroflexus aurantiacus* produced acetate during metabolism but lacks genes for phosphotransacetylase and acetate kinase. Instead, it encodes the gene for acetyl-CoA synthetase (ADP-forming) (Tang et al 2011). The presence of this enzyme was confirmed experimentally by purifying it from the native host and demonstrating catalytic activity. Additionally, it was expressed heterologously in *E. coli* and again displayed the expected activity. Analysis of substrate specificities and kinetic constants of the recombinant enzyme revealed high similarity with the isoform I enzyme of acetyl-CoA synthetase (ADP-forming) from archaea (Schmidt and Schonheit 2013).

Unlike acetyl-CoA synthetase (ADP-forming), acetyl-CoA synthetase (AMP) catalyzes formation of acetate and ATP using acetyl-CoA, AMP, and PP_i. The activity of acetyl-CoA synthetase (AMP) has been demonstrated in a model syntrophic bacterium, *Syntrophus aciditrophicus*, using a combination of transcriptomic, proteomic, metabolite, and enzymatic approaches (James et al 2016). Shotgun transcriptomics of *S. aciditrophicus* revealed that gene (*SYN_02635*) for acetyl-CoA synthetase (AMP) was highly expressed; shotgun proteomic analysis revealed that protein encoded by *SYN_02635* was one of the most abundant proteins in the proteome of *S. aciditrophicus*; the cell extract of *S. aciditrophicus* had high acetyl-CoA synthetase activity that was dependent on AMP and PP_i.

Butyryl-CoA:acetate CoA-transferase catalyzes conversion of acetyl-CoA with butyrate to form acetate and butyryl-CoA. This pathway was reported in glutamate fermentation to form acetate and butyrate in *Clostridium tetanomorphum* (Buckel 2001). Butyryl-CoA is next converted to butyrate via phosphotransbutyrylase and butyrate kinase.

Pathways for acetate production in eukaryotes

Eukaryotes employ four pathways to form acetate from acetyl-CoA, three of which are also found in bacteria, including phosphotransacetylase and acetate kinase, acetyl-CoA synthetase (ADP-forming), and acetyl-CoA synthetase (AMP). There is one more pathway that has not been reported in archaea and bacteria, the succinyl-CoA:acetate CoA-transferase and succinyl-CoA synthetase pathway.

Both phosphotransacetylase and acetate kinase activity were reported in mitochondria prepared from a green alga, *Chlamydomonas reinhardtii* (Atteia et al 2006, Kreuzberg et al 1987). Acetyl-CoA synthetase (ADP-forming) was purified from *Entamoeba histolytica*, a human parasite, under anaerobic conditions. The purified acetyl-CoA synthetase (ADP-forming) did not form ATP from AMP and PP_i but rather formed ATP and acetate from acetyl-CoA, ADP and phosphate (Reeves et al 1977). A gene encoding acetyl-CoA (ADP-forming) from the amitochondriate eukaryote *Giardia lamblia* was identified and expressed in *E. coli* (Sánchez et al 2000). Acetyl-CoA synthetase (AMP) activity was discovered in a fungus, *Aspergillus nidulans*, during ammonia fermentation. The gene encoding this enzyme was identified and the corresponding protein was purified from the fungus (Takasaki et al 2004).

The succinyl-CoA:acetate CoA-transferase (SCACT) and succinyl-CoA synthetase (SCS) pathway (SCACT/SCS pathway) was observed in some anaerobic protozoa, such as *Tritrichomonas foetus, Trichomonas vaginalis*, and *Trypanosoma brucei*. Succinyl-CoA:acetate CoA-transferase catalyzes conversion of acetyl-CoA and succinate to acetate and succinyl-CoA; succinyl-CoA synthetase catalyzes reaction of succinyl-CoA, ADP, and phosphate to form succinate, CoA, and ATP. This pathway was first reported in the hydrogenosomes of *T. foetus* (Lindmark 1976). Dependence of succinate to form acetate was reported in *T. foetus* and *T.*

vaginalis (Steinbuchel and Muller 1986). The gene encoding succinyl-CoA:acetate CoA-transferase was identified and confirmed to encode this enzyme in *T. brucei* by the combination of genetic, enzymatic, and biochemical approach (Riviere et al 2004). This pathway was also found in other eukaryotes (Muller et al 2012, Tielens et al 2010).

Evidence for another new pathway for forming acetate in bacteria

Although bacteria have the four recognized pathways for forming acetate as mentioned above, there is evidence of a fifth pathway. Recent genomic analysis revealed that some rumen bacteria could use SCACT/SCS pathway to form acetate from acetyl-CoA during fermentation (Hackmann et al 2017). *Mitsuokella jalaludinii* M 9 and three *Selenomonas* lacks all known pathways to form acetate in bacteria, but they encode genes for succinyl-CoA:acetate CoA-transferase and succinyl-CoA synthetase, implying that this pathway could be used for acetate production in these rumen bacteria, although the biochemical evidence is lacking.

S. ruminantium HD4 is a rumen bacterium that may use the SCACT/SCS pathway to form acetate. It has long been known that *S. ruminantium* HD4 forms acetate but does not have activities for phosphotransacetylase and acetate kinase (Joyner and Baldwin 1966, Melville et al 1988). It was suggested to use acetyl-CoA ligase (ADP forming), also called acetyl-CoA synthetase (ADP-forming), as alternative for the missing activities based on several points of evidence (Michel and Macy 1990). A protein complex was purified from *S. ruminantium* HD4 grown on glucose and fumarate by chromatography. This purified enzyme had molecular weight 230 kDa and had activity towards acetyl-CoA, propionyl-CoA, and succinyl-CoA, measured by an uncommon enzymatic assay (Michel and Macy 1990). However, the proposed acetyl-CoA synthetase (ADP-forming) may not be used for acetate formation *in S. ruminantium* HD4; instead, the SCACT/SCS pathway could be the alternative pathway (Hackmann et al 2017). First, genomic evidence

suggested that it encodes the SCACT/SCS pathway, rather than gene for acetyl-CoA synthetase (ADP-forming). Second, the enzymatic assay for measuring activity of acetate-forming enzyme from *S. ruminantium* HD4 is not specific for acetyl-CoA (ADP-forming). Indeed, the observed enzymatic results are consistent with predicted results for succinyl-CoA:acetate CoA-transferase plus succinyl-CoA transferase, rather than the predicted results for acetyl-CoA synthetase (ADP-forming) (Hackmann et al 2017).

Efforts had been made to test the SCACT/SCS pathway in *S. ruminantium* HD4. Succinyl-CoA synthetase activity was observed in *S. ruminantium* HD4, but not the activity of succinyl-CoA:acetate CoA-transferase (McCourt 2019). It was found that the methods used to biochemically test presence of acetyl-CoA synthetase (ADP-forming) were not specific to acetyl-CoA synthetase (ADP-forming). These methods measured off target activity of succinyl-CoA synthetase. Other assays were performed and verified the activity of succinyl-CoA synthetase but not succinyl-CoA:acetate CoA-transferase nor acetyl-CoA synthetase (ADP-forming) in *S. ruminantium* HD4. Therefore, it is still unclear how this strain forms acetate during fermentation.

Some propionibacteria encode the SCACT/SCS pathway, but it is unclear which pathway they use for forming acetate, some examples include *Cutibacterium granulosum* (formerly *Propionibacterium granulosum*), *Cutibacterium acnes* (formerly *Propionibacterium acidipropionici*), and *Acidipropionibacterium acidipropionici* (formerly *Propionibacterium acidipropionici*) (Parizzi et al 2012, Scholz and Kilian 2016). *C. granulosum* and *C. acnes* are commonly found on human skin and are occasionally associated with inflammatory diseases (Allaker et al 1985), while *A. acidipropionici* is an important propionate-forming bacterium, and has been widely studied for propionate production in industry (Zhu et al 2010). These bacteria form propionate as well as acetate as a byproduct. Efforts were made to knock out the typical

pathway for forming acetate, aiming to increase propionate production in *A. acidipropionici*, but the levels of propionate did not change significantly (Suwannakham et al 2006), suggesting that other pathway could be used for forming acetate. The possible pathways are the SCACT/SCS pathway and acetyl-CoA synthetase (ADP-forming), since they were identified by genomic and proteomic analysis (Parizzi et al 2012). Further, the pathway for forming acetate in *C. granulosum* has not yet been reported.

Missing step in redox balance for fermentative succinate/propionate production

Redox cofactors are electron carriers that transfer electrons from one substrate to the other. Redox related enzymes, including Rnf, can regenerate redox cofactors during metabolism. The process of regenerating redox cofactors by redox related enzymes is critical to metabolism, including fermentation.

Regenerating redox cofactors to maintain redox balance

Redox balance has to be maintained during fermentation for it to continue (Chen et al 2014). During anaerobic fermentation, oxidation of the substrate is coupled to the reduction of another substrate or an intermediate derived from the oxidation. Redox cofactors, such as NAD, NADP, and ferredoxin, serve as electron carriers. The number of redox cofactors in the cell is limited, so they are regenerated to be able to continuously transfer electrons. During fermentation of glucose to ethanol, for example, NAD_{ox} is first reduced to NAD_{red} by glyceraldehyde-3-phosphate. It is then reoxidized to NAD_{ox} by acetaldehyde. If not reoxidized, fermentation cannot continue. The same principle applies with Fd_{ox} and Fd_{red}.

Several enzymes can reduce or oxidize redox cofactors. Enzymes that reduce NAD_{ox} or oxidize NAD_{red} in the cytoplasm are glyceraldehyde-3-phosphate dehydrogenase, lactate

dehydrogenase, pyruvate dehydrogenase, aldehyde dehydrogenase, alcohol dehydrogenase, malate dehydrogenase. Some respiratory enzymes located on the cell membrane are able to accept electrons from NAD_{red}, such as NADH dehydrogenase, NADH:ubiquinone oxidoreductase, and NADH-quinone oxidoreductase. The redox potential of ferredoxin is in the range of -450 to -500 mV (Buckel and Thauer 2013). An electron donor must have a sufficiently lower redox potential than ferredoxin in order to reduce ferredoxin. Consequently, only a few compounds can reduce Fd_{ox}. Glyceraldehyde-3-phosphate ferredoxin oxidoreductase, carbon monoxide dehydrogenase, and pyruvate:ferredoxin oxidoreductase reduce Fd_{ox} with glyceraldhydrate-3-phosphate, carbon monoxide (CO), and pyruvate, respectively. The oxidation of Fd_{red} with NAD_{ox} or H^+ can be catalyzed by Rnf or various hydrogenase (Sondergaard et al 2016), respectively.

Flavin-based electron bifurcation is another mechanism to regenerate ferredoxin. In flavin-based electron bifurcation, reduction of the high-potential electron acceptor drives the reduction of the low-potential electron acceptor (usually ferredoxin). This electron bifurcation has been employed by several enzymes. The butyryl-CoA/EtfAB complex in *Clostridium kluyveri* couples the reaction of crotonyl-CoA and NAD_{red} with the reduction of Fd_{ox} with NAD_{red} (Herrmann et al 2008). The NADH-dependent reduced ferredoxin:$NADP^+$ oxidoreductase complex NfnAB from *C. kluyveri* couples the reaction of $NADP_{ox}$ and Fd_{red} with reduction of $NADP_{ox}$ with NAD_{red} (Wang et al 2010). Using the same mechanism, the caffeyl-CoA reductase complex CarCDE from *Acetobacterirum woodii* reduces Fd_{ox} with NAD_{red} by coupling it to NADH-dependent reduction of caffeyl-CoA. A soluble electron-bifurcating hydrogenase identified in *A. woodii* catalyzes NAD-dependent ferredoxin reduction with H_2 (Schuchmann and Muller 2012). Ferredoxin- and NAD-dependent formate dehydrogenase (Wang et al 2013) and ferredoxin-and NAD-dependent lactate dehydrogenase catalyze reduction of Fd_{ox} from NAD_{red} using flavin-based electron

bifurcation (Weghoff et al 2015). The electron bifurcating hydrogenase HydABC from *Ruminococcus albus* 7 catalyzes consumption of Fd_{red} and NAD_{red} to produced H_2 (Zheng et al 2014).

Ferredoxin:NAD^+ oxidoreductase activity and ion translocating activity of Rnf

As mentioned above, Rnf can also regenerate ferredoxin. This enzyme is an ion pump located on the cell membrane and has activity of ferredoxin:NAD^+ oxidoreductase activity. It catalyzes the oxidation of Fd_{red} and reduction of NAD_{ox}. Genes for *rnf* were first discovered in *Rhodobacter capsulatus* and predicted to encode a protein cable of transporting electron to nitrogenase (Saeki et al 1993, Schmehl et al 1993). In 2005, it was demonstrated that the membrane associated complex catalyzed reaction of Fd_{red} with NAD_{ox} in a bacterium, *C. tetanomorphum* (Boiangiu et al 2005). Enzymes purified from *C. tetanomorphum* had 6 subunits and N-termini of these subunits were encoded by putative *rnfABCDEG* genes of sequenced genome of *Clostridium tetani* (Bruggemann et al 2003). The activity of ferredoxin:NAD^+ oxidoreductase of Rnf was demonstrated in *A. woodii* and this activity was coupled to Na^+ translocation (Biegel and Muller 2010). The Rnf from *A. woodii* requires Na^+ and the ferredoxin:NAD^+ oxidoreductase activity is reversely coupled to the membrane potential (Hess et al 2013). Studies with genetic mutants suggested that Rnf has role in energetically linking cellular pools of ferredoxin and NAD (Westphal et al 2018). Purified Rnf was incorporated into artificial liposomes, and this enzyme catalyzed transport of Na^+, which was coupled to ferredoxin dependent reduction of NAD_{ox} (Wiechmann et al 2020).

Genes for Rnf complex have been identified in many anaerobic microorganisms such as acetogenic bacteria (Imkamp et al 2007), butyrivibrios (Hackmann and Firkins 2015), sulfate reducers (Strittmatter et al 2009), and methanogens (Schlegel et al 2012, Wang et al 2014). The

ferredoxin:NAD^+ oxidoreductase activity of Rnf has been identified in many Gram-positive bacteria and Gram-negative bacteria (Hess et al 2016). Some examples of Gram-positive bacteria include *C. tetanomorphum* and *Clostridium ljungdahlii*. Some examples of Gram-negative bacteria include *B. fragilis* and *Vibrio cholerae*. Rnf genes are widely distributed in aerobes, facultative anaerobes, and anaerobes. In total, there have been about 260 genomes encoding Rnf genes identified until 2010 (Biegel et al 2011), but it is still unclear the distribution of Rnf genes in genomes of fermentative prokaryotes.

Role of Rnf in fermentation

Rnf has an important role for forming butyrate production. The most common pathway leading to butyrate formation is the conversion of acetyl-CoA to crotonyl-CoA and the latter is reduced to butyryl-CoA, which is catalyzed by butyryl-CoA dehydrogenase. Butyryl-CoA dehydrogenase catalyzes reduction of ferredoxin and crotonyl-CoA with NAD_{red} via flavin-based electron bifurcation. Electron bifurcation with crotonyl-CoA may be the only pathway to butyrate in anaerobic microorganisms (Buckel 2021). Rnf oxidizes the Fd_{red} for butyrate formation during sugar fermentation, glutamate formation, and glucose/xylose fermentation (Buckel 2021, Hackmann and Firkins 2015, Schoelmerich et al 2020).

The presence of Rnf is critical for redox balance and energy conservation during glutamate fermentation in C. *tetanomorphum*. *C. tetanomorphum* ferments glutamate via two pathways, 2-hydroxyglutarate and 3-methylaspartate pathway. In the 2-hydroxyglutarate pathway, ferredoxin is reduced via flavin-based electron bifurcation. The Fd_{red} donates electrons to proton and NAD_{ox} via [FeFe]-hydrogenase and Rnf, respectively. In the 3-methylaspartate pathway, in addition to butyryl-CoA dehydrogenase, pyruvate:ferredoxin oxidoreductase also reduces Fd_{ox}. The Fd_{red} is oxidized by Rnf and [FeFe]-hydrogenase (Buckel 2021).

Rnf and Ech catalyze oxidation of Fd_{red} during carbohydrate fermentation in a rumen bacterium, *P. ruminis* (Schoelmerich et al 2020). This organism ferments glucose into lactate, formate, acetate, butyrate, H_2, and CO_2. Fd_{red} was produced by pyruvate:ferredoxin oxidoreductase and butyryl-CoA dehydrogenase. Rnf and Ech were involved in oxidizing Fd_{red} and generating ion gradients driving ATP synthesis via two types of ATP synthase.

The electron transfer from Fd_{red} to NAD_{ox} catalyzed by Rnf is critical for ethanol production in *R. thermocellum* (Lo et al 2017). NAD_{red} and $NADP_{red}$ are produced via glycolysis and oxidized by the aldehyde dehydrogenase and alcohol dehydrogenase in *R. thermocellum*. Pyruvate:ferredoxin oxidoreductase reduces Fd_{ox} and then the Fd_{red} is oxidized by Rnf, Ech, and the enzyme NADH-dependent reduced ferredoxin:$NADP^+$ oxidoreductase. Electrons from Fd_{red} and NAD_{red} or $NADP_{red}$ are transferred to proton via electron bifurcation. Deletion of the NADH-dependent reduced ferredoxin:$NADP^+$ oxidoreductase did not change the distribution of fermentation products. However, deletion of Rnf genes resulted in a decrease in ethanol formation. Overexpression of Rnf genes lead to 30% increase of ethanol production if the hydrogenase was deleted.

These examples suggest that Rnf plays an important role in both amino acids and carbohydrate fermentation. It helps to regenerate redox cofactors and generate ion gradient contributing to extra energy conservation. Rnf is not the only enzyme that oxidizes Fd_{red}. Other enzymes, such as electron bifurcating hydrogenase and Ech, are involved in oxidizing Fd_{red}. No bacteria have been identified where Rnf is the sole enzyme to oxidize Fd_{red}. The involvement of Rnf in succinate and propionate production has not been reported.

Missing step in fermentative production of succinate and propionate

The pathway for forming propionate has been studied extensively in propionibacteria (Allen et al 1964). Propionibacteria, such as *P. freudenreichii*, form propionate using the succinate pathway. They have pyruvate dehydrogenase and glyceraldehyde-3-phosphate dehydrogenase to reduce NAD_{ox}. Then NAD_{red} donates electrons to oxaloacetate and fumarate for succinate production. Recent genomic analysis found that some *Prevotella* species isolated from rumen have genes encoding pyruvate:ferredoxin oxidoreductase rather than pyruvate dehydrogenase. These species were *Prevotella albensis*, *Prevotella brevis*, *Prevotella bryantii*, and *P. ruminicola* (Hackmann et al 2017). The involvement of pyruvate:ferredoxin oxidoreductase during fermentation leads to two problems. First, Fd_{red} is formed by pyruvate:ferredoxin oxidoreductase. The Fd_{red} has to be oxidized. Second, reduction of oxaloacetate and fumarate with NAD_{red} forms extra NAD_{ox} that cannot be completely reduced by glyceraldehyde-3-phosphate dehydrogenase, according to the stoichiometry analysis (Hackmann et al 2017). The extra NAD_{ox} must be reduced. The missing step is how to reduce NAD_{ox} and how to oxidize Fd_{red}.

Genomic investigation of redox related enzymes led to the proposal that Rnf could fill in the missing step for succinate and propionate formation during carbohydrate fermentation (Hackmann et al 2017). According to genomic information of these *Prevotella*, Rnf is the only enzyme that can simultaneous reduce NAD_{ox} and oxidize Fd_{red}. No genes for other enzymes reducing NAD_{ox} or oxidizing Fd_{red} were identified except pyruvate:ferredoxin oxidoreductase, glyceraldehyde-3-phosphate dehydrogenase, malate dehydrogenase, and NADH:quinione oxidoreductase and fumarate reductase complex.

However, the biochemical evidence for Rnf involvement in succinate and propionate production has not been reported, leaving the missing step in succinate and propionate production

unsolved. Further experimentation should be conducted to demonstrate that Rnf is expressed in the cell during fermentation, and it has the activity to oxidize Fd_{red} and reduce NAD_{ox}.

Conclusion

Microbial fermentation is important to industry, agriculture, and human health. In this chapter, we described general features of microbial fermentation, energy conservation, and pathways for producing fermentation products (e.g., acetate, propionate, and butyrate). Microbial fermentation occurs in various anaerobic settings. We focused on microbial fermentation that occurs in the rumen, highlighting the members of ruminal microbial community and their roles in the rumen. We pursued this as knowing the biochemical pathways in fermentation is critical for manipulating fermentation. Recent development in DNA sequencing and multi-omics analysis promotes identification of new enzymes in fermentation.

Fermentation involves breaking down large organic compounds into small molecule metabolites using organic compounds as the electron donor and the electron acceptor. Microbial fermentation occurs in the rumen, which confers ruminants the unique ability to convert plant carbohydrates into milk and meat. Microbial fermentation also occurs in the gut of many different animals, food industry, aquatic environment, and anaerobic digesters, demonstrating the importance of microbial fermentation to many aspects of human life.

Many metabolites are formed during fermentation. The major products of fermentation are acetate, ethanol, acetone, lactate, propionate, isopropanol, butyrate, n-butanol, 2,3-butanediol, and succinate. Studies have revealed many pathways for forming these metabolites. Despite previous efforts in identifying pathways for forming fermentation products, some steps are still unsolved or unknown. It is unclear how bacteria form acetate during fermentation without known pathways for

forming acetate in bacteria. The SCACT/SCS pathway could be alternative to the typical pathway for acetate formation (Hackmann et al 2017), but no biochemical evidence has been documented to support it. Furthermore, there are missing steps for fermentative propionate formation in bacteria. It is unclear which enzymes regenerate redox cofactors for propionate formation. It has been proposed that Rnf can reduce NAD_{ox} and oxidize Fd_{red}, but more experimentation is necessary to prove it.

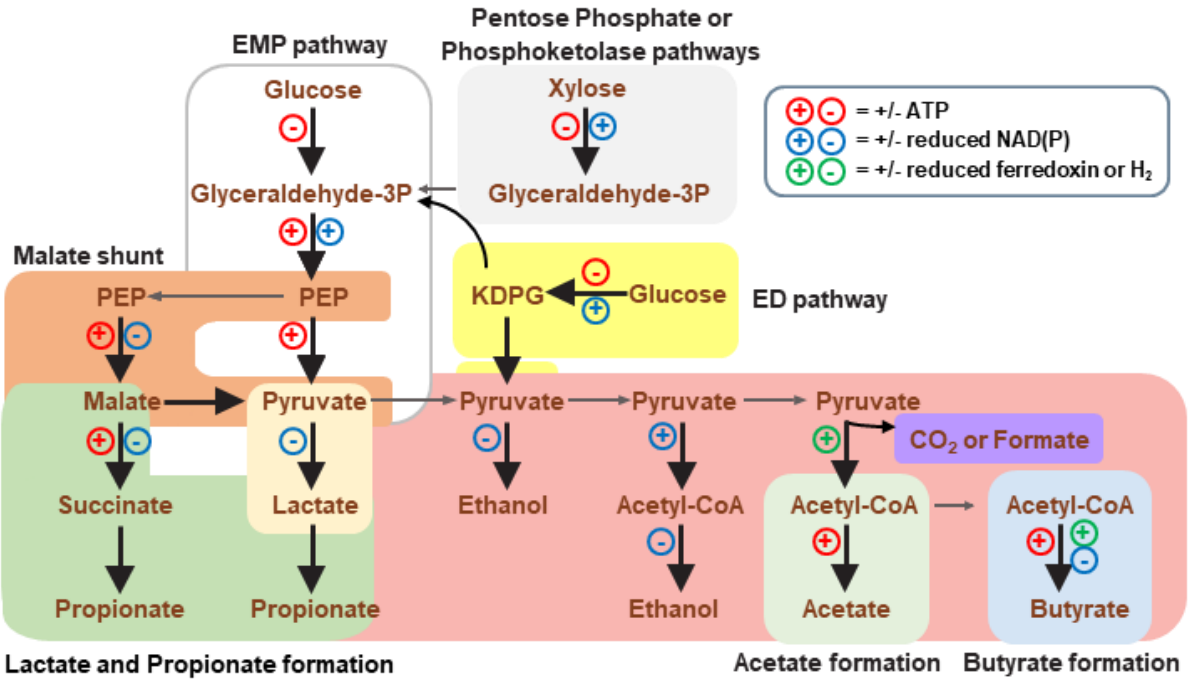

Figure 1. Overview of fermentation pathways. Modified from the reference (Ungerfeld and Hackmann 2020). Abbreviations: PEP, phosphoenolpyruvate; glyceraldehyde-3P, glyceraldehyde-3-phosphate; KDPG, 2-keto-3-deoxy-6-phosphogluconate; EMP pathway, Embden-Meyerhof-Parnas pathway; ED pathway, Entner–Doudoroff pathway.

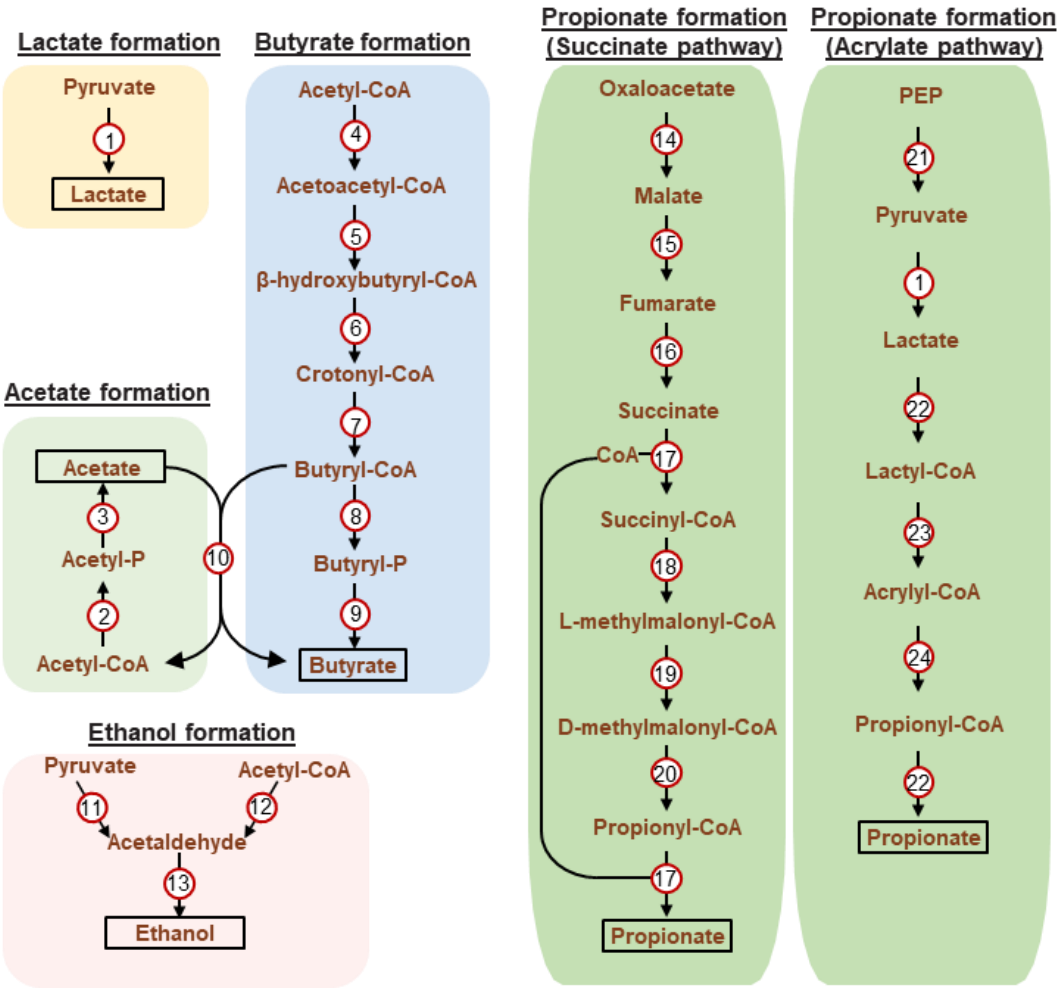

Figure 2. Typical pathways for forming acetate, ethanol, lactate, propionate, and butyrate during fermentation. Enzymes: 1, lactate dehydrogenase (EC 1.1.1.27); 2, phosphotransacetylase (PTA; EC 2.3.1.8); 3, acetate kinase (AK; EC 2.7.2.1); 4, acetyl-CoA-acetyltransferase (EC 2.3.1.9); 5, β-hydroxybutyryl-CoA dehydrogenase (EC 1.1.1.157); 6, β-hydroxybutyryl-CoA dehydratase (EC 4.2.1.55); 7, butyryl-CoA dehydrogenase complex (EC 1.3.1.109); 8, phosphotransbutyrylase (EC 2.3.1.19); 9, butyrate kinase (EC 2.7.2.7); 10, butyryl-CoA:acetate CoA-transferase (EC 2.8.3.8); 11, pyruvate decarboxylase (EC 4.1.1.1); 12, acetaldehyde dehydrogenase (EC 1.2.1.10); 13, alcohol dehydrogenase (EC 1.1.1.1); 14, malate dehydrogenase (EC 1.1.1.37); 15, fumarate hydratase (EC 4.2.1.2); 16, fumarate reductase/succinate dehydrogenase (EC 1.3.5.1, EC 1.3.5.4);

17, propionyl-CoA:succinate-CoA transferase (EC 2.8.3.27); 18, methylmalonyl-CoA mutase (EC 5.4.99.2); 19, methylmalonyl-CoA epimerase (EC 5.1.99.1); 20, methylmalonyl-CoA decarboxylase (EC 4.1.1.41), or methylmalonyl-CoA transcarboxylase (EC 2.1.3.1); 21, pyruvate kinase (EC 2.7.1.40); 22, propionyl-CoA transferase (EC 2.8.3.1); 23, lactyl-CoA dehydratase (EC 4.2.1.54); 24, acrylyl-CoA reductase (EC 1.3.1.84). Abbreviations: acetyl-P, acetyl-phosphate; butyryl-P, butyryl-phosphate; CoA, coenzyme A; PEP, phosphoenolpyruvate.

Chapter 2. A new pathway for forming acetate and synthesizing ATP during fermentation in bacteria

Abstract

Many bacteria and other organisms carry out fermentations forming acetate. These fermentations have broad importance to foods, agriculture, and industry. They are also important to bacteria themselves because they often generate ATP. Here we found a biochemical pathway for forming acetate and synthesizing ATP that was unknown in fermentative bacteria. We found the bacterium *Cutibacterium granulosum* formed acetate during fermentation of glucose. It did not use phosphotransacetylase or acetate kinase, enzymes found in nearly all acetate-forming bacteria. Instead, it used a pathway involving two different enzymes. The first enzyme, succinyl-CoA:acetate CoA-transferase (SCACT), forms acetate from acetyl-CoA. The second enzyme, succinyl-CoA synthetase (SCS), synthesizes ATP. We identified the genes encoding these enzymes, and they were homologs of SCACT and SCS genes found in other bacteria. The pathway resembles one described in eukaryotes, but the present pathway uses bacterial gene homologs. To find other instances of the pathway, sequences of all biochemically-characterized homologs of SCACT and SCS (103 enzymes from 64 publications) were analyzed. Homologs with similar enzymatic activity had similar sequences, enabling a large-scale search for them in genomes. Nearly 600 genomes of bacteria known to form acetate were searched, and 36 genomes of bacteria were found to encode homologs with SCACT and SCS activity. This included >30 species belonging to 5 different phyla, showing a diverse range of bacteria encode the SCACT/SCS pathway. This work suggests the SCACT/SCS pathway is important to forming acetate in many branches of the tree of life.

Introduction

Many bacteria and other organisms carry out anaerobic fermentations forming acetate (Caspi et al 2016, Gottschalk 1986, Muller et al 2012, White et al 2012). Such acetate-yielding fermentations have importance to foods, agriculture, and industry. Acetate is found in many fermented foods (e.g., Swiss cheese) (Fröhlich-Wyder et al 2017), and it is an energy source for cattle harboring fermentative microbes (Bergman 1990). Further, acetate is an often unwanted byproduct in industrial fermentations (e.g., those producing succinate or propionate) (Wang et al 2016). These fermentations also have importance to the energy metabolism of fermentative organisms themselves. If the organism forms acetate from acetyl-CoA or acetyl phosphate, it can generate ATP by substrate-level phosphorylation (Thauer et al 1977). This is crucial because fermentative metabolism otherwise yields few ATP.

Reflecting this broad importance, the biochemical pathways for forming acetate and ATP during fermentation have been studied for over 80 years (Lipmann 1939). Over the course of their study, a total of five pathways have been reported (Figure 3). For four of the pathways, the high energy precursor is acetyl-CoA. For one pathway, the precursor is either acetyl-CoA or acetyl phosphate.

Curiously, one of the five pathways has been found missing in bacteria. The pathway missing in bacteria involves the enzymes succinyl-CoA:acetate CoA-transferase (SCACT; EC 2.8.3.18) and succinyl-CoA synthetase (SCS; EC 6.2.1.5). It was first reported in a flagellate protozoan (Lindmark 1976), and then other eukaryotes (Muller et al 2012, Tielens et al 2010). No report of this SCACT/SCS pathway has been made in bacteria or archaea. In bacteria, the pathway commonly used involves phosphotransacetylase (PTA; EC 2.3.1.8) and acetate kinase (AK; EC 2.7.2.1) instead (Thauer et al 1977).

Recently, we found evidence of the SCACT/SCS pathway in some bacteria of the rumen (Hackmann et al 2017). These bacteria form acetate during fermentation, yet do not have genes for the PTA/AK pathway. They do have genes of the SCACT/SCS pathway, suggesting they may use this pathway instead. We have since tried to find bacteria with biochemical, not just genomic, evidence of the pathway (McCourt 2019).

Here we find biochemical evidence of the SCACT/SCS pathway in the bacterium *Cutibacterium granulosum*. We confirmed it has the appropriate genes, the gene products have enzymatic activity, and they form a functional pathway. Strikingly, the genes are bacterial homologs of SCACT and SCS, suggesting the pathway in this bacterium did not originated from eukaryotes. Moreover, this pathway appears to be common and is encoded by 36 type strains of bacteria that form acetate. This work suggests the SCACT/SCS pathway is important to acetate formation in many branches of the tree of life.

Materials and Methods

Organisms, media and growth

The Deutsche Sammlung von Mikroorganismen und Zellkulturen (DSMZ) was the source for all bacterial strains. The strains used were *Acidipropionibacterium acidipropionici* 4, *Butyrivibrio fibrisolvens* D1, *Cutibacterium acnes* DSM 1897, *Cutibacterium granulosum* VPI 0507, and *Propionibacterium freudenreichii* E11.1.

Strains were grown anaerobically under O_2-free CO_2 and with Balch tubes with butyl rubber stoppers, using techniques previously described (Tao et al 2019, Tao et al 2016). Propionibacteria (*A. acidipropionici*, *P. freudenreichii*, *C. acnes*, *C. granulosum*) were grown in the PYG medium (DSMZ medium 104). Per liter, PYG medium contained 5 g glucose, 5 g

Trypticase peptone (product 211921, BD), 5 g peptone (product 211677, BD), 10 g Bacto yeast extract (product 212750, BD), 5 g beef extract (product LP0029, Oxoid), 2.04 g K_2HPO_4, 40 mg KH_2PO_4, 80 mg NaCl, 20 mg $MgSO_4 \cdot 7H_2O$, 10 mg $CaCl_2 \cdot 2H_2O$, 1 mL Tween 80, 5 mg haemin, 1 µL vitamin K_1, 4 g $NaHCO_3$, and 449 mg cysteine-HCl. Resazurin was added as a redox indicator. The haemin was added as a 0.5 g/L solution containing 10 mM NaOH as the diluent. The vitamin K_1 was added as a 5 mL/L solution containing 95% ethanol as the diluent.

B. fibrisolvens D1 was grown on DSMZ medium 712. Per liter, DSMZ medium 712 contained 9 g glucose, 8.3 g Bacto yeast extract (product 212750, BD), 383 mg K_2HPO_4, 384 mg KH_2PO_4, 751 mg $(NH_4)_2SO_4$, 760 mg NaCl, 73 mg $MgSO_4$, 100 mg $CaC1_2 \cdot 2H_2O$, 10.669 g $NaHCO_3$, 16.7 mL vitamin solution, and 1.616 g cysteine hydrochloride monohydrate. Per liter, the vitamin solution contained 2 mg biotin, 2 mg folic acid, 10 mg pyridoxine-HCl, 5 mg thiamine-HCl, 5 mg riboflavin, 5 mg nicotinic acid, 5 mg D-Ca-pantothenate, 0.1 mg vitamin B_{12}, 5 mg p-aminobenzoic acid, and 5 mg lipoic acid. Resazurin was added as redox indicator.

The temperature for *A. acidipropionici* and *P. freudenreichii* was 30°C. The temperature for *B. fibrisolvens*, *C. acnes*, and *C. granulosum* was 37°C.

Cell extracts and supernatant

Eight, 9-mL cultures were grown to mid-exponential phase and then pooled. Cells were harvested by centrifugation (12,000 *g* for 10 min at 4°C; F15-8x50cy rotor and Sorvall Legend XTR centrifuge), washed twice in buffer (50 mM Tris [pH 7.2] and 10 mM $MgCl_2$), and resuspended to 3.8 mL in same buffer. All steps after growing the cultures were performed aerobically.

The resuspended cells were lysed with a French press (Glen Mills). The resuspended cells were transferred to a mini cell pressure cell and lysed at 110 MPa. Cell debris was removed by centrifugation (12,000 × *g* for 15 min at 4°C).

Cell extract was prepared three or more different times for each bacterial strain. It was stored at -80°C until use.

One 9-mL culture was grown to mid-exponential phase. Cells were removed from supernatant by centrifugation (12,000 × *g* for 10 min at 4°C). Supernatants were prepared three or more different times for each bacterial strain. They were stored at -20°C until use.

Enzymatic assays

We measured enzymatic activity of cell extracts as well as purified SCACT and SCS (see below). Assays were performed at room temperature following conditions in Table 1. Assay products were monitored by measuring absorbance with a Molecular Devices M3 spectrophotometer. The path length of assay mix in 96-well plates (0.288 cm) was determined using a solution of known absorbance (NADH). Activity was calculated over the time that absorbance increased (or decreased) linearly. Values were corrected by subtracting off the activity of controls (where water replaced cell extract, substrate, or cofactor). One unit of activity is defined as one µmol of product formed per min.

Several assays (for SCS, ACS, butyrate kinase [BK], AK) measured formation of hydroxamic acids. For these assays, we stopped the reaction at intervals by addition of 0.286 volumes of development solution (0.25 M $FeCl_3$, 2.5 M HCl, and 15% [w/v] trichloroacetic acid) (Fowler et al 2011). Afterwards, we held the assay mix for 5 to 60 min at room temperature, centrifuged it at 18,000 × *g* for 2 min, and then measured absorbance of the supernatant.

One assay measured formation of acetyl-CoA. The assay mix sometimes formed a precipitate when cell extract was added, and this interfered with measurements. The cause could not be determined, and we discarded results from any affected experiments.

One assay measured formation of ATP from ADP and other substrates. We found our source of ADP was contaminated with trace amounts of ATP, which interfered with measurements. To overcome this interference, the assay was pre-incubated for 80 min to allow all ATP to be consumed. Only after this pre-incubation was the sample (purified SCACT and SCS) added.

When available, purified enzymes were used as additional controls. Specifically, assays were spiked with purified enzyme at the end of the incubation. The enzymes were obtained from Megazyme. They were SCS from an unspecified prokaryotic source (product code E-SCOAS), ACS (AMP-forming) from *Bacillus subtilis* (product code E-ACSBS), PTA from *B. subtilis* (product code E-PTABS), and AK from an unspecified source (product code K-ACETRM).

We determined if activity was different from 0 using an analysis of variance (ANOVA). The statistical model was

$$Y_{ij} = \mu + T_i + \varepsilon_{ij}$$

where Y_{ij} is the observation, μ is the overall mean, T_i is the fixed effect of treatment (bacterial strain), and ε_{ij} is the residual error. For assays measuring acetyl-CoA or ATP formation, T_i refers to treatments with different combinations or substrates or enzymes. All analyses were conducted in R. The model was fit using the aov function. Least squares means, standard error of the mean, and degrees of freedom were taken from the emmeans package. *P*-values were calculated using a one-sided *t*-test.

For purified SCACT and SCS, we determined if activity was different from 0 using a one-sided *t*-test. We determined if SCACT and SCPCT activities were different with a paired, two-sided *t*-test.

Protein concentration in the cell extract and purified proteins was measured using a Pierce BCA protein assay kit (product 23227, Thermo Scientific).

Cloning of genes, production and purification of proteins

Cloning of genes. Genes encoding SCACT and SCS in *C. granulosum* were cloned into a plasmid vector. First, genes were PCR-amplified from cell extracts of *C. granulosum* with Q5 Hot Start High-Fidelity DNA polymerase (New England BioLabs M0493S) according to the instruction manual included in the kit. Briefly, cell extracts of *C. granulosum* were prepared as described above and used as the DNA template. Different primer pairs were designed, synthesized, and used to amplify genes encoding SCACT and SCS. For SCACT, forward and reverse primers were AAGAAGGAGATATACATATGTCAGAGCGGATTGCCAATGCAG and CAGTGGTGGTGGTGGTGGTGGCCCTGCTGCATGGTGCC. For SCS, they were AAGAAGGAGATATACATATGGACCTGTATGAATACCAAGCC and CAGTGGTGGTGGTGGTGGTGCTTCTTGAGCGACGCCATC. The primers for SCS amplified both α and β subunits as part of the same fragment. The amplified gene fragment was inserted into the expression plasmid pET-30a-Novagen plasmid (Sigma-Aldrich 69909) with the NEBuilder HiFi DNA Assembly Master Mix (New England BioLabs E2621S) according to the instruction manual. Briefly, the plasmid fragment was PCR-amplified using forward primer CACCACCACCACCACCAC and reverse primer CATATGTATATCTCCTTCTTAAAGTTAAACAAAATTATTTCTAGAGG. The amplified gene fragment was then incubated with plasmid fragment in the presence of the NEBuilder HiFi

DNA Assembly Master Mix at 50°C for 15 min. The mixture was used to transform *E. coli* 5-alpha competent cells (New England BioLabs C2987I). Positive colonies were selected by sequencing the assembled plasmid. Sanger sequencing verified that the assembled plasmids had the correct inserts. To enable later purification, the gene fragment was inserted upstream of a hexahistidine tag sequence.

Production and purification of proteins. We produced SCACT and SCS proteins from *C. granulosum* by using *E. coli* as the expression system. The assembled plasmid containing SCACT or SCS genes were chemically transformed into *E. coli* BL21(DE3)pLysS (Promega L1191). After transformation, *E. coli* cells were grown overnight in Terrific Broth (TB) medium with 30 µg/mL kanamycin and 34 µg/mL chloramphenicol. Next, 16 mL of this overnight culture was used to inoculate 0.4 L of TB medium with kanamycin and chloramphenicol. Cells from the 0.4-L culture were grown at 37°C to optical density (OD_{600}) of 0.6-0.7, and then the culture bottle was placed in ice water for 4 min with gentle shaking to decrease the culture temperature. After that, expression was induced with 0.1 mM IPTG (isopropyl ß-D-1-thiogalactopyranoside) for 10 hours at 23 to 25°C. Cells were harvested by centrifugation (12,000 × *g* for 5 min at 4°C), washed with buffer (50 mM Tris [pH 7.2] and 10 mM $MgCl_2$), then stored at -80°C.

Protein was purified from harvested cells using affinity chromatography. The frozen cells were lysed by thawing and vortex-mixing in 12 mL of binding buffer (see below). About 100 U of Pierce Universal Nuclease (product PI88700, Fisher) was added to the mixture and incubated on ice for 30 min with frequent vortexing. Then the mixture was centrifuged at 12,000 × *g* for 30 min at 4°C. The supernatant (12 mL) was filtered through 0.2-µm membrane, mixed with 1 mL 50% (v/v) slurry of Profinity IMAC Resin (Bio-Rad 1560131) for 1.5 hour at 4°C with gentle shaking, and transferred to a chromatography column (Bio-Rad 7311550). The column was

washed with 13 mL of binding buffer, 2 mL of washing buffer and 8 mL of elution buffer. After purification, protein was concentrated with Amicon Ultra-15 Centrifugal Filter (3 kDa cutoff). It was used immediately or stored at -80°C.

All buffers for affinity chromatography contained 50 mM Tris (pH 7.2) and 100 mM NaCl. Binding buffer additionally contained 10 mM imidazole (pH 8.0). Washing buffer contained either 50 mM imidazole (SCACT) or 10 mM imidazole (SCS). Elution buffer contained either 100 mM imidazole (SCACT) or 20 mM imidazole (SCS).

Purity was checked using SDS-PAGE (12% T, 29:1 acrylamide:bis-acrylamide) and staining with Coomassie Brilliant Blue G-250. The sequence of proteins was correct when determined with LC-MS/MS (below).

Untargeted proteomics

We used LC-MS/MS to identify if SCACT and SCS proteins were expressed in cell extracts of *C. granulosum*. We also used it to verify the amino acid sequence of recombinant SCACT and SCS.

Proteins in the sample (e.g., cell extract) were prepared for LC-MS/MS. Proteins were precipitated by adding 1000 µL of chilled 15% (w/v) trichloroacetic acid and 0.2% (w/v) dithiothreitol in acetone to 250 µL of sample and incubating at -80°C for 20 min. Incubation was continued at -20°C overnight. Proteins were harvested by centrifugation (21,100 *g* for 20 min at 4°C), air-dried to remove acetone, and then resuspended in 100 µL of 6 M urea in 50 mM ammonium bicarbonate (AMBIC). They were reduced with 2.5 µL of 200 mM dithiothreitol in AMBIC at 37°C for 30 min, then alkylated with 7.7 µL of 194.6 mM iodoacetamide in AMBIC for 30 min at room temperature in the dark. Alkylation was stopped by adding 20 µL of 200 mM dithiothreitol in AMBIC and incubating at room temperature for 10 min. Proteins were digested

to peptides with trypsin/Lys-C mix (Promega V5073) in a 1:25 enzyme:protein (w/w) ratio at 37°C for 4 hours. The trypsin in the mixture was activated by adding 550 µL of AMBIC and then continued for 16 h at 37°C. Digestion was terminated by adding trifluoroacetic acid (TFA) to a final concentration of 1% (v/v). Peptides were desalted with the Millipore C_{18} ZipTips (ZTC18S096). The tip was wet by slowly aspiring 10 µL of 100% (v/v) acetonitrile (ACN), discarding the solvent, and repeating once. The tip was then equilibrated by aspiring 10 µL of 0.1% TFA, discarding solvent, and repeating once. The digested sample containing 1% TFA was slowly aspirated in and out of the tip for 10 cycles to maximize binding. The tip was rinsed with 20 µL of 0.1% TFA/5% ACN and eluted by 100 µL of 0.1% (v/v) acetic acid/60% ACN. The eluted peptides were dried by vacuum centrifugation and resuspended in 40 µL of 0.1% TFA.

The resulting peptides were analyzed using LC-MS. The LC was a Dionex UltiMate 3000 RSLC system (Thermo Fisher) equipped with a PepMap C_{18} column (75 µm × 25 cm with 2 µm pore size; Thermo Scientific). The amount of peptide injected was 1 µg, the flow rate of mobile phase was 200 µL/min, and the column temperature was 40°C. The mobile phases were 0.1% formic acid in water (A) and 0.1% formic acid in acetonitrile (B), and they were used in a gradient elution. The concentration of B was decreased from 10% to 8% over 3 min, increased to 46% over 66 min, increased to 99% over 3 min, held at 99% for 2 min, decreased to 2% over 0.5 min, and held at 2% for 15 min.

The MS was an Orbitrap Fusion Lumos (Thermo Scientific). The instrument was operated in a data-dependent acquisition mode. Peptides were ionized and transferred to the mass analyzer with a spray voltage of 1.8 kV, radio frequency lens level of 46%, and ion transfer tube temperature of 275°C. Survey full-scan MS spectra were then acquired with *m/z* range of 375 to 1575, resolution of 60,000, automatic gain control (AGC) target of 4×10^5, and ion filling time of 50 ms.

After the survey scan, MS/MS was performed on the most abundant precursors with charge state between 2 and 3. Precursors were isolated using a 3-s cycle with window width of 1.2 *m/z*. Fragmentation of precursors was done by collisionally induced dissociation (CID) with normalized collision energy of 30%, and the resulting fragments were detected using the rapid rate in the ion trap. MS/MS spectra were acquired with AGC target of 5×10^3, ion filling time of 35 ms, and dynamic exclusion time of 50 s with 10 ppm mass window.

Peptides and proteins were identified from LC-MS/MS data using X!TandemPipeline (Langella et al 2017). The version of X! Tandem (Craig and Beavis 2004) used was Alanine. The sequence database contained all proteins in *C. granulosum* predicted by IMG/M (Chen et al 2019). Parameters were set according to Dataset S4.

Analysis of supernatant and media

Glucose concentration was measured with the glucose oxidase-peroxidase method (Karkalas 1985). To overcome interference from cysteine, 2 moles *N*-ethylmaleimide was added per mole cysteine in samples (Hackmann et al 2013a, Haugaard et al 1981).

Acetate was measured enzymatically. Before analysis, supernatant was heated at 100°C for 10 min to inactivate enzymes. The assay mix contained 150 mM triethanolamine (pH 8.4), 3 mM $MgCl_2$, 10 mM L-malate, 1 mM NAD, 5 mM ATP, 0.4 mM CoA, 1.8 U/mL malate dehydrogenase (product code M1567-5KU, Sigma), 1.4 U/mL citrate synthase (product code C3260-200UN, Sigma), and 0.5 U/mL ACS (AMP-forming) (product code E-ACSBS, Megazyme). Supernatant was replaced with water as a control. Reduced NAD was measured, and acetyl-CoA formed was calculated as above.

Formate was measured using an assay mix containing 50 mM KPO_4 buffer (pH 7.6), 4 mM NAD, and 0.5 U/mL formate dehydrogenase (product code E-FDHCB, Megazyme). Reduced NAD was measured. Whereas most assays were performed in 96-well plates, this assay was performed in microcuvettes (product code 13-878-122, Fisher). Absorbance was measured with a Thermo Scientific Genesys 20 spectrophotometer.

Succinate, L-lactate, and D-lactate were measured using commercial kits (product code 10176281035 and 11112821035, R-Biopharm).

Other fermentation products (propionate, butyrate, isobutyrate, isovalerate) were measured using gas chromatography. Samples were prepared by combining supernatant (350 µL), 10 mM 2-ethylbutyric acid (50 µL), formic acid (100 µL), and methanol (500 µL). The gas chromatograph was a Trace 1300 equipped with AI 1310 autosampler, split/splitless injector, and flame ionization detector (FID) (Thermo Scientific). The column was a Trace GOLD-WaxMS (30 m × 0.32 mm i.d. coated with 1 µm film thickness; Thermo Scientific). N_2 (2.5 mL/min) was the carrier gas. The injection was performed in splitless mode (1 min splitless time. The front inlet had a temperature of 230°C. The initial oven temperature was 45°C, maintained for 0.5 min, raised to 235°C at 25°C/min, and finally held at 235°C for 2 min. The FID had a temperature of 240°C, and flow rates for air, hydrogen, and nitrogen of 350, 35, and 40 mL/min. The injected sample volume was 1 µL and the total run time for each analysis was 10.1 min. Data handling was carried out with Chromeleon Chromatography Data System software (Thermo Scientific). The amount of glucose consumed was calculated from concentrations measured in the media and supernatant. The amount of fermentation products formed was calculated similarly. Least squares means and standard error of the mean were calculated as for enzymatic assays.

Annotation of SCACT and SCS genes and homologs

Annotation of SCACT genes and homologs. We annotated SCACT genes and homologs with KEGG Orthology (KO) (Kanehisa et al 2017), TIGRFAM (Haft et al 2013), Pfam (El-Gebali et al 2019), or COG (Galperin et al 2015) IDs. For TIGRFAM and Pfam, annotation was done using HMMER v. 3.3 and hmmscan on the HMMER webserver (Potter et al 2018). For KEGG, annotation was done with KofamKOALA (Aramaki et al 2020). For COG, annotation was done with NCBI conserved domain search (Lu et al 2020) with COG v.1.0.

Genes were annotated with IDs producing significant bit scores (as defined by the database). For Pfam, outcompeted hits were not kept. For COG, only specific hits were kept.

We also annotated these genes with pHMMs built in this work. Genes were annotated by using pHMMs along with HMMER and hmmsearch (Eddy 2011). For SCACT, a significant bit score was ≥700. For BCACT, it was ≥550.

The pHMMs were built using HMMER and hmmbuild. Protein sequences included are indicated in Figure 10 and Figure 11, and they were aligned with Clustal Omega (Bodenhofer et al 2015, Sievers et al 2011) beforehand.

From annotations, we predicted if genes had SCACT or other enzymatic activities. Predicted activity was compared against that observed experimentally. The accuracy of prediction was calculated as (TP+TN)/(TP+TN+FP+FN), where TP = true positive, TN = true negative, FP = false positive, and FN = false negative.

Annotation of SCS genes and homologs. We annotated SCS genes and homologs following the same process as for SCACT. For SCS, a significant bit score was ≥340 for the α subunit and ≥190 for the β subunit. For ACS, it was ≥550 and ≥270 for the α and β subunits. Some

SCS homologs had α and β subunits that were fused (part of the same protein). To include these subunits in pHMMs, we had to identify the boundaries of the subunits. We did this by using a separate pHMM built with sequences of non-fused subunits.

Gene searches in bacterial genome sequences and construction of phylogenetic trees

Gene searches in bacterial genome sequences. We searched genomes of bacteria and archaea for genes encoding pathways of acetate formation. We used a set of genomes assembled in the reference (Hackmann and Zhang 2021). This set includes genomes for 2,925 type strains of bacteria and archaea, including 590 strains that form acetate during fermentation. See Dataset S1 and reference (Hackmann and Zhang 2021)for details.

We performed searches using IMG/M database (Chen et al 2019), the IMG/M genome ID for each genome (Dataset S1), and KEGG Orthology (KO) ID for each gene (Kanehisa et al 2017) (Dataset S5). The locus tags found by these searches are in Dataset S1.

We searched for acetyl-CoA transferase genes (SCACT and BCACT) using a different method. We searched genomes for these genes first using IMG/M and pfam IDs (El-Gebali et al 2019) (Dataset S5). The pfam ID was used because it was the most sensitive; all known acetate-CoA transferase genes were annotated with pfam IDs. We downloaded all sequences, then annotated them as BCACT or SCACT with pHMMs described above. A more direct approach would have been to search IMG/M using the pHMMs, but IMG/M does not support this type of search.

We searched for acyl-CoA transferase genes (SCS and ACS) similarly to acetyl-CoA transferase genes. Instead of pfam IDs, we used COGs IDs to search IMG/M (Dataset S5). We annotated them as SCS or ACS with pHMMs.

Following our previous work (Hackmann et al 2017), we considered that a pathway was encoded if genes for all enzymes was found. If an enzyme had multiple genes (subunits), all genes for that enzyme had to be found. If a gene had multiple domains, database IDs for all domains had to be found, also. If a pathway could be catalyzed by multiple isozymes, genes for only one isozyme had to be found.

Construction of phylogenetic trees. We constructed a phylogenetic tree of the genomes described above. The construction used sequences of 14 ribosomal proteins and was done as in reference (Hackmann and Zhang 2021). Briefly, we downloaded amino acid sequences of the ribosomal proteins from IMG/M (Chen et al 2019). We aligned sequences and concatenated these sequences in R. We then used aligned and concatenated sequences to create a phylogenetic tree with RAxML (Stamatakis 2014). Branch lengths of the consensus tree were calculated using phytools (Revell 2012). The consensus tree was visualized using ggtree (Yu et al 2017). Because no archaea encoded the SCACT/SCS pathway, they were not included in the final visualization of the tree. A total of 2,464 genomes were included in this visualization.

We constructed phylogenetic trees of SCACT and SCS homologs using the same approach as for genome sequences. For SCS, we concatenated α and β subunits (after alignment).

Results

C. granulosum forms acetate using the SCACT/SCS pathway

We investigated if *C. granulosum* uses the SCACT/SCS pathway to form acetate anaerobically because its genome encodes this pathway, but not others in Figure 3. Other propionibacteria and bacteria were included for comparison.

To confirm that *C. granulosum* forms acetate during fermentation, we measured the concentration of acetate in the culture supernatant when it grew on glucose. Acetate was produced as a major end product of fermentation by *C. granulosum* and other propionibacteria (Figure 4A). The only product produced in larger quantities was propionate (Table 2).

To determine if the SCACT/SCS pathway was responsible for forming this acetate, we measured activities of the appropriate enzymes (Figure 4B-E). High activity of both SCACT and SCS were observed in cell extracts of *C. granulosum*. No activity of enzymes from any other pathway to form acetate was observed. These measurements suggest that *C. granulosum* forms acetate exclusively by the SCACT/SCS pathway (Figure 4F). Similar measurements suggest two other propionibacteria (*C. acnes*, *Acidipropionibacterium acidipropionici*) use this same pathway, whereas a third (*Propionibacterium freudenreichii*) does not.

To support the accuracy of these measurements, multiple controls were included. When measuring activity of each enzyme, we included one or more bacteria that displayed activity. This supports that our experimental conditions were appropriate to detect activity—i.e., we would have detected activity were any present. Additionally, purified enzyme was spiked to cell extracts at the end of experiments (see Materials and Methods). Activity was observed after spiking (data not shown). This again supports that our conditions were appropriate to detect activity.

We further supported our enzymatic measurements by analyzing which enzymes each bacterium encoded (Figure 4B-E, Dataset S1). In general, bacteria displayed high activity only when they encoded the appropriate enzymes. One exception was for acetyl-CoA synthetase (ACS; EC 6.2.1.13, EC 6.2.1.1). One bacterium (*P. freudenreichii*) did not encode ACS, but it still displayed high activity. This is due to interference from AK and PTA activity; our assay cannot distinguish it from ACS activity. Further, two bacteria (*A. acidipropionici*, *P. freudenreichii*)

encoded ACS, but they did not display high activity. The absence of activity appears genuine, given we included appropriate controls (see above).

One last experiment was performed to determine if *C. granulosum* forms acetate through the SCACT/SCS pathway. If *C. granulosum* uses this pathway, it should be able to form acetyl-CoA from acetate, succinate, ATP, and CoA. Indeed, cell extracts formed acetyl-CoA from these four substrates (Figure 5). No acetyl-CoA was formed if any of the four substrates was missing, as expected. In sum, enzymatic and genomic evidence supports that *C. granulosum* forms acetate through the SCACT/SCS pathway.

C. granulosum encodes the SCACT/SCS pathway with bacterial gene homologs

We identified the genes that encode the SCACT/SCS pathway in *C. granulosum*. We did this not only to confirm that *C. granulosum* uses this pathway, but also to determine if its pathway is bacterial in origin or not.

We identified the genes for SCACT and SCS using genomics, proteomics, and enzymatic assays. We searched the genome sequence of *C. granulosum*, and we found one candidate gene for SCACT (Figure 6A). By performing untargeted proteomics, we confirmed this gene was expressed (part of the bacterium's proteome) (Figure 6B). We expressed the protein recombinantly in *E. coli*, and it had SCACT activity (Figure 6C). This demonstrates this gene encodes SCACT in *C. granulosum*. Following a similar process, we found the genes that encode SCS (Figure 7A-C).

We compared SCACT and SCS in *C. granulosum* to all known proteins with SCACT and SCS activity. For SCACT, this included 19 proteins described in 15 publications (see Dataset S2). For SCS, it included 28 proteins described in 22 publications (see Dataset S3). The sequence of SCACT and SCS in *C. granulosum* were closely related to bacterial, not eukaryotic, homologs

(Figure 6D and 7D). This suggests SCACT/SCS pathway in *C. granulosum* is bacterial, not eukaryotic, in origin.

Purified SCACT and SCS form a functional pathway

Based on their individual activities, SCACT and SCS together should form the pathway illustrated in Figure 3. To determine if they indeed form this pathway, we determined if they form acetyl-CoA from acetate, succinate, ATP, and CoA. This experiment was similar to that performed in cell extracts, except it used purified SCACT and SCS. We found that the enzymes together formed acetyl-CoA from these four substrates (Figure 8A). When any enzyme or substrate was missing, no acetyl-CoA was formed (Figure 8A). These results are consistent with the pathway in Figure 3.

Next, we determined if the enzymes could form ATP from acetyl-CoA, succinate, and ADP. This experiment was not possible in cell extracts because of high ATPase activity (~100-fold higher than the expected rate of ATP formation). We found the purified enzymes together formed ATP when all three substrates were present (Figure 8B). Little or no ATP was formed when an enzyme or substrate was missing (Figure 8B). In sum, SCACT and SCS in *C. granulosum* together form a functional pathway as illustrated in Figure 3. This SCACT/SCS pathway forms ATP, representing a new way for bacteria to conserve energy during fermentation.

SCACT also serves a role in producing propionate

In many organisms, SCACT forms not only acetate from acetyl-CoA, but also propionate from propionyl-CoA (Allen et al 1964, Fleck and Brock 2008, Fleck and Brock 2009, Sasikaran et al 2014, Schulman and Wood 1975, van Grinsven et al 2009). Specifically, it can act as a succinyl-CoA:propionate CoA-transferase (SCPCT; EC 2.8.3.27). This activity is important because it can form propionate during fermentation (Allen et al 1964, van Grinsven et al 2009). Indeed, in some

eukaryotes, SCACT is thought to be responsible for forming both acetate and propionate (Muller et al 2012, van Grinsven et al 2009). We determined if SCACT played a similar role in *C. granulosum*.

We measured SCPCT activity in cell extracts and purified protein. In cell extracts of *C. granulosum*, we found SCPCT activity was 0.09171 (0.012 SEM) U/mg. This was nearly equal to SCACT activity [0.0846 (0.0043 SEM) U/mg], and the activities did not differ statistically (P = 0.562). We continued measurements with purified protein, and again found activities of SCPCT and SCACT were nearly equal (Figure 6C) (P = 0.246). The magnitude of SCPCT and SCACT activities is similar to that of purified enzyme of *P. freudenreichii* (Schulman and Wood 1975). The enzyme of *P. freudenreichii* has been shown to be responsible for forming propionate during fermentation (Allen et al 1964, Deborde et al 1999, Schulman and Wood 1975). These findings suggest that SCACT in *C. granulosum* is important in forming both acetate and propionate, just as in some eukaryotes.

Several bacteria encode the SCACT/SCS pathway in their genome

We found that *C. granulosum* encodes the SCACT/SCS pathway by performing a preliminary search of bacterial genomes. To determine how many other bacteria encode this pathway, we searched for SCACT and SCS genes in 2,733 genomes of bacteria (Dataset S1). These genomes represent all type strains in *Bergey's Manual of Systematics of Archaea and Bacteria* (Whitman 2020) with an available genome sequence [see reference (Hackmann and Zhang 2021)]. We focused in particular on 585 genomes from bacteria experimentally observed to form acetate during fermentation (Hackmann and Zhang 2021). The profile hidden Markov models (pHMMs) developed in this work (see below) were used to search for these genes.

With this search, we found 36 type strains that encode the SCACT/SCS pathway and form acetate during fermentation (Figure 9, Dataset S1). These strains belong to 5 different phyla (*Acidobacteria*, *Actinobacteria*, *Bacteroidetes*, *Firmicutes*, *Proteobacteria*). This suggests that many different bacteria could use the SCACT/SCS pathway to form acetate.

We did not find any archaea that encoded the SCACT/SCS pathway (Dataset S1). Instead, all archaea encoded the ACS (ADP-forming) pathway. With the exception of archaea, the SCACT/SCS pathway is widely distributed across the tree of life.

SCACT and SCS genes can be accurately identified

When we first searched bacterial genomes, we failed to find many known SCACT and SCS genes. Databases had annotated many genes with the wrong enzymatic activity, or no activity at all (see Dataset S2 and Dataset S3). Accordingly, we developed our own method, based on pHMMs, to identify genes for these enzymes.

We built and tested pHMMs using 103 biochemically-characterized enzymes from 64 publications. To build a pHMM for SCACT, we used sequences of 19 proteins with SCACT activity (Dataset S2). To test it, we used these proteins, plus 32 others that are close homologs but with no SCACT activity (Dataset S2). A similar process for SCS was done by using 28 proteins with SCS activity and 24 close homologs (Dataset S3). The proteins, phylogenetic trees, and pHMMs are in Figure 10 and Figure 11.

We tested the pHMM for SCACT, and it accurately predicted which proteins had SCACT activity (Figure 12A, Dataset S2). Its accuracy also exceeded that of existing databases (Figure 12A), including TIGRFAM (Haft et al 2013), KEGG (Kanehisa et al 2017), and COG (Galperin et al 2015). We found similarly high accuracy for SCS (Figure 12A, Dataset S3).

With the same set of 103 enzymes, we discovered that we could build pHHMs for butyryl-CoA:acetate CoA-transferase (BCACT; EC 2.8.3.8) and ACS (ADP) (EC 6.2.1.13), also. These pHMMs gave more accurate predictions than did existing databases (Figure 12B, Dataset S2, Dataset S3).

We built pHMMs using all protein sequences available, and some of the same sequences were later used to test their accuracy. Because building and testing were not independent, accuracy may be overstated. To see if this was a problem, we performed 10-fold cross validation, in which building and testing are independent. To do this, we built pHMMs with 90% of the available sequences. We then tested accuracy with the 10% of sequences we left out. This process was repeated 10 times. Accuracy was still high (90.2% for SCACT, 90.3% for SCS, and 92.2% for BCACT, 88.5% for ACS [ADP]). This supports that our pHMMs would be accurate when tested with new sequences (not used for building).

In sum, we developed a method that accurately identifies proteins with SCACT or SCS activity. With this method, we could confidently search for SCACT and SCS genes in bacterial genomes (see Figure 9). This method has uses beyond the current work and can improve annotation of genes in databases.

Discussion

We have found a biochemical pathway for forming acetate and synthesizing ATP that was previously unrecognized in bacteria. Pathways for forming acetate during fermentation have been studied for over 80 years (Lipmann 1939), and so our discovery of the SCACT/SCS pathway is surprising. Nonetheless, it appears to be a common pathway, given it is encoded by 6% of all bacteria that form acetate during fermentation.

The SCACT/SCS pathway has been thought to be exclusively eukaryotic (Muller et al 2012). Our study with *C. granulosum* shows that bacteria can have the pathway, but with bacterial gene homologs. One gene homolog (SCS) originates from the TCA cycle (Thauer 1988). The other (SCACT) is used to form propionate during fermentation (Allen et al 1964, Deborde et al 1999, Schulman and Wood 1975), or it is part of a modified TCA cycle (Kwong et al 2017, Mullins et al 2008, Thauer 1988). In this way, the pathway may have been easy to evolve, and it is unsurprising bacteria would have it.

We focused on *C. granulosum* in this study because it is one bacterium that encodes only the SCACT/SCS pathway. Earlier, we had performed experiments with *Selenomonas ruminantium* HD4, a rumen bacterium that encodes only this pathway (Hackmann et al 2017) for acetate formation. In those experiments, we could detect SCS, but not SCACT (McCourt 2019). The reason is unknown but may be because SCACT was degraded to an acetyl-CoA hydrolase, an enzyme that we did detect. The present experiments confirm that the SCACT/SCS pathway is used in bacteria, even as it leaves the identity of the pathway in *S. ruminantium* unknown.

Our finding of the SCACT/SCS pathway in bacteria is important for two practical reasons. First, it is important to manipulating yield of fermentation products through genetic engineering. One study tried to engineer *A. acidipropionici* to produce less acetate (more propionate), but it focused on deleting AK (Suwannakham et al 2006). Our study suggests that enzymes of the SCACT/SCS pathway would be more appropriate targets. Indeed, other studies have decreased acetate yield by deleting SCACT, albeit in bacteria not growing by fermentation (Litsanov et al 2012, Yasuda et al 2007).

Second, our finding is important for predicting metabolic pathways from genome sequences. These predictions are used to determine the metabolic capabilities of bacteria,

especially ones not cultured in the lab. When studies predict metabolic pathways for fermentation, most search for enzymes of the PTA/AK pathway only (Magnusdottir et al 2017). Some also search for enzymes of the ACS (ADP) pathway (Wrighton et al 2012). The current study shows the importance of looking for enzymes of the SCACT/SCS pathway. Otherwise, studies will overlook pathways (or bacteria) that can form acetate.

In sum, our work shows that the SCACT/SCS pathway is important to many fermentative organisms. It suggests there is still much to learn about fermentation, despite being one of the best studied types of metabolism.

Table 1. Conditions used to measure enzymatic activity

Enzyme or reaction	Reference	Assay components	Product measured (wavelength)	Controls
Succinyl-CoA: acetate CoA-transferase of *C. granulosum* (SCACT; EC 2.8.3.18)	After (Hilpert et al 1984)	50 mM KPO_4 buffer (pH 8.0), 100 mM KCl, 1.5 mM 5,5'-dithiobis-(2-nitrobenzoic acid), 30 U/mL phosphotransacetylase[1], 300 mM potassium acetate (pH 7.0), 1.5 mM succinyl-CoA	5-thio-2-nitrobenzoic acid (412 nm)[2]	Succinyl-CoA, acetate, or cell extract replaced with water
Succinyl-CoA:acetate CoA-transferase of other strains (SCACT; EC 2.8.3.18)	(Schulman and Wood 1975)	100 mM Tris (pH 8.0), 0.6 mM succinyl-CoA, 60 mM potassium acetate (pH 7.0), 0.4 mM L-malate, 1 mM NAD, 2.84 mM KPO_4 (pH 6.8), 8.8 U/mL malate dehydrogenase[3], 1.4 U/mL citrate synthase[4]	Reduced NAD (340 nm)[5]	Succinyl-CoA, acetate, or cell extract replaced with water
Succinyl-CoA:propionate CoA-transferase (SCPCT; EC 2.8.3.-)	After (Hilpert et al 1984)	50 mM KPO_4 buffer (pH 8.0), 100 mM KCl, 1.5 mM 5,5'-dithiobis-(2-nitrobenzoic acid), 30 U/mL phosphotransacetylase[1], 300 mM potassium propionate (pH 7.0), 1.5 mM succinyl-CoA	5-thio-2-nitrobenzoic acid (412 nm)[2]	Succinyl-CoA, propionate or acetate, or cell extract replaced with water
Succinyl-CoA synthetase (SCS; EC 6.2.1.5)	(Dijkhuizen et al 1980)	50 mM Tris (pH 7.2), 10 mM $MgCl_2$, 10 mM succinate (pH 7.0), 1.2 mM ATP, 0.4 mM CoA, 200 mM hydroxylamine (pH 7.0)	Succino-hydroxamate (540 nm)[6]	Succinate replaced with water
Acetyl-CoA synthetase (ACS) (EC 6.2.1.13, EC 6.2.1.1)	(Rado and Hoch 1973)	50 mM Tris (pH 7.2), 10 mM $MgCl_2$, 40 mM potassium acetate (pH 7.0), 1.2 mM ATP, 0.4 mM CoA, 200 mM hydroxylamine (pH 7.0)	Aceto-hydroxamate (540 nm)[7]	Potassium acetate replaced with water
Phosphotransbutyrylase (PTB; EC 2.3.1.19)	After (Rado and Hoch 1973)	76 mM Tris (pH 7.6), 10 mM NH_4Cl, 2.5 mM butyryl phosphate, 0.25 mM CoA	Butyryl-CoA (233 nm)[8]	Butyryl phosphate replaced with water

CONTINUED

Table 1: CONTINUED

Butyrate kinase (BK; EC 2.7.2.7)	After (Dijkhuizen et al 1980)	50 mM Tris (pH 7.2), 10 mM $MgCl_2$, 200 mM butyrate (pH 7.0), 5 mM ATP, 200 mM hydroxylamine (pH 7.0)	Butyryl-hydroxamate (540 nm)[7]	butyrate replaced with water
Phosphotransacetylase (PTA; EC 2.3.1.8)	(Rado and Hoch 1973)	76 mM Tris (pH 7.6), 10 mM NH_4Cl, 5 mM acetyl phosphate, 0.25 mM CoA	Acetyl-CoA (233 nm)[8]	Acetyl phosphate replaced with water
Acetate kinase (AK; EC 2.7.2.1)	After (Dijkhuizen et al 1980)	50 mM Tris (pH 7.2), 10 mM $MgCl_2$, 100 mM potassium acetate (pH 7.0), 5 mM ATP, 200 mM hydroxylamine (pH 7.0)	Aceto-hydroxamate (540 nm)[7]	Potassium acetate replaced with water
Acetyl-CoA formation of cell extract	After (Schulman and Wood 1975)	100 mM Tris (pH 8.0), 10 mM $MgCl_2$, 2.84 mM KPO_4 (pH 6.8), 1 mM NAD, 4 mM L-malate, 8.8 U/mL malate dehydrogenase, 1.4 U/mL citrate synthase, 30 mM succinate (pH 7.0), 60 mM potassium acetate (pH 7.0), 5 mM ATP, and 2 mM CoA	Reduced NAD (340 nm)[5]	None
Acetyl-CoA formation of purified SCACT and SCS	After (Schulman and Wood 1975)	100 mM Tris (pH 8.0), 2.84 mM KPO_4 (pH 6.8), 10 mM $MgCl_2$, 4 mM L-malate, 1 mM NAD, 8.8 U/mL malate dehydrogenase, 1.4 U/mL citrate synthase, 5 mM succinate (pH 7.0), 10 mM potassium acetate (pH 7.0), 5 mM ATP, and 0.4 mM CoA	Reduced NAD (340 nm)[5]	None
ATP formation	After (Lamprecht and Trauschold 1974)	38 mM triethanolamine (pH 7.4), 3 mM KPO_4 (pH 6.8), 6.6 mM $MgCl_2$, 2 mM NADP, 1 mM acetyl-CoA, 25 mM succinate (pH 7.0), 5 mM ADP, 50 mM glucose, 2 U/mL glucose-6-phosphate dehydrogenase[9], and 5.4 U/mL hexokinase[10]	Reduced NADPH (340 nm)[5]	None

[1]From *Bacillus subtilis* (Megazyme E-PTABS)

[2]Extinction coefficient 14,150 M^{-1} cm^{-1} (Eyer et al 2003)

[3]From porcine heart (Sigma M1567-5KU)

[4]From porcine heart (Sigma C3260-200UN)

[5]Extinction coefficient of 6,220 M^{-1} cm^{-1}

[6]Succinic anhydride was used as a standard and prepared in 50 mM Tris (pH 7.2), 10 mM $MgCl_2$, and 200 mM hydroxylamine (Lipmann and Tuttle 1945)

[7]Acetyl phosphate was used as a standard and prepared in 50 mM Tris (pH 7.2), 10 mM $MgCl_2$, and 200 mM hydroxylamine (pH 7.0)

[8]Extinction coefficient of 4,440 M^{-1} cm^{-1} (value for S-acetyl-*N*-succinylcysteamine) (Michal and Bergmeyer 1983)

[9]From *Saccharomyces cerevisiae* (Sigma G7877-250UN)

[10]From *Saccharomyces cerevisiae* (Sigma H4502-1KU)

Table 2. Net change in concentrations of glucose and fermentation products in different propionibacteria cultures

	Strain[1]				
Product[2]	*C. gran.*	*C. acnes*	*A. acid.*	*P. freud.*	SEM[3]
	mmol/L media				
Glucose	-6.75	-9.04	-9.03	-6.18	0.34
Formate	-0.25	-0.18	-0.18	-0.18	0.01
Acetate	4.38	2.77	3.53	4.25	0.07
Propionate	9.29	6.99	10.03	7.37	0.15
Butyrate	-0.02	0.00	-0.03	-0.02	0.02
Isobutyrate	0.58	0.44	0.63	0.77	0.06
Isovalerate	0.00	0.03	-0.02	-0.01	0.02
D-Lactate	-0.48	-0.20	-0.69	-0.74	0.01
L-Lactate	-1.03	-0.38	-0.98	-1.03	0.03
Succinate	2.37	1.00	0.56	2.76	0.06

[1]Abbreviations: *A. acid.*, *Acidipropionibacterium acidipropionici*; *C. acnes*, *Cutibacterium acnes*; *C. gran.*, *Cutibacterium granulosum*; and *P. freud*, *Propionibacterium freudenreichii*.

[2]Products with negative values were consumed from the media

[3]Standard error of the mean

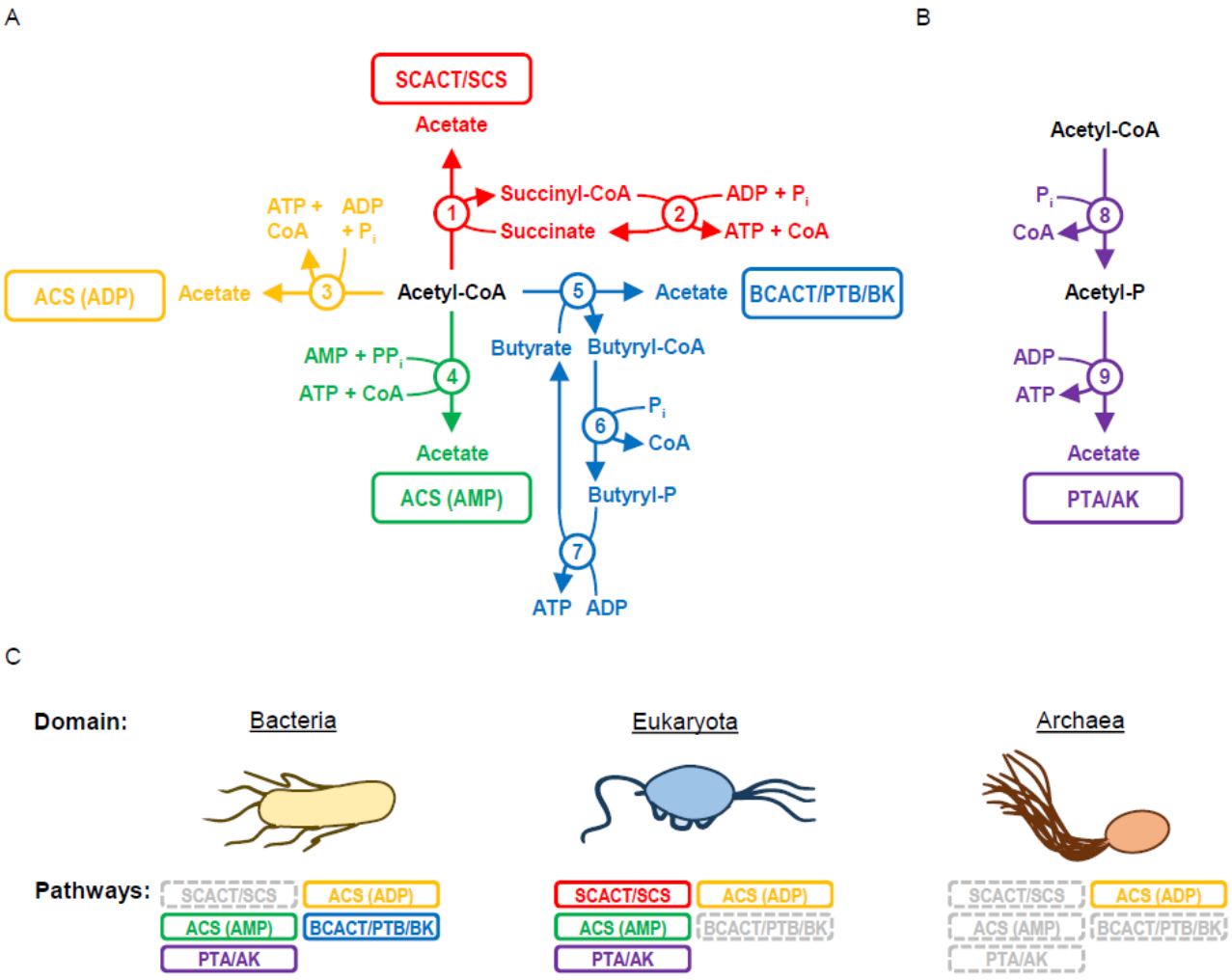

Figure 3. Pathways for forming acetate during fermentation in living organisms. Bacteria use many pathways to form acetate and ATP during fermentation, but none are reported to use the SCACT/SCS pathway. Pathways for forming acetate and ATP from (A) acetyl-CoA and (B) acetyl-CoA or acetyl phosphate. (C) Reported use of pathways by domain. Pathways that form acetate without ATP (e.g., acetyl-CoA hydrolase; EC 3.1.2.1) are not included. The PTA/AK pathway can use both PTA and AK, or it can use AK alone. Enzymes: 1, succinyl-CoA:acetate CoA-transferase (SCACT; EC 2.8.3.18); 2, succinyl-CoA synthetase (ADP-forming) (SCS; EC 6.2.1.5); 3, acetyl-CoA synthetase (ADP-forming) (ACS [ADP]; EC 6.2.1.13); 4, acetyl-CoA synthetase (ACS [AMP]; EC 6.2.1.1); 5, butyryl-CoA:acetate CoA-transferase (BCACT; EC

2.8.3.8); 6, phosphotransbutyrylase (PTB; EC 2.3.1.19); 7, butyrate kinase (BK; EC 2.7.2.7); 8, phosphotransacetylase (PTA; EC 2.3.1.8); and 9, acetate kinase (AK; EC 2.7.2.1). For bacteria, see ref. (Schmidt and Schonheit 2013) for ACS (ADP) pathway, ref. (James et al 2016) for ACS (AMP) pathway, ref. (Buckel and Barker 1974, Buckel 2001) for BCACT/PTB/BK pathway, and ref. (Thauer et al 1977) for PTA/AK pathway. For eukaryotes, see ref. (Lindmark 1976, Riviere et al 2004) for SCACT/SCS pathway, ref. (Reeves et al 1977, Sanchez et al 2000) for ACS (ADP) pathway, ref. (Takasaki et al 2004) for ACS (AMP) pathway, and ref. (Atteia et al 2006, Kreuzberg et al 1987) for PTA/AK pathway. For archaea, see ref. (Musfeldt et al 1999, Schafer and Schonheit 1991) see ref. for ACS (ADP) pathway. Abbreviations: ACS (ADP), acetyl-CoA synthetase (ADP-forming); ACS (AMP), acetyl-CoA synthetase; AK, acetate kinase; BCACT, butyryl-CoA:acetate CoA-transferase; BK, butyrate kinase; CoA, coenzyme A; P, phosphate; P_i, inorganic phosphate; PP_i, pyrophosphate; PTA, phosphotransacetylase; PTB, phosphotransbutyrylase; SCACT**,** succinyl-CoA:acetate CoA-transferase; and SCS, succinyl-CoA synthetase (ADP-forming).

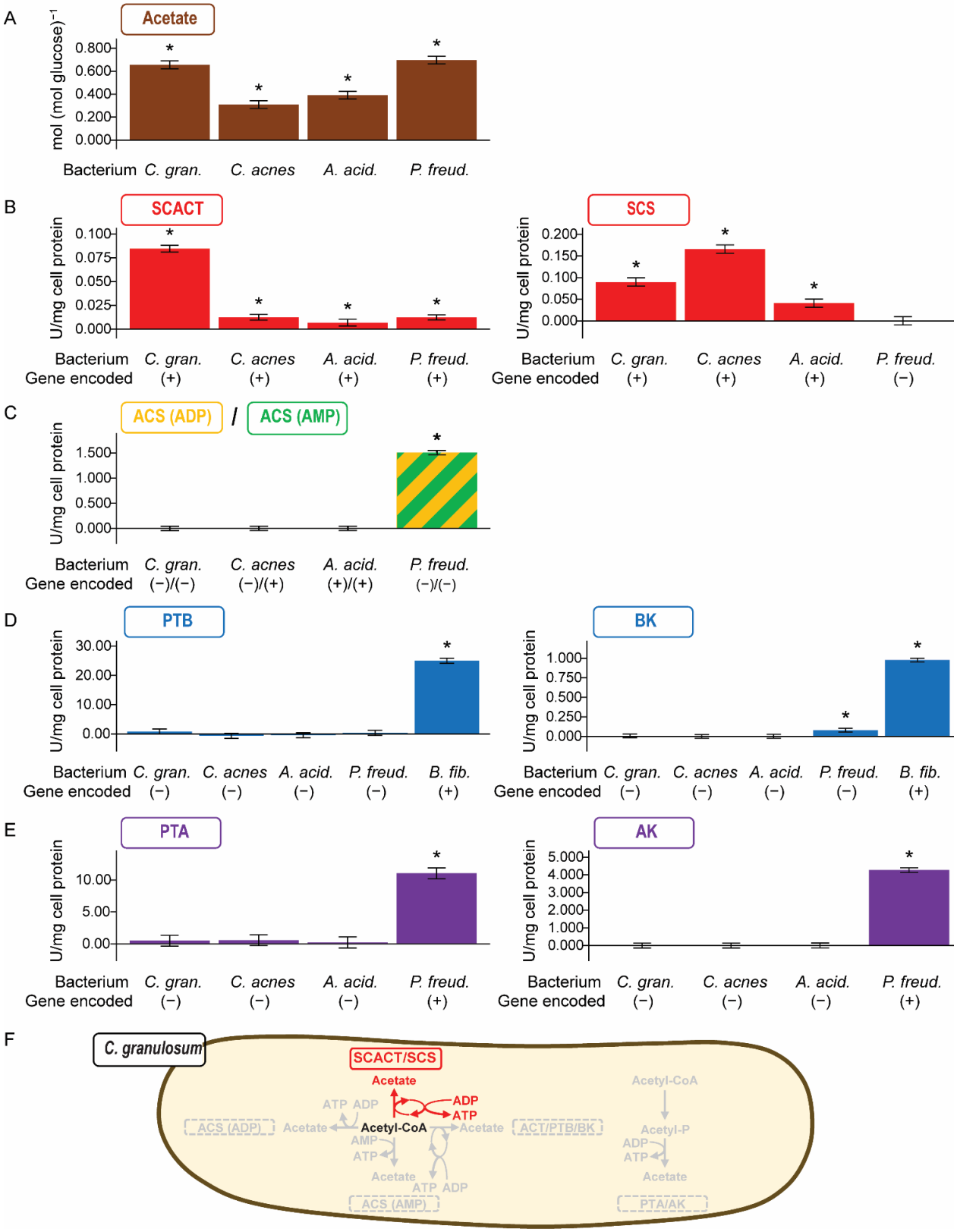
A
Acetate
mol (mol glucose)$^{-1}$
0.800
0.600
0.400
0.200
0.000
Bacterium C. gran. C. acnes A. acid. P. freud.
B
SCACT
U/mg cell protein
0.100
0.075
0.050
0.025
0.000
Bacterium C. gran. C. acnes A. acid. P. freud.
Gene encoded (+) (+) (+) (+)
SCS
U/mg cell protein
0.200
0.150
0.100
0.050
0.000
Bacterium C. gran. C. acnes A. acid. P. freud.
Gene encoded (+) (+) (+) (−)
C
ACS (ADP) / ACS (AMP)
U/mg cell protein
1.500
1.000
0.500
0.000
Bacterium C. gran. C. acnes A. acid. P. freud.
Gene encoded (−)/(−) (−)/(+) (+)/(+) (−)/(−)
D
PTB
U/mg cell protein
30.00
20.00
10.00
0.00
Bacterium C. gran. C. acnes A. acid. P. freud. B. fib.
Gene encoded (−) (−) (−) (−) (+)
BK
U/mg cell protein
1.000
0.750
0.500
0.250
0.000
Bacterium C. gran. C. acnes A. acid. P. freud. B. fib.
Gene encoded (−) (−) (−) (−) (+)
E
PTA
U/mg cell protein
10.00
5.00
0.00
Bacterium C. gran. C. acnes A. acid. P. freud.
Gene encoded (−) (−) (−) (+)
AK
U/mg cell protein
5.000
4.000
3.000
2.000
1.000
0.000
Bacterium C. gran. C. acnes A. acid. P. freud.
Gene encoded (−) (−) (−) (+)
F
C. granulosum
SCACT/SCS
Acetate
ATP ADP
ADP
ATP
ACS (ADP)
Acetate
Acetyl-CoA
Acetate
ACT/PTB/BK
AMP
ATP
Acetate
ATP ADP
ACS (AMP)
Acetyl-CoA
Acetyl-P
ADP
ATP
Acetate
PTA/AK

Figure 4. Acetate production and enzymatic activities of various acetate-forming pathways in propionibacteria. The bacterium *C. granulosum* forms acetate using the SCACT/SCS pathway. Other propionibacteria are included for comparison. (A) Acetate formed during glucose fermentation. (B to E) Activity of enzymes in different pathways for forming acetate. (F) Summary of pathways in *C. granulosum*. In panel C, the assay cannot distinguish between the enzymes of ACS (ADP) and ACS (AMP) pathways. In panel D, a nonpropionibacterium (*Butyrivibrio fibrisolvens*) was included as a control. No attempt was made to measure the activity of BCACT in the BCACT/PTB/BK pathway. Results are means ± standard error of at least 3 biological replicates (batches of cell extract prepared from independent cultures). Means different from 0 ($P < 0.05$) are marked with an asterisk. Abbreviations for enzymes: ACS (ADP), acetyl-CoA synthetase (ADP-forming); ACS (AMP), acetyl-CoA synthetase; AK, acetate kinase; BCACT, butyryl-CoA:acetate CoA-transferase; BK, butyrate kinase; PTA, phosphotransacetylase; PTB, phosphotransbutyrylase; SCACT, succinyl-CoA:acetate CoA-transferase; and SCS, succinyl-CoA synthetase (ADP-forming). Abbreviations for bacteria: *A. acid*., *Acidipropionibacterium acidipropionici*; *C. acnes*, *Cutibacterium acnes*; *C. gran*., *Cutibacterium granulosum*; and *P*. *freud*, *Propionibacterium freudenreichii*.

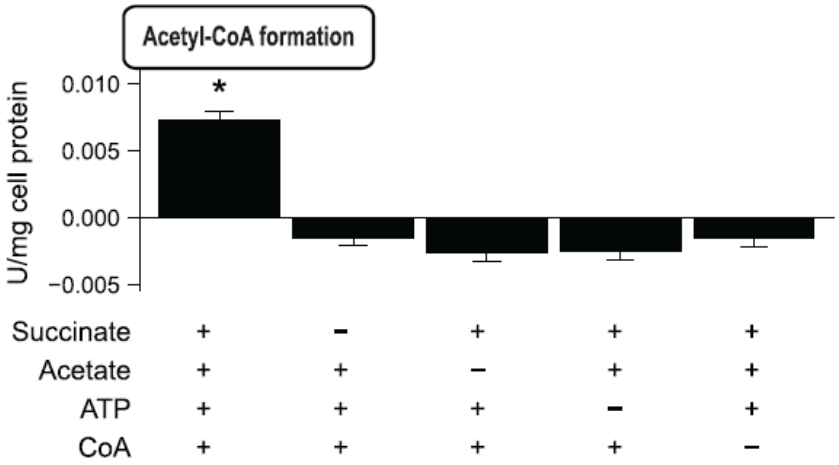

Figure 5. Acetyl-CoA formation measured in the presence of different substrates. The bacterium *C. granulosum* forms acetyl-CoA only when provided all four substrates of the SCACT/SCS pathway. In different treatments, substrates were provided (+) or withheld (-). Results are means ± standard error of 3 biological replicates. Means different from 0 ($P < 0.05$) are marked with an asterisk. Abbreviations: CoA, coenzyme A; SCACT, succinyl-CoA:acetate CoA-transferase; and SCS, succinyl-CoA synthetase (ADP-forming).

A SCACT gene in genome

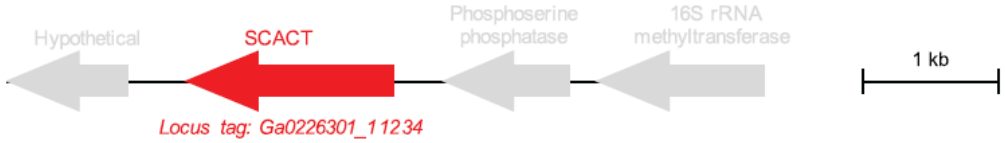

B SCACT protein in proteome

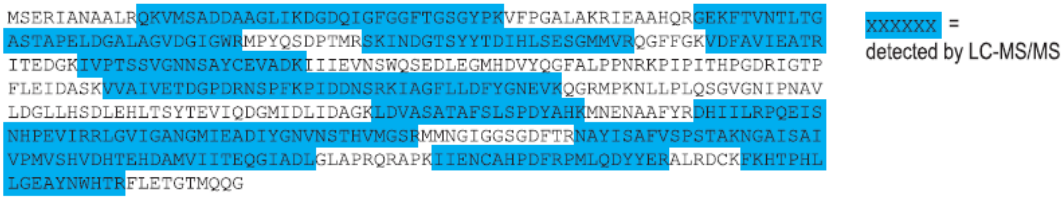

XXXXXX = detected by LC-MS/MS

C SCACT purified protein and activity

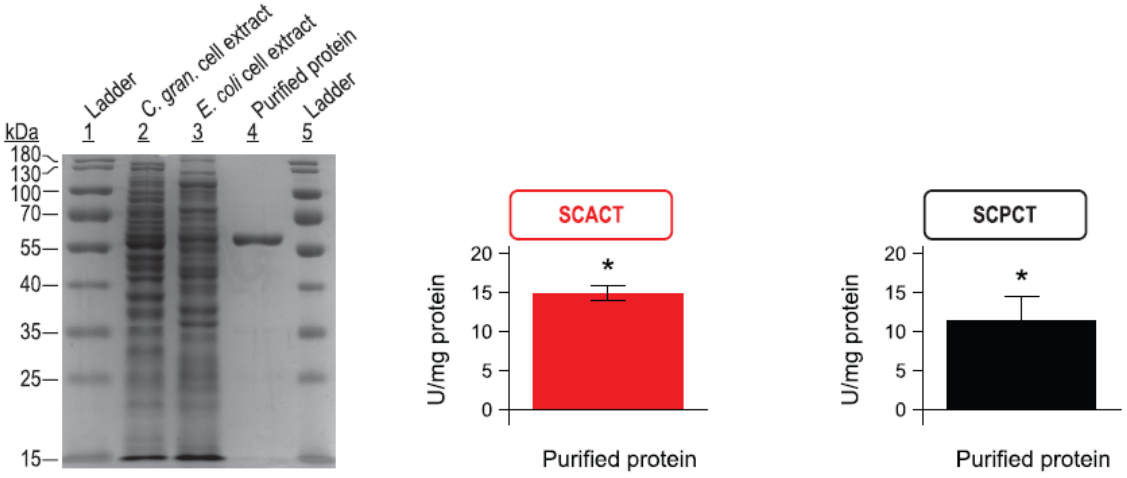

D Phylogenetic origin of SCACT gene

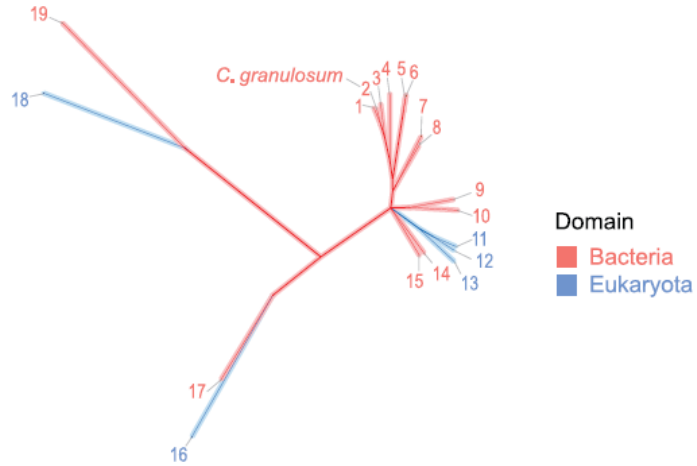

Figure 6. Identification of gene encoding SCACT in *C. granulosum*. The gene encoding SCACT in *C. granulosum* is a bacterial homolog, pointing to a bacterial origin of the SCACT/SCS pathway. (A) Location of the SCACT gene in the genome of *C. granulosum*. (B) Detection of SCACT protein in the proteome of *C. granulosum*. Specific peptides detected by LC-MS/MS are highlighted in the full protein sequence. Peptides shown were detected in each of two biological replicates (batches of protein prepared from independent cultures). (C) Production and enzymatic activity of recombinant SCACT protein in *E. coli*. Purity shown by SDS-PAGE was 92%. The amount of protein loaded was 7.7, 5.8, and 0.8 µg for lanes 2, 3, and 4. Enzymatic activity is mean ± standard error of 3 biological replicates. Means different from 0 ($P < 0.05$) are marked with an asterisk. (D) Phylogenetic tree of SCACT protein sequences, showing that SCACT in *C. granulosum* is a bacterial homolog. Proteins included are those with experimental evidence of enzymatic activity. Protein sequences are 1. *Acidipropionibacterium acidipropionici*, 2. *Cutibacterium granulosum*, 3. *Propionibacterium freudenreichii*, 4. *Corynebacterium diphtheriae*, 5. *Acetobacter cerevisiae*, 6. *Acetobacter aceti*, 7. *Snodgrassella alvi*, 8. *Moraxella catarrhalis*, 9. *Bacteroides fragilis*, 10. *Escherichia coli* (homolog 1), 11. *Aspergillus nidulans*, 12. *Saccharomyces cerevisiae*, 13. *Trichomonas vaginalis*, 14. *Acinetobacter baumannii*, 15. *Clostridium kluyveri*, 16. *Fasciola hepatica*, 17. *Yersinia pestis*, 18. *Trypanosoma brucei* (homolog 1), and 19. *Ralstonia eutropha*. Full information on proteins is in Dataset S2. Abbreviations: *C. gran.*, *Cutibacterium granulosum*; SCACT, succinyl-CoA:acetate CoA-transferase; SCPCT, succinyl-CoA:propionate CoA-transferase; and SCS, succinyl-CoA synthetase (ADP-forming).

A SCS genes in genome

B SCS proteins in proteome

Subunit α

VAIILDENAKIIVQGMTGSEGMKHTQRMIDSGSQIVGGTNPRKAGQKVEFRDGVSVPVFGTVKEAMAAT
GANVSVIFVPAKFTKSAVMESIEAEIPLVVCITEGVPVKDTAEFFTAAQRSGKTRIIGPNCPGIISPGK
SNAGIVPADITGPGRVGLVSKSGTLTYQLMYEVRDLGISTAIGIGGDPVIGTTHIDALKYFEEDPETDV
IVMIGEIGGDAEERAAKYISEHVSKPVVGYIAGFTAPKGKTMGHAGAIVSGSSGTAAAKKEALEAAGVR
VGKTPTETAKLAHEAMASLKK

XXXXXX = detected by LC-MS/MS

Subunit β

VDLYEYQARDLFEKHGVPVLRGIVAENPEQASQAAAELGTSVVAVKAQVKIGGRGKAGGVKIAKSPEEA
AQHAEKILGMDIKGHTVHKVMIAEGADIAEEYYFSILLDRSERRYLVMCSREGGMDIETLAKERPEALA
KVPVDPIEGIDEAVAGTILTEAGFPAEEHAAIVPAIVKLWETYRDEDATLVEVNPLIKTKDGKVLAIDA
KMTVDDNASFRQPDHAALVDRATTDPLELRAKELGLNYVKLDGNVGVIGNGAGLVMSTLDVTAYAGEEF
PGSPKPANFLDIGGGASAEVMANGLDVILSDPQVRSVFVNIFGGITACDQVAKGVKGALEKLGDQASKP
LVVRLDGNAVEEGRAILSEYNHPLVTMVETMDEAARKAAELASKEA

C SCS purified proteins and activity

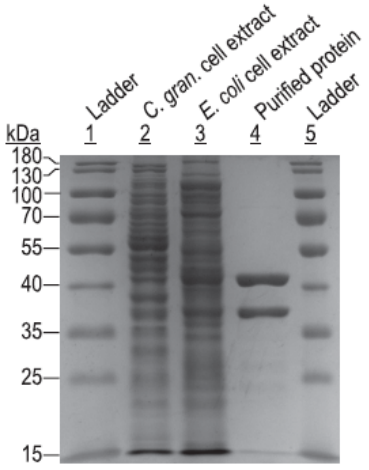

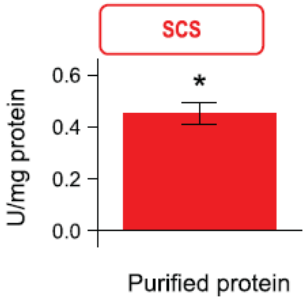

D Phylogenetic origin of SCS genes

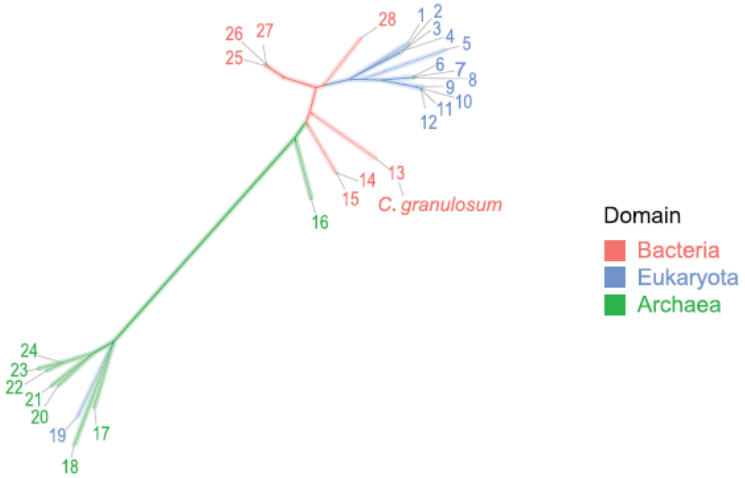

Figure 7. Identification of gene encoding SCS in *C. granulosum*. The gene encoding SCS in *C. granulosum* is a bacterial homolog, pointing to a bacterial origin of the SCACT/SCS pathway. As Figure 6, except genes are for SCS instead of SCACT. Purity shown by SDS-PAGE was 96%. The amount of protein loaded was 7.7, 7.2, and 1.4 µg for lanes 2, 3, and 4. Protein sequences are 1. *Toxoplasma gondii*, 2. *Blastocystis* sp., 3. *Solanum lycopersicum* (homolog 2), 4. *Solanum lycopersicum* (homolog 1), 5. *Saccharomyces cerevisiae*, 6. *Columba livia* (homolog 2), 7. *Mus musculus*, 8. *Homo sapiens* (homolog 1), 9. *Columba livia* (homolog 1), 10. *Homo sapiens* (homolog 2), 11. *Sus scrofa* (homolog 1), 12. *Sus scrofa* (homolog 2), 13. *Cutibacterium granulosum*, 14. *Thermus thermophilus*, 15. *Thermus aquaticus*, 16. *Korarchaeum cryptofilum* (homolog 4), 17. *Archaeoglobus fulgidus* (homolog 1), 18. *Archaeoglobus fulgidus* (homolog 2), 19. *Giardia lamblia*, 20. *Thermococcus kodakarensis* (homolog 3), 21. *Thermococcus kodakarensis* (homolog 4), 22. *Thermococcus kodakarensis* (homolog 1), 23. *Pyrococcus furiosus* (homolog 5), 24. *Pyrococcus furiosus* (homolog 6), 25. *Escherichia coli*, 26. *Alcanivorax borkumensis*, 27. *Pseudomonas aeruginosa*, and 28. *Advenella mimigardefordensis*. Full information on proteins is in Dataset S3. Abbreviations: *C. gran.*, *Cutibacterium granulosum*; SCACT, succinyl-CoA:acetate CoA-transferase; and SCS, succinyl-CoA synthetase (ADP-forming).

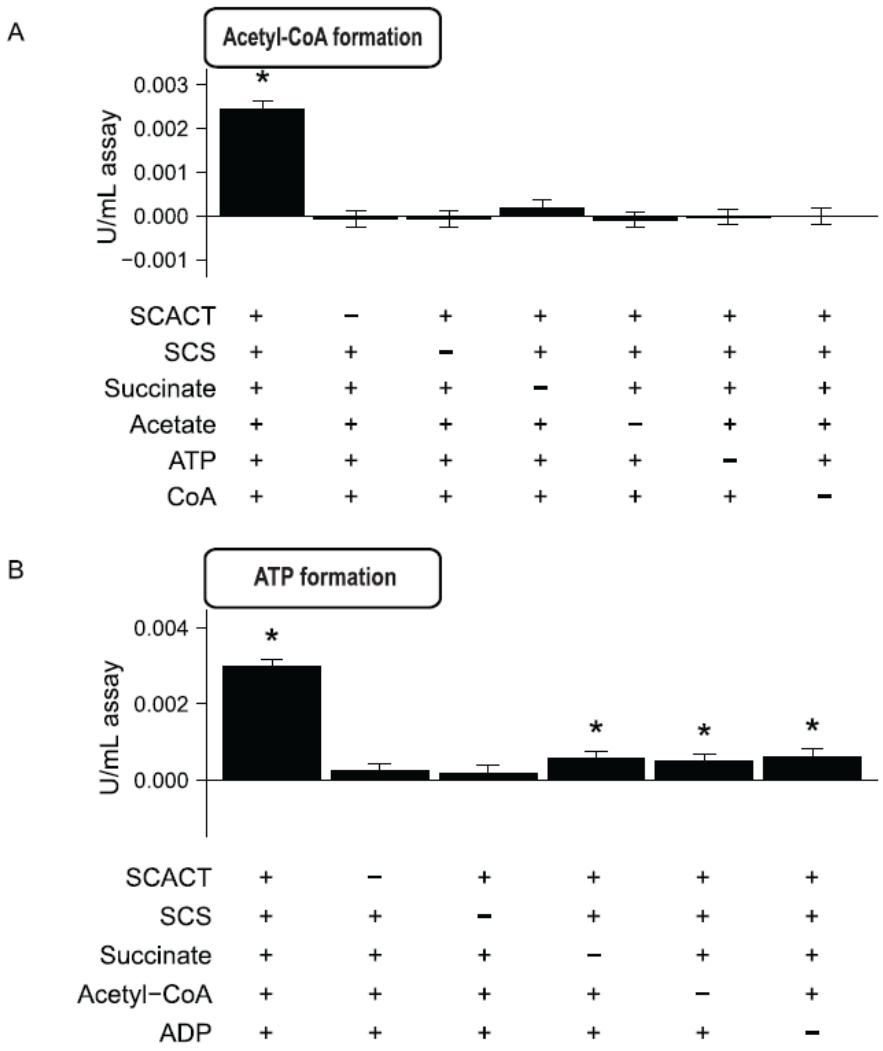

Figure 8. Acetyl-CoA and ATP formation in the presence of different substrates and purified enzymes. Purified SCACT and SCS form a functional pathway. (A) Acetyl-CoA formation by SCACT and SCS from succinate, acetate, ATP, and CoA. (B) ATP formation by SCACT and SCS from succinate, acetyl-CoA, and ADP. In different treatments, enzymes or substrates were provided (+) or withheld (-). Each milliliter of assay mix contained 4.5 µg for SCACT and 4.5 µg for SCS. Results are mean ± standard error of 3 biological replicates (batches of SCACT and SCS prepared from independent cultures). Means different from 0 ($P < 0.05$) are marked with an asterisk. Abbreviations: CoA, coenzyme A; SCACT, succinyl-CoA:acetate CoA-transferase; and SCS, succinyl-CoA synthetase (ADP-forming).

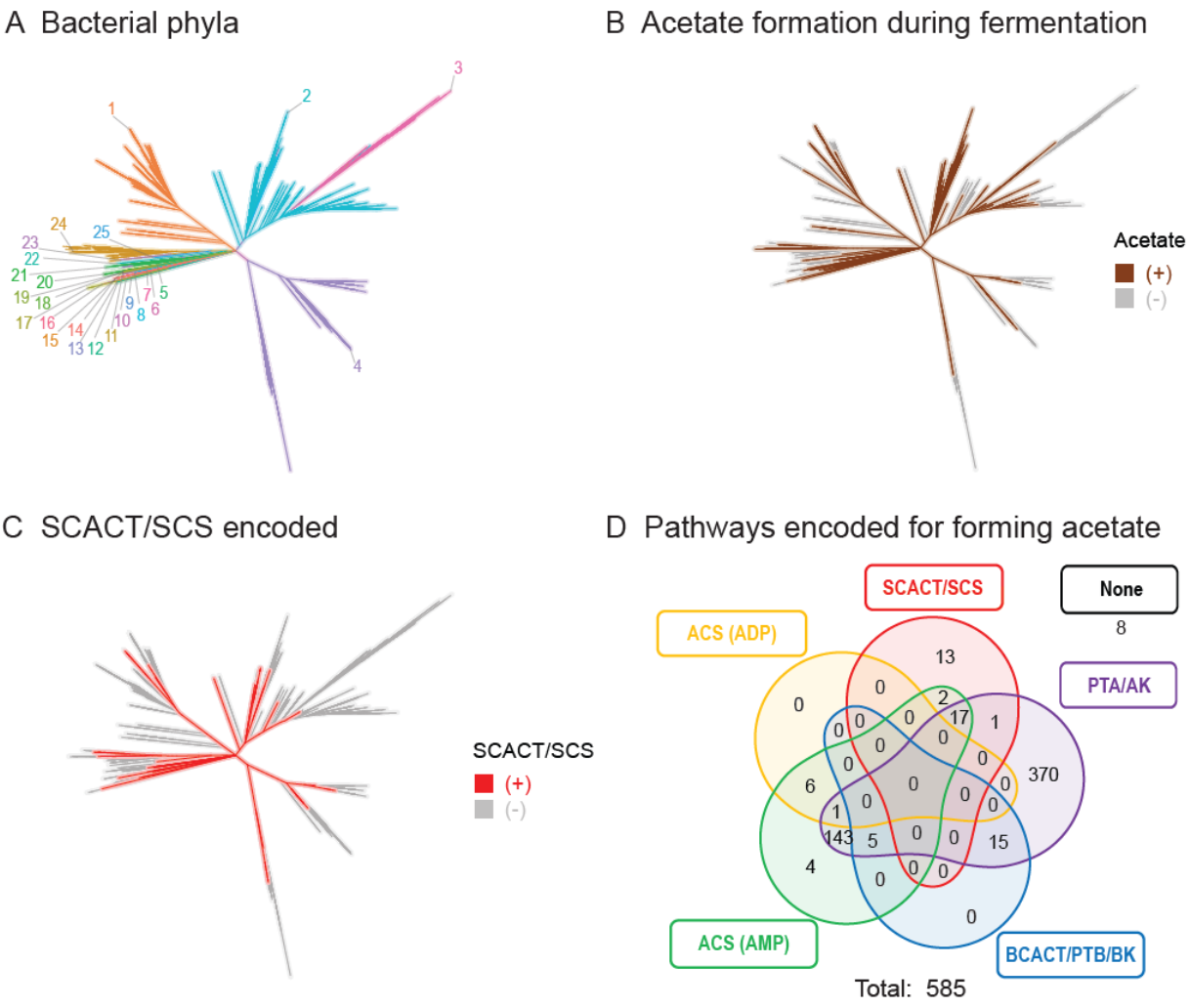

Figure 9. Distribution of the SCACT/SCS pathway among bacteria. Many bacteria encode enzymes of the SCACT/SCS pathway. Phylogenetic tree of type strains of bacteria in *Bergey's Manual of Systematics of Archaea and Bacteria* (Whitman 2020), highlighting (A) phyla (B) strains reported to form acetate during fermentation, and (C) strains that encode the SCACT/SCS pathway in their genome. (D) Venn diagram for strains that encode the SCACT/SCS vs. other pathways for forming acetate. In C and D, only strains reported to form acetate during fermentation are included. Phyla are 1. *Actinobacteria*, 2. *Firmicutes*, 3. *Tenericutes*, 4. *Proteobacteria*, 5. *Dictyoglomi*, 6. *Synergistetes*, 7. *Thermotogae*, 8. *Fusobacteria*, 9.

Lentisphaerae, 10. *Spirochaetes*, 11. *Elusimicrobia*, 12. *Planctomycetes*, 13. *Acidobacteria*, 14. *Verrucomicrobia*, 15. *Chlamydiae*, 16. *Caldiserica*, 17. *Aquificae*, 18. *Coprothermobacterota*, 19. *Deinococcus-Thermus*, 20. *Chloroflexi*, 21. *Desulfobacterota*, 22. *Fibrobacteres*, 23. *Rhodothermaeota*, 24. *Ignavibacteriae*, and 25. *Bacteroidetes*. Abbreviations: ACS (ADP), acetyl-CoA synthetase (ADP-forming); ACS (AMP), acetyl-CoA synthetase; AK, acetate kinase; BCACT, butyryl-CoA:acetate CoA-transferase; BK, butyrate kinase; PTA, phosphotransacetylase; PTB, phosphotransbutyrylase; SCACT, succinyl-CoA:acetate CoA-transferase; and SCS, succinyl-CoA synthetase (ADP-forming).

A

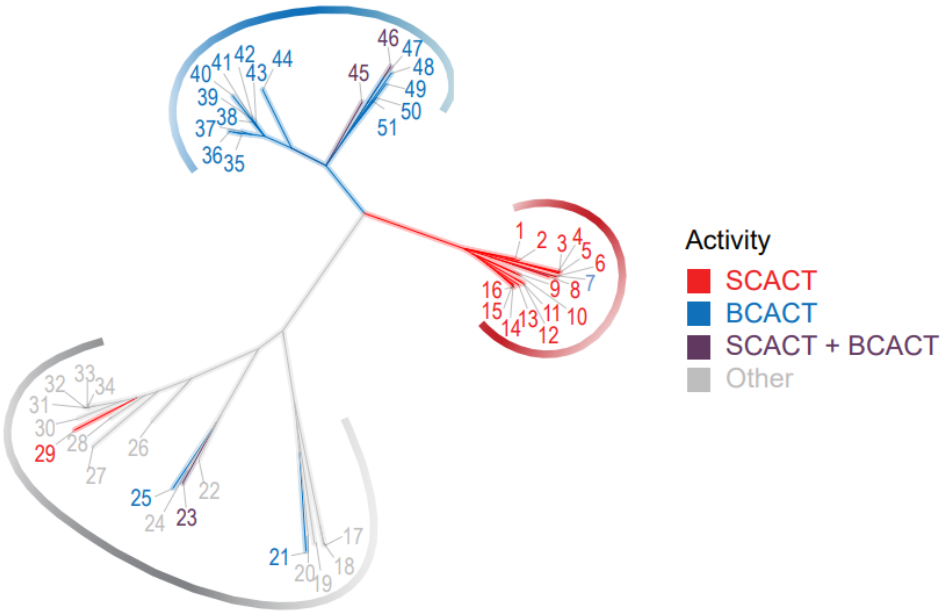
Activity
SCACT
BCACT
SCACT + BCACT
Other

B

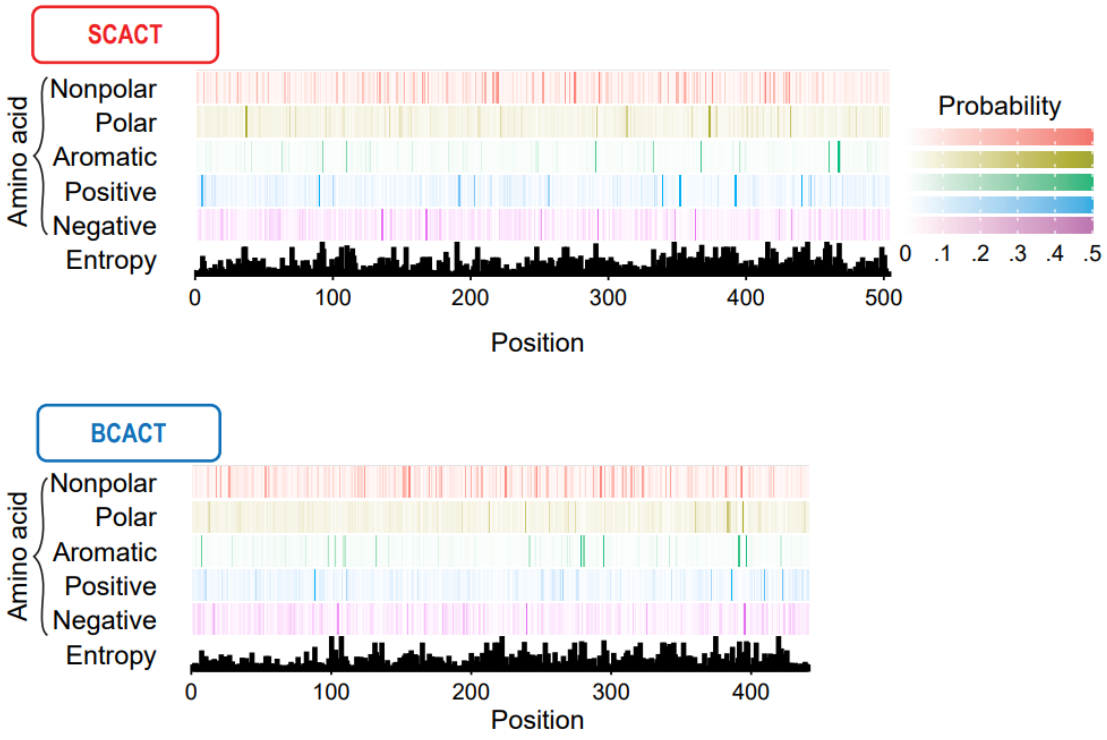
SCACT
Amino acid
Nonpolar
Polar
Aromatic
Positive
Negative
Entropy
Probability
0 .1 .2 .3 .4 .5
0 100 200 300 400 500
Position
BCACT
Amino acid
Nonpolar
Polar
Aromatic
Positive
Negative
Entropy
0 100 200 300 400
Position

Figure 10. A large number of proteins used to build and test profile hidden Markov models (pHMMs) for SCACT. (A) Phylogenetic tree of protein sequences, which is highlighted by their activity. (B) pHMMs for SCACT and BCACT. Protein sequences are 1. *Clostridium kluyveri*, 2. *Acinetobacter baumannii*, 3. *Trichomonas vaginalis*, 4. *Saccharomyces cerevisiae*, 5. *Aspergillus nidulans*, 6. *Escherichia coli* (homolog 1), 7. *Porphyromonas gingivalis* (homolog 3), 8. *Bacteroides fragilis*, 9. *Moraxella catarrhalis*, 10. *Snodgrassella alvi*, 11. *Acetobacter aceti*, 12. *Acetobacter cerevisiae*, 13. *Corynebacterium diphtheriae*, 14. *Propionibacterium freudenreichii*, 15. *Cutibacterium granulosum*, 16. *Acidipropionibacterium acidipropionici*, 17. *Mycobacterium tuberculosis*, 18. *Rhodococcus jostii*, 19. *Myxococcus xanthus*, 20. *Pseudomonas knackmussii*, 21. *Acidaminococcus fermentans*, 22. *Acetobacterium woodii*, 23. *Ralstonia eutropha*, 24. *Clostridium propionicum*, 25. *Escherichia coli* (homolog 2), 26. *Clostridium acetobutylicum*, 27. *Pseudomonas putida*, 28. *Helicobacter pylori*, 29. *Trypanosoma brucei* (homolog 1), 30. *Drosophila melanogaster*, 31. *Homo sapiens*, 32. *Sus scrofa*, 33. *Mus musculus*, 34. *Rattus norvegicus*, 35. *Anaerostipes* sp. 494a, 36. *Anaerostipes caccae* (homolog 1), 37. *Anaerostipes* sp. 992a, 38. *Butyricicoccus* sp. BB10, 39. *Intesimonas butyriciproducens*, 40. *Peptoniphilus* sp. 35-6-1, 41. *Roseburia hominis*, 42. *Roseburia* sp. 831b, 43. *Roseburia* sp. 499, 44. *Megasphaera elsdenii*, 45. *Yersinia pestis*, 46. *Fasciola hepatica*, 47. *Artemia franciscana*, 48. *Porphyromonas gingivalis* (homolog 2), 49. *Clostridium aminobutyricum*, 50. *Anaerostipes caccae* (homolog 2), 51. *Porphyromonas gingivalis* (homolog 1). Full information on proteins is in Dataset S2. For SCACT, HMMs were built using sequences of enzymes 1-6 and 8-16. For BCACT, they were build using sequences of enzymes 35-51. Amino acids were grouped as non-polar (G, A, P, V, L, I, M), polar (S, T, C, N, Q), aromatic (F, Y, W), positive (K, H, R), or negative (D, E). Entropy refers to bits

of information. Abbreviations: BCACT, butyryl-CoA:acetate CoA-transferase; and SCACT, succinyl-CoA:acetate CoA-transferase.

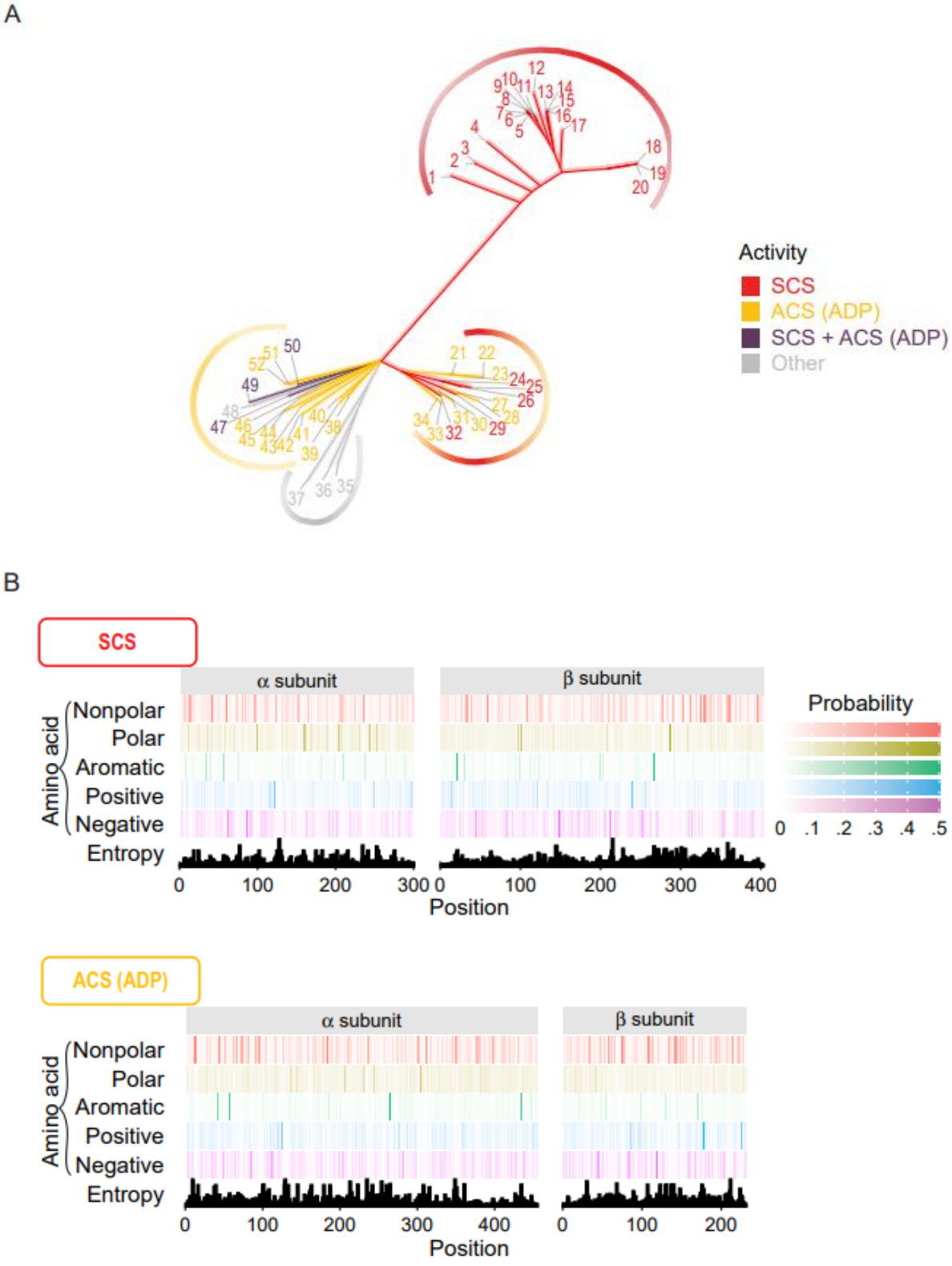
A
Activity
SCS
ACS (ADP)
SCS + ACS (ADP)
Other
B
SCS
α subunit
β subunit
Amino acid
Nonpolar
Polar
Aromatic
Positive
Negative
Entropy
Probability
0 .1 .2 .3 .4 .5
0 100 200 300
0 100 200 300 400
Position
ACS (ADP)
α subunit
β subunit
Amino acid
Nonpolar
Polar
Aromatic
Positive
Negative
Entropy
0 100 200 300 400
0 100 200
Position

Figure 11. A large number of proteins used to build and test profile hidden Markov models (pHMMs) for SCS. As Figure 10, except sequences are for proteins with SCS activity and their homologs. Protein sequences are 1. *Korarchaeum cryptofilum* (homolog 4), 2. *Thermus aquaticus*, 3. *Thermus thermophilus*, 4. *Cutibacterium granulosum*, 5. *Sus scrofa* (homolog 2), 6. *Columba livia* (homolog 1), 7. *Sus scrofa* (homolog 1), 8. *Homo sapiens* (homolog 2), 9. *Columba livia* (homolog 2), 10. *Mus musculus*, 11. *Homo sapiens* (homolog 1), 12. *Saccharomyces cerevisiae*, 13. *Solanum lycopersicum* (homolog 1), 14. *Solanum lycopersicum* (homolog 2), 15. *Blastocystis* sp., 16. *Toxoplasma gondii*, 17. *Advenella mimigardefordensis*, 18. *Pseudomonas aeruginosa*, 19. *Escherichia coli*, 20. *Alcanivorax borkumensis*, 21. *Pyrococcus furiosus* (homolog 4), 22. *Pyrococcus furiosus* (homolog 3), 23. *Thermococcus kodakarensis* (homolog 2), 24. *Pyrococcus furiosus* (homolog 6), 25. *Thermococcus kodakarensis* (homolog 1), 26. *Pyrococcus furiosus* (homolog 5), 27. *Pyrococcus furiosus* (homolog 8), 28. *Pyrococcus furiosus* (homolog 7), 29. *Thermococcus kodakarensis* (homolog 4), 30. *Pyrococcus furiosus* (homolog 10), 31. *Pyrococcus furiosus* (homolog 9), 32. *Thermococcus kodakarensis* (homolog 3), 33. *Pyrococcus furiosus* (homolog 1), 34. *Pyrococcus furiosus* (homolog 2), 35. *Ralstonia eutropha* (homolog 2), 36. *Ralstonia eutropha* (homolog 1), 37. *Delftia acidovorans*, 38. *Korarchaeum cryptofilum* (homolog 3), 39. *Korarchaeum cryptofilum* (homolog 1), 40.*Korarchaeum cryptofilum* (homolog 2), 41. *Entamoeba histolytica* (homolog 1), 42. *Entamoeba histolytica* (homolog 2), 43. *Pyrobaculum aerophilum*, 44. *Methanosarcina mazei*, 45. *Haloarcula marismortui*, 46. *Chloroflexus aurantiacus*, 47. *Giardia lamblia*, 48. *Nitrosopumilus maritimus* (homolog 1), 49. *Archaeoglobus fulgidus* (homolog 2), 50. *Archaeoglobus fulgidus* (homolog 1), 51. *Methanocaldococcus jannaschii*, and 52. *Nitrosopumilus maritimus* (homolog 2). Full information on proteins is in Dataset S3. For SCS, pHMMs were built using sequences of enzymes 1-20, 24-26, 29, and 32. For

ACS, they were built using sequences of enzymes 21-23, 27-28, 30-31, 33-34, 38-47, and 49-52. Abbreviations: ACS (ADP), acetyl-CoA synthetase (ADP-forming); and SCS, succinyl-CoA synthetase (ADP-forming).

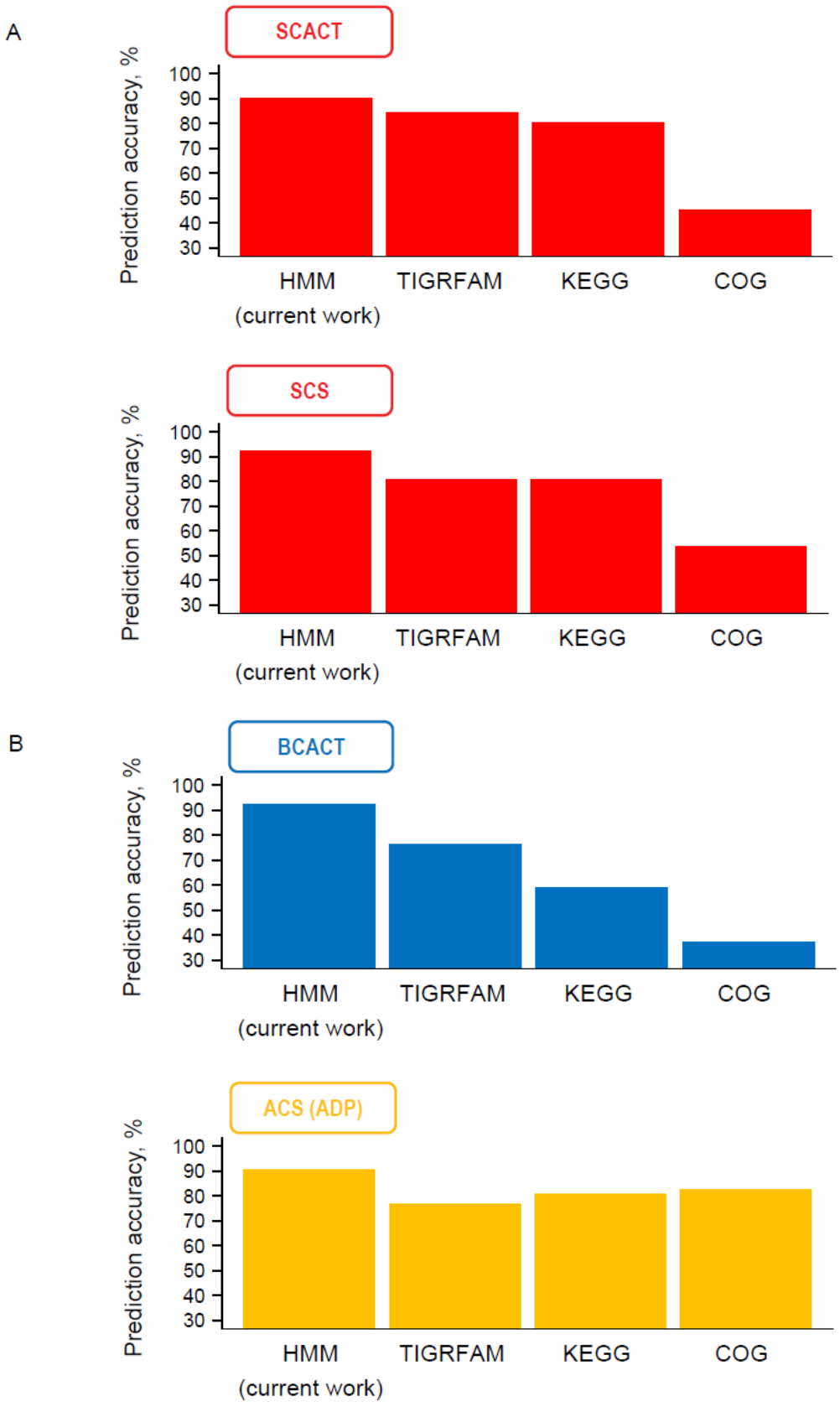
A
SCACT
Prediction accuracy, %
100
90
80
70
60
50
40
30
HMM
(current work)
TIGRFAM
KEGG
COG
SCS
Prediction accuracy, %
100
90
80
70
60
50
40
30
HMM
(current work)
TIGRFAM
KEGG
COG
B
BCACT
Prediction accuracy, %
100
90
80
70
60
50
40
30
HMM
(current work)
TIGRFAM
KEGG
COG
ACS (ADP)
Prediction accuracy, %
100
90
80
70
60
50
40
30
HMM
(current work)
TIGRFAM
KEGG
COG

Figure 12. Prediction accuracy of HMM, TIGRFAM, KEGG, and COG. Proteins with SCACT or SCS activity can be accurately predicted using profile hidden Markov models (pHMMs) from this work. The same is observed for proteins with BCACT and ACS (ADP) activity. Accuracy of other databases (TIGRFAM, KEGG, COG) shown for comparison. Abbreviations: ACS (ADP), acetyl-CoA synthetase (ADP-forming); BCACT, butyryl-CoA:acetate CoA-transferase; SCACT, succinyl-CoA:acetate CoA-transferase; and SCS, succinyl-CoA synthetase (ADP-forming). See Dataset S2 and Dataset S3 for details of the prediction.

Appendix 1

Dataset S1: Genomes searched, pathways encoded, reported acetate formation, and locus tags found.

Download Dataset S1 by searching https://journals.asm.org/doi/suppl/10.1128/AEM.02959-20/suppl_file/aem02959-20_supp_1_seq12.xls

Dataset S2: Proteins with experimental evidence of SCACT, BCACT, or other activity.

Download Dataset S2 by searching https://journals.asm.org/doi/suppl/10.1128/AEM.02959-20/suppl_file/aem02959-20_supp_2_seq13.xls

Dataset S3: Proteins with experimental evidence of SCS, ACS (ADP), or other activity.

Download Dataset S3 by searching https://journals.asm.org/doi/suppl/10.1128/AEM.02959-20/suppl_file/aem02959-20_supp_3_seq14.xls

Dataset S4: Parameters used in X!TandemPipeline.

Download Dataset S4 by searching https://journals.asm.org/doi/suppl/10.1128/AEM.02959-20/suppl_file/aem02959-20_supp_4_seq15.xls

Dataset S5: Genes and database IDs searched on IMG/M.

Download Dataset S5 by searching https://journals.asm.org/doi/suppl/10.1128/AEM.02959-20/suppl_file/aem02959-20_supp_5_seq16.xls

Chapter 3. Rnf regenerates redox cofactors for propionate production during fermentation in bacteria

Abstract

Fermentation is an important type of metabolism carried out by many prokaryotes in the environment. It is vital to many systems studies by microbial ecologists. One important metabolite formed during fermentation is propionate. This short-chain fatty acid provides energy for host metabolism and other microbes in the environment. However, one major biochemical pathway for forming propionate has unknown steps. No steps are known to regenerate redox cofactors, oxidized ferredoxin (Fd_{ox}) and reduced NAD (NAD_{red}). The hypothesis of this study is that the enzyme Rnf can regenerate these redox cofactors. Our recent study found Rnf genes in many propionate-forming bacteria from the rumen. Here, we studied two of these rumen bacteria, *Prevotella ruminicola* 23 and *Prevotella brevis* GA33. Analysis of fermentation products verified that they formed propionate (or its precursor, succinate) and acetate during the fermentation of glucose. The quantitative analysis of fermentation products and cells showed that without Rnf, fermentation is unbalanced; it produced almost equal excess amounts of reduced ferredoxin (Fd_{red}) and oxidized NAD (NAD_{ox}). With enzymatic assays, the ferredoxin:NAD^+ oxidoreductase activity of Rnf was observed in both bacteria. The genes encoding Rnf were identified and their expression was confirmed by shotgun proteomics. These results show that Rnf handles the excess Fd_{red} and NAD_{ox} by converting them back to Fd_{ox} and NAD_{red}. Similarly, we confirmed the involvement of other enzymes in regenerating redox cofactors. The fermentation products of more than 1,400 species of prokaryotes were cataloged, and nearly 10% of these fermentative species carry out a fermentation forming propionate/succinate and acetate. Over 40% of species carrying out this

fermentation also have genes for Rnf. These species come from several habitats (gut, aquatic sediments, and anaerobic digesters). This work suggests Rnf is important to propionate formation in many bacteria from the environments.

Introduction

Fermentation is a major type of metabolism, and prokaryotes isolated from many habitats can carry out fermentation (Hackmann and Zhang 2021). Fermentative prokaryotes are abundant in many habitats, including the gastrointestinal tract, aquatic environment, and anaerobic digesters (Whitman 2020). Fermentation is also carried out by eukaryotes (Muller et al 2012). Therefore, this type of metabolism is important in a variety of systems studied by microbial ecologists.

One important metabolite produced during fermentation is propionate. This short chain fatty acid is produced at high level in the gut, and then it is absorbed by the gut and utilized for energy metabolism by the host (Bergman 1990). In other environments, such as anaerobic digesters, it is formed (Zhou et al 2018) and then metabolized by other microbes (Dyksma and Gallert 2019). Organisms can form propionate outright, or they form succinate, a precursor rapidly converted to propionate by other microbes (Scheifinger and Wolin 1973, Stewart and Flint 1989, Van Gylswyk 1995). Because of its importance in these environments, it is critical to know at the biochemical level how propionate is formed.

Despite decades of study (Allen et al 1964), one major biochemical pathway for forming propionate has unknown steps. Propionate is most commonly produced via the succinate pathway and it is usually produced in combination with acetate (Allen et al 1964, Gottschalk 1986, Muller et al 2012). The pathway has a problem when glucose is utilized as the substrate: it forms excess amounts of reduced ferredoxin (Fd_{red}), a redox cofactor (Figure 13A) (Hackmann et al 2017). This

redox cofactor is formed by pyruvate:ferredoxin oxidoreductase, and no step is known to oxidize it back to oxidized ferredoxin (Fd_{ox}). Similarly, this pathway forms oxidized NAD (NAD_{ox}), with no step to reduce it back to reduced NAD (NAD_{red}). This is an apparent problem in both prokaryotes (Hackmann et al 2017, McCubbin et al 2020) and eukaryotes (Muller et al 2012). The unknown steps are important because fermentation stops if Fd_{ox} and NAD_{red} are not regenerated.

We hypothesize that the enzyme Rnf fills the unknown steps (Figure 13B). This enzyme (EC 7.2.1.2) simultaneously oxidizes Fd_{red} and reduces NAD_{ox}, solving two problems at once. This enzyme plays a similar role in other pathways, such as the pathway metabolizing caffeate (Imkamp et al 2007). Recently, we found Rnf genes in many propionate-forming bacteria from the rumen (Hackmann et al 2017). Here we study two of these rumen bacteria in detail and find that they indeed use Rnf to form propionate (or its precursor, succinate). This is demonstrated by the combination of biochemical, proteomic, and other approaches. Further, we find Rnf is common in bacteria that form propionate (or succinate), with 44 type strains from many habitats encoding it. This work suggests Rnf is important to propionate formation in bacteria from various environments.

Materials and Methods

Organisms

The American Type Culture Collection (ATCC) was the source for *Prevotella brevis* GA33 and *Prevotella ruminicola* 23. The Deutsche Sammlung von Mikroorganismen und Zellkulturen (DSMZ) was the source for *Clostridium pasteurianum* 5. Michael Flythe (USDA-ARS, Lexington, KY) was the source for *Selenomonas ruminantium* HD4.

Media and growth

Strains were grown anaerobically under O_2-free CO_2 and with serum bottles with butyl rubber stoppers, using previously described techniques (Tao et al 2019, Tao et al 2016). The bottles were 150-mL in volume and contained 70-mL of culture. Balch tubes with 10-mL of culture were also used. In each case, 0.1 mL volume of a stationary-phase culture was used as the inoculant (seed). The temperature of growth was 37°C.

Growth of cultures was measured by removing 1-mL aliquots with a syringe and measuring optical density at 600 nm (OD_{600}) in cuvettes. The instrument used was a Thermo Scientific Genesys 20 spectrophotometer. The sample was diluted with 0.9% (w/v) NaCl as needed to remain within the linear range of the instrument.

P. brevis GA33 and *S. ruminantium* HD4 were cultured on the medium PC+VFA. Per liter, this medium contained 4 g glucose, 1 g Trypticase peptone (product 211921; BD), 0.5 g Bacto yeast extract (product 212750; BD), 292 mg K_2HPO_4, 292 mg KH_2PO_4, 480 mg $(NH_4)_2SO_4$, 480 mg NaCl, 49 mg $MgSO_4$, 64 mg $CaCl_2 \cdot 2H_2O$, 3.1 mL VFA solution, 0.5 mL 0.1% (w/v) resazurin, 4 g Na_2CO_3, and 0.6 g L-cysteine·HCl·H_2O. The VFA solution was a mixture of 6 mL propionic acid, 4 mL n-butyric acid, 1 mL n-valeric acid, 1 mL isovaleric acid, 1 mL isobutyric acid, 1 mL DL-α-methyl butyric acid, and 17 mL acetic acid.

P. ruminicola 23 was cultured on medium BZ. This is a defined medium developed in the current work by modifying a complex medium reported in ref. (Villas-Boas et al 2006). Per liter, the medium contained 8 g glucose, 0.6 g K_2HPO_4, 0.45 g KH_2PO_4, 0.45 g $(NH_4)_2SO_4$, 0.9 g NaCl, 92 mg $MgSO_4$, 0.12 g $CaCl_2 \cdot 2H_2O$, 2 mL hemin, 1 mL 0.1% (w/v) resazurin, 1 mL trace element SL-9 (Tschech and Pfennig 1984), 10 mL DSMZ-medium-141 vitamin solution, 0.1 mg vitamin

B_{12}, 322.7 µL isobutyric acid, 322.7 µL 2-methylbutyric acid, 322.7 µL valeric acid, 322.7 µL isovaleric acid, 4 g Na_2CO_3, and 1.2 g L-cysteine·HCl·H_2O. One liter of the trace element SL-9 contained 12.8 g nitrilotriacetic acid, 2 g $FeCl_2$·4 H_2O, 190 mg $CoCl_2$·6 H_2O, 100 mg $MnCl_2$·4 H_2O, 70 mg $ZnCl_2$, 6 mg H_3BO_3, 24 mg $NiCl_2$·6 H_2O, 2 mg $CuCl_2$·2 H_2O, 36 mg Na_2MoO_4·2 H_2O. The trace element SL-9 was made by dissolving nitrilotriacetic acid in 200 mL of distilled water, adjusting pH to 6.5 with KOH, dissolving mineral salts, adjusting pH to 6.5 with KOH, and adding distilled water to make up to 1000 mL. One liter of the DSMZ-medium-141 vitamin solution contained 2 mg biotin, 2 mg folic acid, 10 mg pyridoxine-HCl, 5 mg thiamine-HCl, 5 mg riboflavin, 5 mg nicotinic acid, 5 mg D-Ca-pantothenate, 0.1 mg vitamin B_{12}, 5 mg p-aminobenzoic acid, and 5 mg lipoic acid. The hemin was added as a 0.5-g/liter solution containing 10 mM NaOH as the diluent. Glucose, the DSMZ-medium-141 vitamin solution, and vitamin B_{12} were added to the medium before inoculation.

For experiments measuring the dependency of growth on sodium, we used media above but removed resazurin and also substituted NaCl, NaOH and Na_2CO_3 with equimolar KCl, KOH and K_2CO_3.

Preparation of cell extract, cytoplasmic fraction, and cell membrane

Three 70-mL cultures were grown to mid-exponential phase (OD_{600} = 1.0 to 1.2 for *P. brevis* GA33 and OD_{600} = 2.7 to 3.0 for *P. ruminicola* 23) and then pooled. All steps for preparing cell extract, cytoplasmic fraction and cell membrane were performed under oxygen-free nitrogen atmosphere. Cells were harvested by centrifugation (21,100 × g for 5 min at 4°C; F15-8x50cy rotor and Sorvall Legend XTR centrifuge), washed twice in the Tris-$MgSO_4$ buffer (50 mM Tris-Cl [pH 7.6], 20 mM $MgSO_4$, 4 mM dithiothreitol, 4 µM resazurin), and resuspended in 20 mL Tris-$MgSO_4$ buffer. Two µL of Pierce Universal Nuclease (250 U/µL, Thermo Scientific) was added to a final

concentration of 25 U per mL cells. The resuspended cells were lysed with a precooled (4°C) French press (Glen Mills) at 110 MPa with a single pass through. Cell debris and unbroken cells were removed by centrifugation (14,000 × g for 30 min at 4°C). An aliquot (c. 2 mL) of the cell extract was stored at -80°C until use. The remainder (c. 17 mL) was further separated into cytoplasmic fraction and cell membrane via ultracentrifugation (208,000 × g for 60 min at 4°C; Type 70Ti Rotor and Beckman L8-70M centrifuge). After ultracentrifugation, the supernatant was stored at -80°C and used as the cytoplasmic fraction. The pellet in the bottom of the centrifuge tube was gently rinsed by adding 5 mL Tris-$MgSO_4$ buffer and dumping the buffer without centrifugation. The pellet was then homogenized in 2 mL Tris-$MgSO_4$ buffer by suspending the pellet in the buffer and mixing them well with a pipette, and stored at -80°C and used as the cell membrane.

Solubilized cell membrane was prepared similarly to cell membrane, with a few modifications. Three 70-mL cultures grown to mid-log phase were centrifuged and washed twice in the Tris-$MgSO_4$ buffer, and resuspended in 21 mL Tris-sucrose buffer (50 mM Tris-Cl [pH 8.0], 20% [w/v] sucrose, 4 mM dithiothreitol, and 0.4 µM resazurin). Lysozyme was added in the form of powder to give a final concentration of 0.1 mg/mL. The suspension was incubated at 37°C for 15 min with occasional mixing (swirling). One volume of 0.1 M Na^+-EDTA (pH 7.0) was then slowly added to 10 volumes of the lysate and then incubated at 37°C for 15 min with occasional mixing (swirling). After centrifugation at 21,100 × g for 15 min at 4°C, the pellet was resuspended in 20 mL Tris-FMN buffer (50 mM Tris-Cl [pH 7.6], 5 µM riboflavin 5'-monophosphate sodium salt hydrate [FMN, sigma F6750], 20 mM $MgSO_4$, 4 mM dithiothreitol, 4 µM resazurin), mixed with 2 µL of Pierce Universal Nuclease (250 U/µL), and further lysed with French press at 110 MPa. Cell debris and unbroken cells were removed by centrifugation at 14,000 × g for 30 min at

4°C. The cell membrane was pelleted via ultracentrifugation as described above, rinsed with 5 mL Tris-FMN buffer, and homogenized in 2.5 mL of the same buffer. An aliquot (c. 200 µL) of the cell membrane was stored at -80°C until use. The remainder (c. 2.3 mL) was incubated with a non-ionic detergent n-dodecyl β-D-maltoside (DDM) on ice with a stir bar inside to mix for 120 min. The mass of DDM added gave a final concentration of 1 mg DDM per mg cell protein. After ultracentrifugation at 208,000 × g for 60 min at 4°C, the supernatant was collected, stored at -80°C, and used as solubilized cell membrane.

Cell extract, cytoplasmic fraction, and cell membrane were prepared three or more times for each strain. Solubilized cell membrane was prepared separately and again at least three times.

Analysis of fermentation products and cells

Three, 70-mL cultures were inoculated and grown to the late-log phase (OD_{600} = 1.3 for *P. brevis* GA33 and OD_{600} = 4.0 for *P. ruminicola* 23). Cells were transferred to centrifuge tubes, with the exact volume measured with a pipette. Cells were harvested by centrifugation (21,100 × *g* for 20 min at 4°C; F15-8x50cy rotor and Sorvall Legend XTR centrifuge). The supernatant was stored at -20°C for later analysis. Cell pellets were resuspended in ddH_2O and harvested again by centrifugation (21,100 × *g* for 30 min at 4°C). Pellets were transferred to aluminum pans with ddH_2O and dried at 105°C overnight.

The dry mass of cells was determined by weighing the pan with dried pellet (while still hot) (Hackmann et al 2013b). After cooling, an aliquot of pellet was submitted for elemental analysis (C, H, N) by Intertek (Whitehouse, NJ). The cooled pellet was reweighed to correct for any water absorbed.

Supernatant was analyzed for glucose and fermentation products were measured as in the reference (Zhang et al 2021). Briefly, glucose was measured using glucose oxidase-peroxidase, adding 2 mol *N*-ethylmaleimide per mol cysteine in samples. Formate was measured using formate dehydrogenase. Succinate, L-lactate, and D-lactate was measured using commercial kits from R-Biopharm (product code 10176281035 and 11112821035). Ethanol was measured with a commercial kit from Megazyme (product code K-ETOH). Other fermentation products (acetate, propionate, butyrate, isobutyrate, and isovalerate) were measured using gas chromatography.

One aliquot of culture (5-mL) was also collected at the start of the incubation. Cells were removed by centrifugation (21,100 × *g* for 20 min at 4°C). The supernatant was stored at -20°C and analyzed as above.

The inoculant for cultures was 0.1 mL of a late-log phase culture. The dry mass of cells in this inoculant was determined by methods above. The elemental composition (C, H, N) was not measured and assumed the same as the samples described above.

Measurement of H_2

H_2 gas was measured using gas chromatography. The gas chromatograph was a Trace 1300 equipped with a thermal conductivity detector (TCD) (Thermo Scientific). Gas was sampled from the culture headspace by a gas-tight syringe (Hamilton, REF # 81356), and manually injected into the gas chromatograph. The column was a TG-BOND Q (30 m × 0.53 mm i.d. coated with 20 µm film thickness; Thermo Scientific). N_2 (2.5 mL/min flow rate) was the carrier gas. The injection was performed in split mode, with the split flow rate 75 mL/min, split ratio to be 30. The purge flow rate 3.0 mL/min. The back inlet had a temperature of 150°C. The initial oven temperature was 40°C, maintained for 3 min, raised to 150°C at 25°C/min, and finally held at 150°C for 2 min.

The TCD had a temperature of 150°C, the filament temperature was 200°C, and the reference gas flow rate was 1.5 mL/min. The injected sample gas volume was 1 mL, and the total run time for each analysis was 10.5 min. Data handling was carried out with Chromeleon Chromatography Data System software (Thermo Scientific).

Recovery of carbon and hydrogen

We calculated recovery of carbon in fermentation products and cells. Recovery is defined as the (total carbon at end)/(total carbon at start) × 100%.

To calculate the total carbon at the start (mmol C L^{-1}), we summed up carbon in glucose, fermentation acids, CO_2, and cells. For glucose, we measured the concentration (mmol L^{-1}) at the start of the incubation and multiplied it by its carbon content (6 mmol C $mmol^{-1}$). We did the same for fermentation acids or alcohols (formate, acetate, propionate, succinate, butyrate, isobutyrate, valerate, isovalerate, D-lactate, L-lactate, ethanol). For cells, we measured the dry mass of the inoculant (g L^{-1}) and multiplied it by the carbon content from elemental analysis (mmol C g^{-1}) (correcting for water). For CO_2, we defined the starting concentration as 0.

To calculate the total carbon at the end (mmol C L^{-1}), we again summed up carbon in glucose, fermentation acids, CO_2, and cells. We used the concentration of glucose and fermentation acids measured at the end of the incubation. For cells, we did the same. For CO_2, we calculated the amount produced from fermentation acids (mmol C L^{-1}) using stoichiometry. We assumed -1 CO_2/formate, 1 CO_2/acetate, -1 CO_2/succinate, 2 CO_2/butyrate, 2 CO_2/isobutyrate, 1 CO_2/valerate, 1 CO_2/isovalerate, and 1 CO_2/ethanol. We did not include for any CO_2 formed during cell synthesis.

Recovery of hydrogen was calculated analogously. For H_2O, we defined the starting concentration (mmol H L^{-1}) as 0. We calculated the ending concentration (mmol H L^{-1}) using

stoichiometry and assuming 1 H_2O/acetate, 1 H_2O/propionate, and 1 H_2O/succinate. We did not include for any H_2O formed during cell synthesis.

Balance of NAD_{ox} and Fd_{red}

The quantity of NAD_{ox} and Fd_{red} formed during fermentation and growth was calculated. We assumed -1 NAD_{ox}/acetate, +1 Fd_{red}/acetate, +1 NAD_{ox}/propionate, +1 NAD_{ox}/succinate, and -1 Fd_{red}/formate (see Figure 20 and 21). The value for formate (-1 Fd_{red}/formate) means that no Fd_{red} is formed when fermentation yields formate and acetate.

We also assumed 2.16 mmol NAD_{ox}/g cell and 1.64 mmol Fd_{red}/g cells (Table 4). This was calculated assuming that cell macromolecules are synthesized from glucose and ammonia, composition of cells in reference (Stouthamer 1973), and pathways for synthesis in MetaCyc (Caspi et al 2020) (see Table 3 for details).

Enzymatic assays

Most of the enzymatic assays were performed anaerobically at 37°C in a 1.4 mL glass cuvette (Hellma HL114-10-20) capped with chlorobutyl stopper (DWK Life Sciences W224100-081) under N_2. The assays for glyceraldehyde-3-phosphate dehydrogenase and malate dehydrogenase were performed at room temperature under aerobic conditions in 96-well plate (Corning UV-transparent microplate, product number 3635). After the start of the reaction, the absorbance at 340nm or 430 nm, or both, was monitored with SpectraMax M3 at 10 seconds or 15 seconds intervals. The reaction rate was calculated as the maximum linear change rate of absorbance over time. The absorbance coefficient for NADH at 340 nm is 6.2/mM/cm. The absorbance coefficient for ferredoxin at 430 nm is 13.1/mM/cm.

Glyceraldehyde-3-phosphate dehydrogenase assay. The activity of glyceraldehyde-3-phosphate dehydrogenase was measured aerobically in the 200-µL assay. The assay contained 50 mM Tricine-Na (pH 8.4), 10 mM KPO_4 buffer (pH 7), 2 mM dithiothreitol (DTT), 2 mM $MgCl_2$, 1 mM glyceraldehyde3-phosphate, 1 µg cell extract, and 1 mM NAD (sodium salt) or NADP (disodium salt). The reaction was initiated by the addition of NAD or NADP. Absorbance at 340 nm was recorded. The assay without cell extract was included as the negative control.

Malate dehydrogenase assay. The 200-µL assay for malate dehydrogenase (forming malate) contained 50 mM Tris-Cl (pH 7.6), 0.2 mM NADH (Sigma N8129) or NADPH (Calbiochem 481973), 1 µg cell extract, and 2 mM freshly prepared oxaloacetic acid (Sigma O4126). The reaction was initiated by the addition of oxaloacetic acid and absorbance at 340 nm was recorded.

Pyruvate:ferredoxin oxidoreductase (PFOR) assay. The PFOR activity was measured anaerobically at 37°C in a 1-mL assay that contained 50 mM Tris-Cl (pH 7.6), 10 mM $MgCl_2$, 4 mM DTT, 0.2 mM coenzyme A (lithium salt, Calbiochem 234101), 0.1 mM thiamine pyrophosphate (TPP), 4 U/mL phosphotransacetylase from *Bacillus subtilis* (product code E-PTABS), 10 mM sodium pyruvate, 30 µM ferredoxin that was isolated from *Clostridium pasteurianum* DSM 525 as described in the reference (Schönheit et al 1978) and about 15.1 µg cell extract or cytoplasmic fraction. The reaction was started by addition of sodium pyruvate. Absorbance at 430 nm was recorded.

Ferredoxin:NAD^+ oxidoreductase activity. The ferredoxin:NAD^+ oxidoreductase activity was measured anaerobically at 37°C in a 1-mL assay containing 50 mM Tris-Cl (pH 7.6), 10 mM $MgCl_2$, 4 mM DTT, 10 mM NaCl, about 80 µg cell membrane (or 40 µg solubilized cell membrane), 2 mM NAD (sodium salt), and a reduced ferredoxin-regenerating system (0.2 mM

CoA [lithium salt], 30 μM ferredoxin, 0.1 mM TPP, 4 U/mL phosphotransacetylase, 36.2 μg cytoplasmic fraction proteins of the corresponding bacteria, and 10 mM sodium pyruvate). The reaction was initiated by adding NAD. Before the addition of NAD, cell membrane sample was incubated with other components at 37°C until the absorbance at both 340 nm and 430 nm were stable. This incubation process was about 15 to 20 min. The assay without cell membrane was used as the blank control. The assay without ferredoxin or NAD was included to verify that the activity was dependent on both ferredoxin and NAD. Absorbance at 340 nm was recorded.

NADH:ubiquinone reductase (Na^+-transporting) and fumarate reductase/succinate dehydrogenase activity. The assay for NADH oxidase was performed anaerobically at 37°C in a 1-mL assay containing 100 mM KPO_4 (pH 6), 100 mM NaCl, 4 mM DTT, 0.4 mM NADH (disodium salt hydrate), and 40 μg of solubilized cell membrane or 80 μg of cell membrane. The reaction was initiated by adding a protein sample (cell membrane or solubilized cell membrane). The activity of NADH:ubiquinone reductase (Na^+-transporting) was calculated by measuring the maximum linear rate of NADH oxidation in the absence of fumarate. To measure fumarate reductase/succinate dehydrogenase activity, 5 mM disodium fumarate was added to the assay described above. The activity of fumarate reductase/succinate dehydrogenase was calculated by subtracting the maximum linear rate of NADH oxidation in the absence of fumarate from that of NADH oxidation in the presence of fumarate. The assays without enzyme sample were used as blank controls for both activities. Absorbance at 340 nm was recorded.

Na^+-dependent ferredoxin:NAD^+ oxidoreductase activity. The activity of ferredoxin:NAD^+ oxidoreductase was measured in the same way as the assays described above but in the presence of different amount of Na^+. NAD sodium salt was replaced with NAD hydrate (Sigma N1511). Sodium pyruvate was replaced with potassium pyruvate. CoA (lithium salt) was

replaced with CoA hydrate (Sigma C4282). The final concentration of Na^+ in the assay was 0, 0.1, 2, and 20 mM. The contaminated Na^+ in the Tris-Cl buffer and $MgCl_2$ was measured by sodium probe (Fisher Accumet 13-620-503A) and it was about 2 µM.

ATPase activity. The ATPase activity was measured according to the reference (Schoelmerich et al 2020). ATPase activity was measured by monitoring phosphate production. The assays were carried out in 1.5-mL tubes at a final liquid volume of 0.1 mL at 37°C. The assay contained 100 mM Tris-Cl (pH 7.4), 5 mM $MgCl_2$, 3.6 mM ATP-DiTris, and 6.25 µg cell membrane protein (cell membrane or solubilized cell membrane). Membrane protein sample was mixed with Tris-Cl and $MgCl_2$, and incubated at 37°C in water bath for 5 min. The reaction was started by the addition of 3.6 mM ATP-DiTris, incubated at 37°C for different time lengths (0, 4, 8, 12 min), and terminated by the addition of 14.3 µL of 30% (w/V) trichloroacetic acid. For the 0 min reaction, trichloroacetic acid was added before the addition of ATP-DiTris. After centrifugation at 13,000 × g for 5 min at room temperature, 90 µL of the supernatant was mixed with freshly-prepared 450 µL of AAM-reagent (acetone: 5N H_2SO_4: 10 mM $(NH_4)_6Mo_7O_{24}$ in a volume ratio of 2:1:1) and incubated at room temperature for 10 min. Absorbance at 355 nm was monitored and calibrated with standard curves.

Proteomics

Preparation of samples. LC-MS/MS was used to determine what genes were expressed in the cells of *P. brevis* GA33 and *P. ruminicola* 23. Peptides of proteins in the cell extract were prepared according to the reference (Zhang et al 2021). Briefly, Proteins were precipitated by trichloroacetic acid/acetone solution, denatured by urea, reduced by dithiothreitol, alkylated by iodoacetamide, digested by trypsin/Lys-C mix (V5073; Promega), cleaned-up by Pierce C_{18} Tips (87784; Thermo Scientific), and resuspended in 0.1% (v/v) trifluoroacetic acid for LC-MS analysis.

Peptides of proteins in the cell membrane were prepared according to reference (Sievers 2018) with several modifications. Cell membrane in the cell extract was pelleted via ultracentrifugation at 208,000 × g for 1 hour at 4°C, rinsed with 5 mL Tris-$MgSO_4$ buffer, and homogenized in 2 mL of the same buffer by suspending it in the buffer with a pipette. The centrifuge tube was filled up to 17 mL with Tris-$MgSO_4$ buffer and the cell membrane was pelleted again.

The following steps were performed aerobically. The pellet was solubilized in 2 mL ice-cold carbonate buffer (100 mM Na_2CO_3, 100 mM NaCl, pH 11), mixed with 8 mL carbonate buffer, and incubated on ice for 60 min with a stir inside to mix well. Every 15 min the sample was further homogenized by drawing it up and down with a syringe five times using a long needle. After ultracentrifugation, the membrane pellet was resuspended in 600 μL solubilization buffer (50 mM Tris-Cl [pH 7.5], 8 M urea, 1% (w/v) 3-[(3-cholamidopropyl)dimethylammonio]-1-propanesulfonate), centrifuged at 12,000 × g for 10 min at 4°C, and transferred to a 2-mL screw tube. A TCEP solution (500 mM Tris(2-carboxyethyl)phosphine [TCEP] in 200 mM Tris-Cl [pH 8]) was added to the sample to give a final concentration of 5 mM TCEP. After incubation at 30°C for 60 min, the sample was alkylated by fresh iodoacetamide (10 mM final concentration) at room temperature for 30 min in the dark. The protein concentration was measured with a Pierce BCA protein assay kit (23227; Thermo Scientific).

The sample was mixed with equal volume of SDS-PAGE sample buffer (125 mM Tris-Cl [pH 6.8], 20% (v/v) glycerol, 20% (w/v) sodium dodecyl sulfate (SDS), a trace of Brilliant blue G-250) and loaded into gel wells. After electrophoresis at 140 V for 60 min, the gel (12% acrylamide, 29:1 acrylamide–bis-acrylamide) was fixed in a solution (40% [v/v] ethanol/10% [v/v] acetic acid), washed with distilled water, and visualized by Blue silver stain solution (100 g/L

ammonium sulfate, 10% [v/v] phosphoric acid, 1.2 g/L Brilliant Blue G-250, 20% [v/v] methanol). The gel lanes loaded with samples were cut into gel pieces. The gel pieces were completely destained with gel washing solution (50% (v/v) acetonitrile LC/MS grade and 50 mM NH_4HCO_3 in water), dehydrated by pure acetonitrile, and mixed with diluted trypsin/Lys-C (V5073; Promega) (10 ng/µL) in 50 mM NH_4HCO_3 for incubation at 37°C for 16 hours. One µg of trypsin/Lys-C was used for digestion per 8 µg of membrane protein.

Peptides were extracted from the gel pieces by dehydration in acetonitrile, rehydration in 1% (v/v) acetic acid, drying in acetonitrile, 10 min ultrasonication in 5% (v/v) acetic acid, 10 min ultrasonication in acetonitrile, and drying in acetonitrile. The supernatants were pooled, reduced to dryness by vacuum centrifugation, and resuspended in 1% (v/v) TFA (trifluoroacetic acid). The peptides were further cleaned and desalted with the 100-µL Pierce C_{18} Tips (87784; Thermo Scientific) according to the instructions. Peptides were eluted with 0.1% (v/v) acetic acid/75% (v/v) acetonitrile, dried by vacuum centrifugation, and resuspended in 0.1% TFA.

Data dependent analysis. The resulting peptides of both cell extract and cell membrane were analyzed with LC/MS according to the reference (Zhang et al 2021). Peptides and proteins were identified from LC-MS/MS data using X!TandemPipeline (Langella et al 2017).

Data independent analysis. The resulting peptides of cell membrane were also processed for data acquisition by data-independent acquisition (DIA). Peptides were desalted and trapped on a Thermo PepMap trap and separated on an Easy-spray C_{18} column (100 µm by 25 cm) using a Dionex Ultimate 3000 nUPLC at 200 nL/min. Solvent A was 0.1% (v/v) formic acid and solvent B was 100% acetonitrile 0.1% (v/v) formic acid. Gradient conditions were 2% B to 50% B over 60 minutes, followed by a 50%-99% B in 6 minutes and then held for 3 minutes than 99% B to 2%B in 2 minutes and total run time of 90 minutes using Thermo Scientific Fusion Lumos mass

spectrometer. The samples were run in DIA mode. Mass spectra were acquired using a collision energy of 35, resolution of 30 K, maximum inject time of 54 ms and an AGC target of 50 K, using staggered isolation windows of 12 Da in the m/z range 400-1000 m/z.

The DIA data was analyzed using Spectronaut 15 using the directDIA workflow with the default settings. Peak area intensities were exported from Spectronaut. Quantitative and statistical analysis was performed processing protein peak areas determined by the Spectronaut software. Prior to library-based analysis of the DIA data, the DIA raw files were converted into htrms files using the htrms converter (Biognosys). MS1 and MS2 data were centroided during conversion, and the other parameters were set to default. The htrms files were analyzed with Spectronaut (version: 15, Biognosys) via directDIA. Precursor and protein identifications were filtered to 1% false discovery rate.

Information for organisms in Bergey's Manual of Systematics of Archaea and Bacteria

The phenotypic, genomic, and other information for organisms in *Bergey's Manual of Systematics of Archaea and Bacteria* (Whitman 2022) were collected. First, all n = 1836 articles for genera in *Bergey's Manual of systematics of Archaea and Bacteria* were downloaded. Then the names and written descriptions of n = 8026 type strains were extracted. R scripts from the reference (Hackmann and Zhang 2021) were used to automate this process.

The written descriptions of the type strains were read to collect phenotypic information. This information included fermentative ability, major fermentation end products, minor fermentation end products, and substrate used to form end products.

The R scripts from the reference (Hackmann and Zhang 2021) were used to collect genomic information. These scripts extracted out GOLD organism ID, GOLD project ID, and IMG genome ID. Other information extracted included the organism's taxonomy and article link.

Searches for genes and proteins

The genomes for genes involved in forming propionate, succinate, and acetate were searched. To perform this search, we used IMG/M database (Chen et al 2019), the IMG/M genome ID for each genome, and the KEGG Orthology (KO) ID for each gene (Kanehisa et al 2021). For some genes, the COG (Galperin et al 2015) or pfam (Mistry et al 2021) ID were instead searched for.

For hydrogenases, the search for genes was more involved. We searched for genes using the pfam ID, then uploaded sequences of matches to HydDB (Sondergaard et al 2016). HydDB classified the sequences as [FeFe] Group A, [NiFe] Group 1c, [NiFe] Group 1d, or other. Following the rules of HydDB (Sondergaard et al 2016), we further classified [FeFe]-Group A hydrogenases as Group A1, A2, A3, or A4 (depending on what genes were adjacent).

For each gene, we report the respective enzyme name, enzyme symbol, EC number, and biochemical reaction. This information came from KEGG (Kanehisa et al 2021) and HydDB (Sondergaard et al 2016). An enzyme was considered present in the genome if genes for all subunits was found. A reaction was considered present if at least one isozyme was found.

Other bioinformatic analyses

Proteomes were searched for proteins using locus tags for genes above. Phylogenetic trees were constructed according to the reference (Hackmann and Zhang 2021). We found habitats of organisms forming propionate, succinate, and acetate using *Bergey's Manual of Systematics of Archaea and Bacteria* (Whitman 2022), BacDive (Reimer et al 2019), and information from public

culture collections. Structures of proteins were predicted using ColabFold (Mirdita et al 2021), then they were visualized with PyMOL according to the reference (Hackmann 2022).

Other analysis

Protein concentration in the cell extract, cell membrane, cytoplasmic fraction, and solubilized cell membrane were measured using the Bradford protein assay (Bradford 1976). The blank controls for these samples are the corresponding buffers. The standards used are bovine serum albumin.

A one-sided *t*-test was used to determine if mean yield of fermentation products was greater than 0. The same test was also used for mean values of enzymatic activity. *P*-values reported are for that test.

Results

Prevotella form propionate, succinate, and acetate during fermentation

Our hypothesis is that fermentation of glucose to propionate, succinate, and acetate uses Rnf. Two bacteria from rumen (*Prevotella brevis* GA33 and *Prevotella ruminicola* 23) were used to test this hypothesis. The first step was to verify that these organisms form propionate, succinate, and acetate and these products are in the ratios expected (Figure 14 and 15). We grew these bacteria on media containing glucose and ammonia, then analyzed the culture for several products. For *P. brevis* GA33, a medium that also contained yeast extract and trypticase was used, as the strain GA33 would not grow on media with glucose only.

Both bacteria fermented glucose to acetate and succinate (Figure 14A and 15A). Propionate was formed in large amounts by *P. ruminicola* 23, whereas it was formed in only trace amounts by *P. brevis* GA33. The ratio of succinate and propionate to acetate was approximately 2:1. They

also formed formate, D-lactate, and L-lactate, but only in trace amounts. No H_2 was observed for either bacterium (Figure 16).

The observation of these fermentation products is consistent with genomic prediction, except the observation of trace amount of propionate from *P. brevis* GA33. To more accurately measure propionate yield, *P. brevis* GA33 was cultured on the medium with no added acetate and propionate. Under these conditions, no propionate was observed (data not shown). This confirms that *P. brevis* GA33 forms mainly acetate and succinate (not propionate). To confirm that our analysis can measure trace amount of H_2, the gas sample from *S. ruminantium* HD4, a rumen bacterium forming trace amount of H_2 (Scheifinger et al 1975), was included as a positive control. We were able to measure the H_2 produced from *S. ruminantium* HD4 (Figure 16), confirming that our analysis works for detecting H_2. Our previous genomic analysis did not identify any genes encoding hydrogenase or bifurcating enzymes, which explains why no H_2 was formed by *P. brevis* GA33 and *P. ruminicola* 23.

Carbon recovery and hydrogen recovery analysis were performed to check how accurately we measured products. The carbon recovery is the ratio total carbon atoms of glucose, fermentation acids, CO_2 and cells in the culture at the harvested time to the total carbon atoms in the culture at the start (immediately after inoculation but before incubation). Hydrogen recovery is defined similarly. If all fermentation products were accurately measured in our analysis, the recovery should be 100%. Indeed, both carbon recovery and hydrogen recovery were near or above 100% (Figure 14B, 14C, 15B, and 15C). For *P. brevis* GA33, values were above 100% because our calculations did not account for trypticase and yeast extract also in the medium of this bacterium. The high recoveries of carbon and hydrogen indicate that we measured all products accurately.

In sum, our work shows that *Prevotella* form propionate, succinate, and acetate as the sole products of fermentation (Figure 14D and 15D). Additionally, they form these products in the ratio expected (Figure 13).

Fermentation in *Prevotella* appears to be unbalanced

We hypothesize that *Prevotella* use Rnf to balance fermentation. Without this enzyme, fermentation should produce excess NAD_{ox} and Fd_{red}. We determined if this was indeed the case for *Prevotella*.

The quantity of NAD_{ox} and Fd_{red} produced during the experiments above was calculated. Our calculations revealed that excess NAD_{ox} and Fd_{red} were indeed formed. The amount was 2.7 NAD_{ox} and 2.3 Fd_{red} per 3 glucose (Table 4). This was even higher than expected (Figure 13) and owed to additional NAD_{ox} and Fd_{red} being formed during production of cells (particularly lipid) (Table 3). This calculation did not include activity of Rnf, and it shows without this enzyme, fermentation would indeed be unbalanced.

We performed calculations on *P. ruminicola* 23 only. To calculate the quantity of NAD_{ox} and Fd_{red} formed during production of cells, we assumed macromolecules were synthesized from glucose and ammonia. This would not have been a good assumption for *P. brevis* GA33, where macromolecules could have also come from trypticase and yeast extract.

Our calculation points to an apparent excess of NAD_{ox} and Fd_{red} formed during fermentation and growth. This points to the need for Rnf.

***Prevotella* have the enzyme Rnf**

Having established a need for Rnf, we determined if this enzyme is indeed possessed by *Prevotella*. The presence of Rnf was tested with a combination of genomics, proteomics, and enzyme assays.

Rnf was found in both genome and proteome (Figure 17 and 18). First, the genome sequence of *P. brevis* GA33 and *P. ruminicola* 23 were searched for genes encoding Rnf. The genomes of both species had genes for all six subunits of the enzyme (Figure 17A and 18A). The gene arrangements are identical in both genomes.

By performing shotgun proteomics, we confirmed Rnf is expressed. We prepared peptide samples from both cell extract and cell membrane for each bacterium. We then performed shotgun proteomics with data-dependent acquisition (DDA) and data-independent acquisition (DIA) methods. This revealed that up to four subunits (RnfB, RnfC, RnfG, and RnfD) were expressed, depending on the species, sample, and method used (Figure 17 and 18). The remaining subunits (RnfA and RnfE) were not detected, likely because they are predicted to be integral proteins (Figure 17 and 18). These subunits have evaded detection even in purified Rnf (Kuhns et al 2020).

To verify that Rnf was present, we measured the ferredoxin:NAD^+ oxidoreductase activity of Rnf using enzymatic assays. To do so, we measured formation of NAD_{red} by cell membranes in the presence of Fd_{red}. We found that NAD_{red} was indeed formed and thus both species had activity (Figure 17C and 18C). Activity depended on adding both Fd_{red} and NAD_{ox}, as expected. At first, activity appeared low and was difficult to detect. However, we found higher activity after correcting for activity of NADH oxidase (also present in membranes). We found higher activity still after performing a partial purification of Rnf (by solubilizing the membrane in detergent) (Figure 17C and 18C). This shows that activity, at first low, is indeed present and on par with other enzymes (see below).

To verify that this activity was due to Rnf, not another enzyme, we determined its dependence on sodium. In most species, Rnf pumps sodium ions to create a gradient and thus depends on them for high activity (Biegel and Muller 2010, Hess et al 2016, Kuhns et al 2020). We found that *P. brevis* GA33 did not grow without sodium, showing a general dependence on this ion (Figure 19A). We found the same for *P. ruminicola* 23 (data not shown). Further, when we directly tested if catalytic activity of Rnf depended on sodium, we found that it did (Figure 19B). In sum, our work at the genomic, proteomic, and enzymatic level establishes that *Prevotella* have Rnf. With it, *Prevotella* can handle excess NAD_{ox} and Fd_{red} produced during fermentation.

Prevotella have other enzymes needed to form fermentation products

After find that Rnf was present in Prevotella, we determined if other enzymes forming propionate, succinate, and acetate were also present. It is important to confirm that redox cofactors (NAD_{ox} and Fd_{red}) are produced in the pathway as expected. Again, this was done by a combination of genomics, proteomics, and enzyme assays.

All enzymes converting glucose to acetate and succinate in *P. brevis* GA33 were detected in the proteome (Figure 20, Table 5 and 6), except that the enzyme (enolase) converting glycerate-2-phosphate to phosphoenolpyruvate was missing. Similarly, all enzymes in the pathway converting glucose to acetate, succinate, and propionate were part of the proteome (Figure 21, Table 5 and 7) of *P. ruminicola* 23, except that enolase and methylmalonyl-CoA decarboxylase were missing.

We focused on enzymes involved in regenerating redox cofactors, NAD or ferredoxin in both bacteria. These enzymes include glyceraldehyde-3-phosphate dehydrogenase, malate dehydrogenase, pyruvate:ferredoxin oxidoreductase, NADH:ubiquinone reductase (Na^+-

transporting), fumarate reductase/succinate dehydrogenase, in addition to Rnf. To verify the function of other redox related enzymes in the cell, we performed enzymatic assays to measure activities of these redox related enzymes. The activities of these enzymes were summarized in Table 8. Overall, all these redox related enzymes displayed measurable activities in the respective fraction, confirming their function in the cell. Glyceraldehyde-3-phosphate dehydrogenase had activity to reduce NAD_{ox} and $NADP_{ox}$ using glyceraldehyde-3-phosphate. Malate dehydrogenase had the activity to oxidize NAD_{red} and $NADP_{red}$ using oxaloacetate. Our work confirms that *Prevotella* have the expected enzymes for forming propionate, succinate, and acetate—including those that form NAD_{ox} and Fd_{red}. Rnf is needed to complete this pathway.

Rnf is important in many organisms forming propionate succinate and acetate

To determine how many microbes could use Rnf to form acetate, propionate/succinate during fermentation, we analyzed prokaryotes reported in the *Bergey's Manual of Systematics of Archaea and Bacteria* (Whitman 2022) according to methods described in the reference (Hackmann and Zhang 2021). The written descriptions for information about fermentation were searched. We found 39 fermentation products reported for over 1,400 type strains (Figure 22, Dataset S6). By analyzing the major fermentation products, we identified that nearly 10% of these fermentative type strains form propionate, succinate, and acetate (Figure 22).

We also searched for Rnf genes in genomes of prokaryotes recorded in the *Bergey's Manual of Systematics of Archaea and Bacteria*. These prokaryotes include all prokaryotes with an available genome sequence. We found that about 20% of prokaryotes encode Rnf in their genomes (Figure 23A, Dataset S7). We then searched genomes of prokaryotes that are also fermentative. About 30% of fermentative prokaryotes encode Rnf genes. Interestingly, Rnf genes are encoded by an even higher percentage of organisms that also form acetate and

succinate/propionate (nearly 40%). The enrichment of genes in such organisms shows an importance of Rnf.

With this search and analysis, we identified 44 type strains that encode Rnf and form acetate and succinate/propionate during fermentation (Dataset S6). A phylogenetic tree shows that these strains are diverse, and they belong to 15 genera (Figure 23B). Examining their habitats shows that they come from the gut, aquatic sediment, anaerobic digesters, and elsewhere (Figure 23C, Dataset S8). Together, these results show that Rnf is important not just to propionate formation in *Prevotella*, but also important to many organisms from various different habitats.

Organisms have alternatives to Rnf, but they are uncommon

By oxidizing Fd_{red} and reducing NAD_{ox}, Rnf is one enzyme that fill in the missing step of the pathway we study. However, other alternatives can be imagined. To see if any alternatives were common, we used the same genomic and phenotypic data for prokaryotes as before.

Five possible pathways were taken into consideration (Figure 24, Dataset S7, Dataset S8). One pathway involves the enzyme pyruvate dehydrogenase. When this enzyme replaces pyruvate:ferredoxin oxidoreductase, the resulting pathway is balanced without Rnf. This in fact is the original pathway proposed for propionate formation 60 years ago (Allen et al 1964). However, it is uncommon; only 17% of organisms that form propionate, succinate, and acetate encode this enzyme. The four other pathways—involving prototypical hydrogenase, bifurcating hydrogenase, formate dehydrogenase, or *Campylobacter*-type Nuo—are even less common. Further, none of these five pathways was found in *Prevotella*. This underscores the importance of Rnf to the myriad organisms forming propionate, succinate, and acetate.

Discussion

Our study shows Rnf is important to forming propionate during fermentation. In *Prevotella*, we show that fermentation is apparently unbalanced and produces excess Fd_{red} and NAD_{ox}. Rnf handles the excess Fd_{red} and NAD_{ox} by converting them back to Fd_{ox} and NAD_{red}. Rnf thus fills in a missing step of the pathway and allows fermentation to continue.

The pathways for forming propionate have been studied for over 60 years (Allen et al 1964), yet the need for an enzyme like Rnf was recognized only recently (Hackmann et al 2017, McCubbin et al 2020). A possible reason it has been overlooked is that the pathway was first elucidated in propionibacteria (Allen et al 1964). Propionibacteria have pyruvate dehydrogenase. If this enzyme is used, it can make the redox balanced without Rnf (Allen et al 1964). A pathway with pyruvate dehydrogenase, though plausible, appears seldom used. First, our work shows few organisms forming propionate also encode pyruvate dehydrogenase (Figure 24A). Second, propionibacteria themselves may not use pyruvate dehydrogenase. Recent work shows they also have pyruvate:ferredoxin oxidoreductase, which is expressed and required for normal growth (McCubbin et al 2020). Thus, a need for an enzyme like Rnf is real.

In earlier work, we proposed Rnf could fill in this missing step (Hackmann et al 2017). Rnf is known to play a similar role in other pathways. Examples include forming the short chain fatty acid butyrate. Rnf and another membrane protein Ech oxidize Fd_{red} generated by pyruvate:ferredoxin oxidoreductase and butyryl-CoA dehydrogenase during glucose and xylose fermentation in *Pseudobutyrivibrio ruminis* (Schoelmerich et al 2020). Similarly, during glutamate fermentation in *Clostridium tetanomophum*, Rnf and a [FeFe]-hydrogenase oxidize the Fd_{red} formed by butyryl-CoA dehydrogenase and pyruvate:ferredoxin oxidoreductase (Buckel 2021). Rnf also plays a role in ethanol production in *Clostridium thermocellum* (Lo et al 2017). Deletion

of Rnf genes in *C. thermocellum* resulted in a decrease in ethanol formation and overexpression of Rnf genes increased ethanol production. The importance of Rnf has not been demonstrated in forming propionate.

Our untargeted proteomics identified all enzymes involved in ferment glucose to acetate and propionate/succinate except enolase in *P. brevis* GA33. The gene encoding enolase in *P. brevis* GA33 is not identified, as reported in previous study (Hackmann et al 2017), which explains why enolase is also missing in the proteome. Further, our genomic and proteomic analysis identified most enzymes in the succinate pathway for forming propionate in *P. ruminicola* 23, while we did not identify genes encoding enzymes for the acrylate pathway. The acrylate pathway was proposed for forming propionate as evidenced by enzymatic assays and labeling patterns in propionate (Joyner and Baldwin 1966, Wallnofer and Baldwin 1967); however, the acrylate pathway cannot explain the vitamin B_{12}-dependent propionate production (Strobel 1992). Although we identified most enzymes in the succinate pathway, the step converting (D)-methylmalonyl-CoA to propionyl-CoA is missing. Preliminary experiment suggested that *P. ruminicola* 23 did not have the methylmalonyl-CoA decarboxylase activity (Strobel 1992), leaving this step to be unknown.

Our work shows Rnf is enriched in organisms that form acetate and propionate/succinate. Not all genomes of fermentative bacteria that form acetate and propionate/succinate encode Rnf. This could be explained by multiple reasons. First, part of these fermentative bacteria may not use the succinate pathway, but use the acrylate pathway to form propionate/succinate, such as *Clostridium propionicum* (Hetzel et al 2003) and *Megasphaera elsdenii* (Hino and Kuroda 1993). Second, some of these propionate-forming bacteria do not use glucose but ferment fucose or rhamnose to form propionate, such as human gut anaerobe *Roseburia inulinivorans* (Scott et al 2006).

We find that many bacteria could use Rnf for propionate/succinate formation. They are identified by searching a set of genomes for Rnf genes. This set of bacteria have special phenotypic features: they are fermentative and also form acetate and propionate/succinate. This method can be used for exploring importance of certain enzyme(s) in the organisms with special features. For instance, we can explore how the enzyme pyruvate:ferredoxin oxidoreductase distributes in prokaryotes, prokaryotes that are fermentative, and fermentative prokaryotes that also form acetate. By performing such genomic search, we could gain the insights about the relevance of pyruvate:ferredoxin oxidoreductase to acetate formation during fermentation.

This work shows Rnf is involved in redox balance for propionate formation during glucose fermentation. In addition of Rnf, hydrogenases and bifurcating enzymes are common in oxidizing Fd_{red} for regenerating redox cofactors (Peters et al 1998, Schut and Adams 2009). The role of these enzymes other than Rnf in forming propionate/succinate has not yet been elucidated. Future work should continue to explore the complicated pathways for redox balance during fermentative propionate production.

Table 3. Consumption and production of $NAD(P)_{ox}$ and Fd_{red} for synthesizing cell components

Component	Amount	Redox cofactors formed[1]			
		$NAD(P)_{ox}$	Fd_{red}	$NAD(P)_{ox}$	Fd_{red}
	mmol/g cells	mmol/mmol component		mmol/g cell	
Amino acids					
Alanine	0.454	0	0	0.00	0.00
Arginine	0.252	4	-1	1.01	-0.25
Asparagine	0.101	0	0	0.00	0.00
Aspartate	0.201	0	0	0.00	0.00
Cysteine	0.101	-2	1	-0.20	0.10
Glutamate	0.353	2	-1	0.71	-0.35
Glutamine	0.201	2	-1	0.40	-0.20
Glycine	0.403	-1	0	-0.40	0.00
Histidine	0.05	-1	0	-0.05	0.00
Isoleucine	0.252	1	-1	0.25	-0.25
Leucine	0.403	-2	1	-0.81	0.40
Lysine	0.403	-2	0	-0.81	0.00
Methionine	0.201	1	1	0.20	0.20
Phenylalanine	0.151	0	0	0.00	0.00
Proline	0.252	4	-1	1.01	-0.25
Serine	0.302	-1	0	-0.30	0.00
Threonine	0.252	2	0	0.50	0.00
Tryptophan	0.05	-2	0	-0.10	0.00
Tyrosine	0.101	0	0	0.00	0.00
Valine	0.302	0	0	0.00	0.00
Ribonucleotides					
AMP	0.14	-1	0	-0.14	0.00

CONTINUED

Table 3: CONTINUED

CMP	0.14	-1	0		-0.14	0.00
GMP	0.14	-2	0		-0.28	0.00
UMP	0.115	-1	0		-0.12	0.00
Deoxyribonucleotides						
dAMP	0.024	-1	0		-0.02	0.00
dCMP	0.024	-1	0		-0.02	0.00
dGMP	0.024	-2	0		-0.05	0.00
dTMP	0.024	-1	0		-0.02	0.00
Lipid						
1,2-Palmitoyl phosphatidylethanolamine	0.14	11	16		1.54	2.24
Carbohydrate						
Glucose (as glycogen)	1.026	0	0		0.00	0.00
				Total	2.16	1.64

[1]Negative values for $NAD(P)_{ox}$ mean it is consumed and $NAD(P)_{red}$ is produced; negative values for Fd_{red} mean it is consumed and Fd_{ox} is produced

Table 4. Consumption and production of NAD_{ox} and Fd_{red} in *P. ruminicola* 23 without Rnf

	Yield		Redox cofactors formed[5,6]	
	mmol/(mmol glucose consumed)[1,2]	mmol/(mmol glucose fermented)[3,4]	mmol $NAD(P)_{ox}$/(mmol glucose fermented)	mmol Fd_{red}/(mmol glucose fermented)
Product[7]				
Ac	0.415	0.646	-0.646	0.646
Pr	0.589	0.917	0.917	0.000
Suc	0.279	0.434	0.434	0.000
For	0.029	0.046	0.000	-0.046
D-Lac	0.001	0.001	0.000	0.000
L-Lac	0.001	0.001	0.000	0.000
Cells	0.060	0.093	0.201	0.152
		Total per 1 glucose fermented	0.91	0.75
		Total per 3 glucose fermented	2.72	2.26

[1]Values from Figure 15A

[2]For cells, units are kg/mol glucose consumed

[3]Assumes 1/2 glucose fermented per 1 Ac, 1 Pr, 1 Suc, 1 D-Lac, and 1 L-Lac

[4]For cells, units are g/mmol glucose fermented

[5]Assumes -1 NAD_{ox}/Ac, +1 Fd_{red}/Ac, +1 NAD_{ox}/Pr, +1 NAD_{ox}/Suc, -1 Fd_{red}/For, -1.08 mmol NAD_{ox}/g cells, +1.33 mmol Fd_{red}/g cells , and 0 elsewhere (see text and also Table 3)

[6]Negative values for $NAD(P)_{ox}$ mean it is consumed and $NAD(P)_{red}$ is produced; negative values for Fdred mean it is consumed and Fd_{ox} is produced

[7]Ac, acetate; Pr, propionate; Suc, succinate; For, formate; D-Lac, D-lactate; L-Lac, L-lactate

Table 5. Reaction ID, enzyme name, database ID, and locus tags of *P. brevis* GA33 and *P. ruminicola* 23

Reaction ID	Enzyme name	Enzyme Commission (EC) number	Database ID	Gene in *P. brevis* GA33 genome (locus tag)[1]	Gene in *P. ruminicola* 23 genome (locus tag)[1]
1	Glucokinase/hexokinase	2.7.1.1, 2.7.1.2	K00845	T433DRAFT_02353, T433DRAFT_00587, T433DRAFT_01666	PRU_0395, PRU_1689, PRU_0241, PRU_2364, PRU_1688, PRU_1690
2	Glucose-6-phosphate isomerase	5.3.1.9	K01810	T433DRAFT_02677	PRU_1785
3	6-Phosphofructokinase	2.7.1.11	K00850	T433DRAFT_01181	PRU_1201
4	Fructose-bisphosphate aldolase	4.1.2.13	K01624	T433DRAFT_00274	PRU_2062
5	Triose-phosphate isomerase	5.3.1.1	COG0149	T433DRAFT_01090	PRU_1860
6	Glyceraldehyde-3-phosphate dehydrogenase (phosphorylating)	1.2.1.12, 1.2.1.59	K00134	T433DRAFT_02421	PRU_1674
7	Phosphoglycerate kinase	2.7.2.3	K00927	T433DRAFT_02583	PRU_1634
8	Phosphoglycerate mutase	5.4.2.11, 5.4.2.12	K15633	T433DRAFT_00046	PRU_2355
			K15635	T433DRAFT_00616	PRU_1017
9	Phosphopyruvate hydratase	4.2.1.11	K01689	NA	PRU_1102
10	Pyruvate kinase	2.7.1.40	K00873	T433DRAFT_00542	PRU_0684
11	Pyruvate:ferredoxin oxidoreductase	1.2.7.1, 1.2.7.11	K00174	T433DRAFT_00478, T433DRAFT_00605	PRU_1149, PRU_2267
			K00175	T433DRAFT_00604, T433DRAFT_00477	PRU_2268
			K03737	T433DRAFT_00909	PRU_1235
12	Phosphate acetyltransferase	2.3.1.8	K00625	T433DRAFT_02303	PRU_2260
13	Acetate kinase	2.7.2.1	K00925	T433DRAFT_02304	PRU_2259
14	Phosphoenolpyruvate carboxykinase (ATP)	4.1.1.49	K01610	T433DRAFT_02048	PRU_2279

CONTINUED

Table 5: CONTINUED

15	Malate dehydrogenase	1.1.1.37	K00024	T433DRAFT_01517	PRU_2158
16	Fumarate hydratase	4.2.1.2	K01676	T433DRAFT_00348	PRU_0119
17	Propionyl-CoA:succinate CoA transferase	2.8.3.27	COG0427	T433DRAFT_00482	PRU_2762
18	Methylmalonyl-CoA mutase	5.4.99.2	K01847	T433DRAFT_00914, T433DRAFT_00915	PRU_1640, PRU_1639
19	Methylmalonyl-CoA epimerase	5.1.99.1	K05606	T433DRAFT_01907	PRU_1230
20	Methylmalonyl-CoA decarboxylase	4.1.1.41	K11264	NA	NA
			K18426	NA	NA
21	Ferredoxin-NAD^+ oxidoreductase (Na^+-transporting)	7.2.1.2	K03617	T433DRAFT_01721	PRU_0809
			COG2878	T433DRAFT_01716	PRU_0804
			K03615	T433DRAFT_01717	PRU_0805
			K03614	T433DRAFT_01718	PRU_0806
			K03613	T433DRAFT_01720	PRU_0808
			K03612	T433DRAFT_01719, T433DRAFT_00349	PRU_0807
22	NADH:ubiquinone reductase (Na^+-transporting)	7.2.1.1	K00346	T433DRAFT_00925	PRU_1250
			K00347	T433DRAFT_00926	PRU_1249
			K00348	T433DRAFT_00927	PRU_1248
			K00349	T433DRAFT_00928	PRU_1247
			K00350	T433DRAFT_00929	PRU_1246
			K00351	T433DRAFT_00930	PRU_1245
23	Fumarate reductase/succinate dehydrogenase	1.3.5.1, 1.3.5.4	K00239	T433DRAFT_02095	PRU_2432
			K00240	T433DRAFT_02094	PRU_2431

CONTINUED

Table 5: CONTINUED

24	ATP synthase	7.1.2.2	K00241	T433DRAFT_02096	PRU_2433
			K02108	T433DRAFT_01651	PRU_1196
			K02109	T433DRAFT_01653	PRU_1194
			K02110	T433DRAFT_01652	PRU_1195
			K02111	T433DRAFT_01655	PRU_1192
			K02112	T433DRAFT_01648	PRU_1199
			COG0224	T433DRAFT_01656	PRU_1191
			K02113	T433DRAFT_01654	PRU_1193
			K02114	T433DRAFT_01649	PRU_1198
25	D-glyceraldehyde-3-phosphate:$NADP^+$ oxidoreductase (phosphorylating)	1.2.1.13, 1.2.1.59	K00150, K05298	NA	NA
26	(S)-malate:$NADP^+$ oxidoreductase	1.1.1.82	K00051	NA	NA
27	Methylmalonyl-CoA carboxytransferase[2]	2.1.3.1	K03416	NA	NA
			K17489	NA	NA
28	Diphosphate-fructose-6-phosphate 1-phosphotransferase[3]	2.7.1.90	K00895	T433DRAFT_00987	PRU_0792
29	Pyruvate, phosphate dikinase[4]	2.7.9.1	K01006	T433DRAFT_02597	PRU_1512
30	H^+-pyrophosphatase[5]	7.1.3.2	K15987	T433DRAFT_00912	PRU_0830
31	Acetate-CoA ligase[6]	6.2.1.1	K01895	T433DRAFT_02325	PRU_2205
32	Formate C-acetyltransferase[7]	2.3.1.54	K00656	T433DRAFT_01500	PRU_1243
33	Phosphate butyryltransferase[8]	2.3.1.19	K00634	T433DRAFT_00012	PRU_2350
34	Butyrate kinase[8]	2.7.2.7	K00929	T433DRAFT_00013	PRU_2349
35	Butyryl-CoA:acetate-CoA transferase[8]	2.8.3.8	COG0427	T433DRAFT_00482	PRU_2762

[1]NA, no locus tag was identified

[2]Alternate to methylmalonyl-CoA decarboxylase and phosphoenolpyruvate carboxykinase (ATP)

[3]Alternate to 6-phosphofructokinase

[4]Alternate to pyruvate kinase

[5]Involved in forming pyrophosphate for diphosphate-fructose-6-phosphate 1-phosphotransferase and pyruvate, phosphate dikinase

[6]Alternate to acetate kinase and phosphate acetyltransferase

[7]Involved in forming formate

[8]Involved in forming butyrate

Table 6. Reactions, genes, and proteins for fermentation in *P. brevis* GA33

Reaction ID	Gene in genome (locus tag) [2]	Protein in proteome (locus tag)[1,2]					
		Cell extract/DDA[3]		Membrane/DDA[3]		Membrane/DIA[4]	
		Replicate 1	Replicate 2	Replicate 1	Replicate 2	Replicate 1	Replicate 2
1	T433DRAFT_02353, T433DRAFT_00587, T433DRAFT_01666	02353, 00587, 01666	02353, 00587, 01666	NA	00587, 01666	01666	00587, 01666
2	T433DRAFT_02677	02677	02677	NA	02677	NA	02677
3	T433DRAFT_01181	01181	01181	NA	01181	01181	NA
4	T433DRAFT_00274	00274	00274	NA	00274	00274	00274
5	T433DRAFT_01090	01090	01090	01090	01090	01090	01090
6	T433DRAFT_02421	02421	02421	02421	02421	02421	02421
7	T433DRAFT_02583	02583	02583	NA	02583	02583	02583
8	T433DRAFT_00046	00046	00046	NA	NA	NA	NA
	T433DRAFT_00616	00616	00616	NA	NA	NA	NA
9	NA	NA	NA	NA	NA	NA	NA
10	T433DRAFT_00542	00542	00542	NA	NA	NA	NA
11	T433DRAFT_00478, T433DRAFT_00605	00478, 00605	00478, 00605	NA	00478, 00605	00605	00478, 00605
	T433DRAFT_00604, T433DRAFT_00477	00477, 00604	00477, 00604	NA	NA	NA	00477
	T433DRAFT_00909	00909	00909	00909	00909	00909	00909
12	T433DRAFT_02303	02303	02303	NA	02303	NA	02303
13	T433DRAFT_02304	02304	02304	NA	02304	NA	02304
14	T433DRAFT_02048	02048	02048	NA	02048	02048	02048
15	T433DRAFT_01517	01517	01517	NA	NA	NA	NA
16	T433DRAFT_00348	00348	00348	NA	00348	NA	NA
17	T433DRAFT_00482	00482	00482	NA	NA	NA	NA

CONTINUED

Table 6: CONTINUED

18	T433DRAFT_00914, T433DRAFT_00915	00914, 00915	00914, 00915	NA	00914, 00915	00914	00914, 00915
19	T433DRAFT_01907	01907	01907	NA	NA	NA	01907
20	NA	NA	NA	NA	NA	NA	NA
	NA	NA	NA	NA	NA	NA	NA
21	T433DRAFT_01721	NA	NA	NA	NA	NA	NA
	T433DRAFT_01716	01716	01716	01716	01716	01716	01716
	T433DRAFT_01717	01717	01717	01717	01717	01717	01717
	T433DRAFT_01718	NA	NA	NA	NA	NA	01718
	T433DRAFT_01720	NA	NA	NA	NA	NA	NA
	T433DRAFT_01719, T433DRAFT_00349	NA	NA	NA	01719	01719	01719
22	T433DRAFT_00925	00925	00925	00925	00925	00925	00925
	T433DRAFT_00926	NA	NA	NA	00926	00926	00926
	T433DRAFT_00927	NA	NA	00927	00927	00927	00927
	T433DRAFT_00928	NA	NA	NA	NA	00928	NA
	T433DRAFT_00929	NA	NA	NA	NA	NA	NA
	T433DRAFT_00930	00930	00930	00930	00930	00930	00930
23	T433DRAFT_02095	02095	02095	02095	02095	02095	02095
	T433DRAFT_02094	02094	02094	02094	02094	02094	02094
	T433DRAFT_02096	NA	NA	NA	02096	NA	02096
24	T433DRAFT_01651	NA	NA	NA	01651	NA	01651
	T433DRAFT_01653	NA	NA	01653	01653	01653	01653
	T433DRAFT_01652	NA	01652	01652	01652	01652	01652
	T433DRAFT_01655	01655	01655	01655	01655	01655	01655
	T433DRAFT_01648	01648	01648	01648	01648	01648	01648
	T433DRAFT_01656	01656	01656	01656	01656	01656	01656
	T433DRAFT_01654	NA	01654	01654	01654	01654	01654

CONTINUED

Table 6: CONTINUED

	T433DRAFT_01649	NA	NA	NA	NA	NA	NA
25	NA	NA	NA	NA	NA	NA	NA
	NA	NA	NA	NA	NA	NA	NA
26	NA	NA	NA	NA	NA	NA	NA
27	NA	NA	NA	NA	NA	NA	NA
28	T433DRAFT_00987	00987	00987	NA	00987	NA	00987
29	T433DRAFT_02597	02597	02597	02597	02597	02597	02597
30	T433DRAFT_00912	NA	NA	NA	00912	00912	00912
31	T433DRAFT_02325	02325	02325	NA	NA	NA	NA
32	T433DRAFT_01500	01500	01500	NA	01500	NA	01500
33	T433DRAFT_00012	00012	00012	NA	NA	NA	NA
34	T433DRAFT_00013	NA	00013	NA	NA	NA	NA
35	T433DRAFT_00482	00482	00482	NA	NA	NA	NA

[1]Locus tag "T433DRAFT_xxxxx" is shorten as "xxxxx"

[2]NA, no locus tag was identified, or the protein was not detected in the proteome

[3]DDA, shotgun proteomics with data-dependent acquisition method

[4]DIA, shotgun proteomics with data-dependent acquisition method

Table 7. Reactions, genes, and proteins for fermentation in *P. ruminicola* 23

Reaction ID	Gene in genome (locus tag)[1]	Protein in proteome (locus tag)[1]					
		Cell extract/DDA[2]		Membrane/DDA[2]		Membrane/DIA[3]	
		Replicate 1	Replicate 2	Replicate 1	Replicate 2	Replicate 1	Replicate 2
1	PRU_0395, PRU_1689, PRU_0241, PRU_2364, PRU_1688, PRU_1690	PRU_0241, PRU_2364, PRU_1688	PRU_1689, PRU_0241, PRU_1688, PRU_1690	NA	PRU_0241	PRU_0241	PRU_0241
2	PRU_1785	NA	PRU_1785	NA	PRU_1785	NA	PRU_1785
3	PRU_1201	PRU_1201	PRU_1201	PRU_1201	PRU_1201	PRU_1201	PRU_1201
4	PRU_2062	PRU_2062	PRU_2062	PRU_2062	PRU_2062	PRU_2062	PRU_2062
5	PRU_1860	PRU_1860	PRU_1860	NA	NA	NA	NA
6	PRU_1674	PRU_1674	PRU_1674	PRU_1674	PRU_1674	PRU_1674	PRU_1674
7	PRU_1634	PRU_1634	PRU_1634	PRU_1634	PRU_1634	PRU_1634	PRU_1634
8	PRU_2355	PRU_2355	PRU_2355	NA	PRU_2355	PRU_2355	PRU_2355
	PRU_1017	PRU_1017	PRU_1017	NA	NA	NA	NA
9	PRU_1102	NA	NA	NA	NA	NA	NA
10	PRU_0684	PRU_0684	PRU_0684	NA	PRU_0684	NA	PRU_0684
11	PRU_1149, PRU_2267	PRU_1149, PRU_2267	PRU_1149, PRU_2267	PRU_2267, PRU_1149	PRU_1149, PRU_2267	PRU_1149, PRU_2267	PRU_1149, PRU_2267
	PRU_2268	PRU_2268	PRU_2268	NA	NA	NA	NA
	PRU_1235	PRU_1235	PRU_1235	PRU_1235	PRU_1235	PRU_1235	PRU_1235
12	PRU_2260	PRU_2260	PRU_2260	NA	PRU_2260	PRU_2260	PRU_2260
13	PRU_2259	PRU_2259	PRU_2259	NA	NA	NA	NA
14	PRU_2279	PRU_2279	PRU_2279	PRU_2279	PRU_2279	PRU_2279	PRU_2279

CONTINUED

Table 7: CONTINUED

15	PRU_2158	PRU_2158	PRU_2158	NA	NA	NA	NA
16	PRU_0119	PRU_0119	PRU_0119	PRU_0119	NA	PRU_0119	NA
17	PRU_2762	PRU_2762	PRU_2762	PRU_2762	NA	NA	NA
18	PRU_1639, PRU_1640	PRU_1639	PRU_1639, PRU_1640	NA	PRU_1639, PRU_1640	PRU_1640	PRU_1639, PRU_1640
19	PRU_1230	NA	PRU_1230	NA	NA	NA	NA
20	NA	NA	NA	NA	NA	NA	NA
	NA	NA	NA	NA	NA	NA	NA
21	PRU_0809	NA	NA	NA	NA	NA	NA
	PRU_0804	NA	NA	PRU_0804	PRU_0804	PRU_0804	PRU_0804
	PRU_0805	NA	NA	PRU_0805	PRU_0805	PRU_0805	PRU_0805
	PRU_0806	NA	NA	NA	NA	NA	NA
	PRU_0808	NA	NA	NA	NA	NA	NA
	PRU_0807	NA	NA	PRU_0807	PRU_0807	PRU_0807	PRU_0807
22	PRU_1250	PRU_1250	PRU_1250	PRU_1250	PRU_1250	PRU_1250	PRU_1250
	PRU_1249	NA	PRU_1249	PRU_1249	PRU_1249	PRU_1249	PRU_1249
	PRU_1248	NA	PRU_1248	PRU_1248	PRU_1248	PRU_1248	PRU_1248
	PRU_1247	NA	NA	NA	NA	NA	NA
	PRU_1246	NA	NA	NA	NA	NA	NA
	PRU_1245	NA	PRU_1245	PRU_1245	PRU_1245	PRU_1245	PRU_1245
23	PRU_2432	PRU_2432	PRU_2432	PRU_2432	PRU_2432	PRU_2432	PRU_2432
	PRU_2431	PRU_2431	PRU_2431	PRU_2431	PRU_2431	PRU_2431	PRU_2431
	PRU_2433	NA	NA	PRU_2433	PRU_2433	NA	PRU_2433
24	PRU_1196	NA	NA	NA	NA	NA	NA
	PRU_1194	NA	NA	PRU_1194	PRU_1194	PRU_1194	PRU_1194
	PRU_1195	NA	PRU_1195	PRU_1195	PRU_1195	PRU_1195	PRU_1195
	PRU_1192	PRU_1192	PRU_1192	PRU_1192	PRU_1192	PRU_1192	PRU_1192
	PRU_1199	PRU_1199	PRU_1199	PRU_1199	PRU_1199	PRU_1199	PRU_1199

CONTINUED

Table 7: CONTINUED

	PRU_1191	NA	NA	PRU_1191	PRU_1191	PRU_1191	PRU_1191
	PRU_1193	NA	NA	NA	PRU_1193	PRU_1193	PRU_1193
	PRU_1198	NA	NA	NA	NA	NA	NA
25	NA	NA	NA	NA	NA	NA	NA
26	NA	NA	NA	NA	NA	NA	NA
27	NA	NA	NA	NA	NA	NA	NA
28	PRU_0792	PRU_0792	PRU_0792	PRU_0792	PRU_0792	PRU_0792	PRU_0792
29	PRU_1512	PRU_1512	PRU_1512	PRU_1512	PRU_1512	PRU_1512	PRU_1512
30	PRU_0830	NA	NA	NA	PRU_0830	NA	PRU_0830
31	PRU_2205	NA	PRU_2205	PRU_2205	NA	PRU_2205	NA
32	PRU_1243	NA	PRU_1243	NA	NA	PRU_1243	PRU_1243
33	PRU_2350	PRU_2350	PRU_2350	NA	PRU_2350	NA	NA
34	PRU_2349	NA	NA	NA	NA	NA	NA
35	PRU_2762	PRU_2762	PRU_2762	PRU_2762	NA	NA	NA

[1]NA, no locus tag was identified, or the protein was not detected in the proteome

[2]DDA, shotgun proteomics with data-dependent acquisition method

[3]DIA, shotgun proteomics with data-dependent acquisition method

Table 8. Enzymatic assays confirming *Prevotella* catalyze key reactions for forming acetate and succinate/propionate

Reaction ID	Reaction equation	Source	*P. brevis* GA33		*P. ruminicola* 23	
			Activity[1]	*P*-value	Activity[1]	*P*-value
6	D-Glyceraldehyde-3-phosphate + Orthophosphate + NAD^+ <=> 3-Phospho-D-glyceroyl phosphate + NADH + H^+	Cell extract	2814 (190)	<0.001	2840 (360)	0.008
11	2 Reduced ferredoxin + Acetyl-CoA + CO_2 + 2 H^+ <=> 2 Oxidized ferredoxin + Pyruvate + CoA	Cell extract	346 (97)	0.035	449 (92)	0.020
15	(S)-Malate + NAD^+ <=> Oxaloacetate + NADH + H^+	Cell extract	979 (30)	<0.001	2420 (260)	0.006
22	NADH + H^+ + ubiquinone + n Na^+[side 1] = NAD^+ + ubiquinol + n Na^+[side 2]	Membrane	17.8 (5.6)	0.043	16.4 (2.6)	0.012
		Solubilized membrane	28.8 (1.7)	0.002	17.2 (3.8)	0.022
23	Quinone + Succinate <=> Hydroquinone + Fumarate	Membrane	155.3 (8.9)	0.002	27.5 (5.4)	0.018
		Solubilized membrane	420 (33)	0.003	42.2 (5.9)	0.009
24	ATP + H_2O + 4 H^+[side 1] = ADP + phosphate + 4 H^+[side 2]	Membrane	97 (23)	0.025	53.3 (1.7)	0.001
		Solubilized membrane	102 (16)	0.012	61.5 (4.2)	0.002
25	D-Glyceraldehyde-3-phosphate + Orthophosphate + $NADP^+$ <=> 3-Phospho-D-glyceroyl phosphate + NADPH + H^+	Cell extract	515 (24)	<0.001	214 (120)	0.106
26	(S)-Malate + $NADP^+$ <=> Oxaloacetate + NADPH + H^+	Cell extract	501.5 (6.7)	<0.001	216 (25)	0.007

[1] Units are mean (SEM) mU/(mg protein)

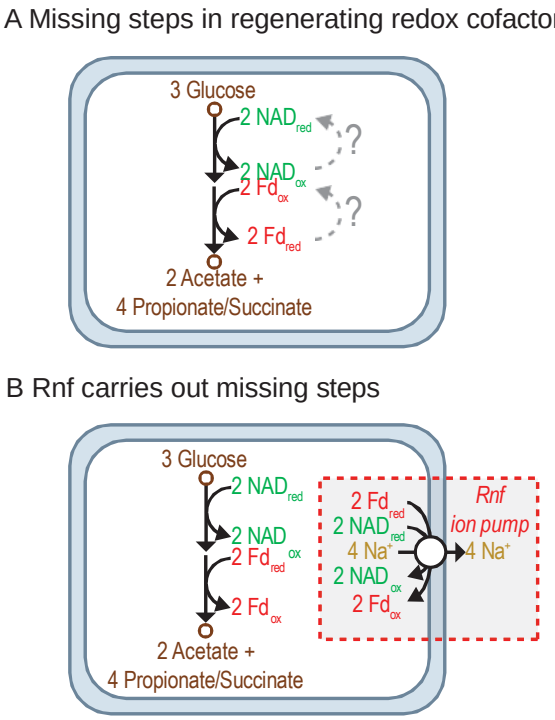

Figure 13. Missing steps during fermentation of glucose to acetate and succinate/propionate. (A) The missing steps are for regenerating redox cofactors. (B) We hypothesize Rnf carries out the missing steps. Abbreviations: Fd_{ox}, oxidized ferredoxin; Fd_{red}, reduced ferredoxin; NAD_{ox}, oxidized NAD, NAD^+; NAD_{red}, reduced NAD, NADH.

A Fermentation products

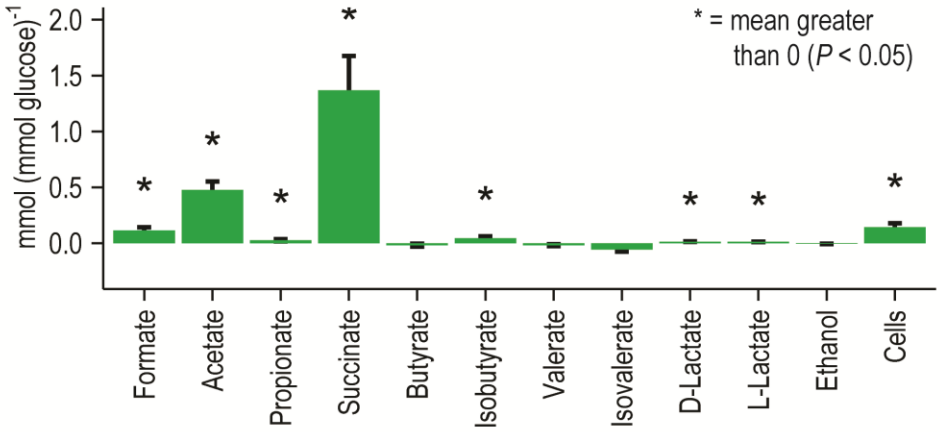

B Carbon recovery

Time	Glucose	Acids	CO_2	Cells	Total
			mean (SEM) mmol C L^{-1}		
Start	93.3 (8.7)	103.3 (0.8)	0 (0)	0 (0)	196.6 (8.3)
End	58.8 (2.6)	136.7 (4.2)	-5.1 (0.6)	31.3 (1.3)	221.7 (4.8)
				Recovery	**113.2 (4.3) %**

C Hydrogen recovery

Time	Glucose	Acids	H_2O	Cells	Total
			mean (SEM) mmol H L^{-1}		
Start	187 (17)	206.6 (1.6)	0 (0)	0 (0)	393 (17)
End	117.5 (5.1)	259.0 (7.0)	9.3 (1.2)	55.0 (1.9)	441.0 (9.5)
				Recovery	**112.6 (4.3) %**

D Summary

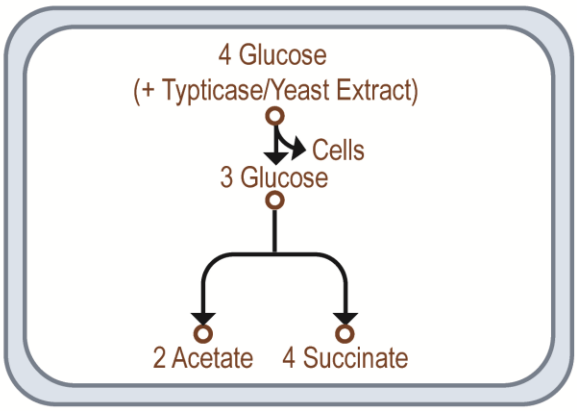

Figure 14. Fermentation products formed during fermentation of glucose in *P. brevis* GA33. (A) Yield of fermentation products. (B) Recovery of carbon is near or above 100%. (C) Recovery of hydrogen is also near or above 100%. (D) Summary of growth and fermentation. In (A), the yield

of cells is g (mmol glucose)$^{-1}$. Results are mean ± standard error of at least 3 biological replicates (culture supernatant or cells prepared from independent cultures).

A Fermentation products

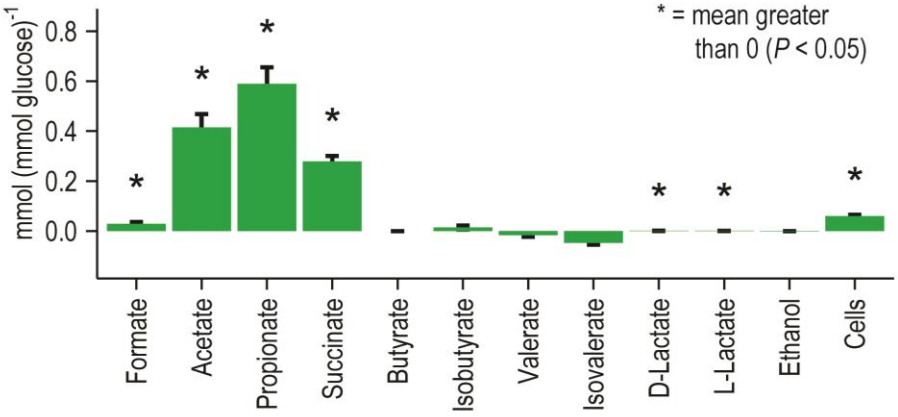

B Carbon recovery

Time	Glucose	Acids	CO_2	Cells	Total
			mean (SEM) mmol C L^{-1}		
Start	232 (14)	57.0 (2.0)	0 (0)	0 (0)	289 (15)
End	78.1 (2.1)	144.6 (4.4)	1.6 (1.5)	61.1 (0.3)	285.0 (5.0)
				Recovery	**99.3 (6.7) %**

C Hydrogen recovery

Time	Glucose	Acids	H_2O	Cells	Total
			mean (SEM) mmol H L^{-1}		
Start	465 (28)	114.0 (4.0)	0 (0)	0 (0)	579 (30)
End	156.3 (4.2)	275.0 (8.7)	23.0 (0.1)	112.7 (2.3)	566.9 (5.3)
				Recovery	**98.5 (5.8) %**

D Summary

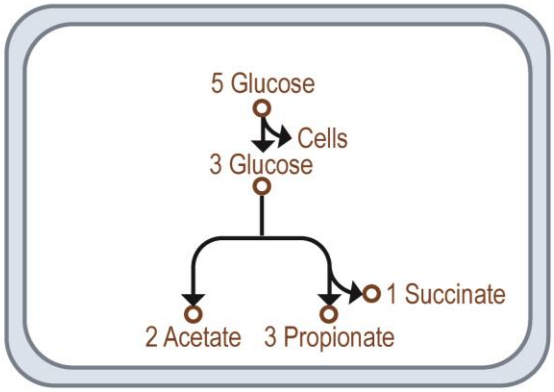

Figure 15. Fermentation products formed during fermentation of glucose in *P. ruminicola* 23. (A) Yield of fermentation products. (B) Recovery of carbon is near or above 100%. (C) Recovery of hydrogen is also near or above 100%. (D) Summary of growth and fermentation. In (A), the yield

of cells is g (mmol glucose)$^{-1}$. Results are mean ± standard error of at least 3 biological replicates (culture supernatant or cells prepared from independent cultures).

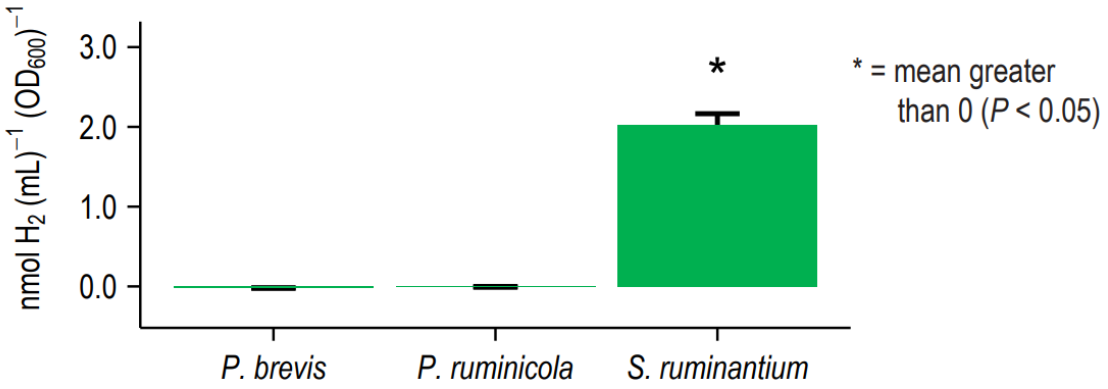

Figure 16. Measurement of H_2. *Prevotella* do not form H_2 during fermentation of glucose. *Selenomonas ruminantium* HD4 is known to form trace amounts of H_2 (Scheifinger et al 1975) and is included as a control.

A Rnf in genome

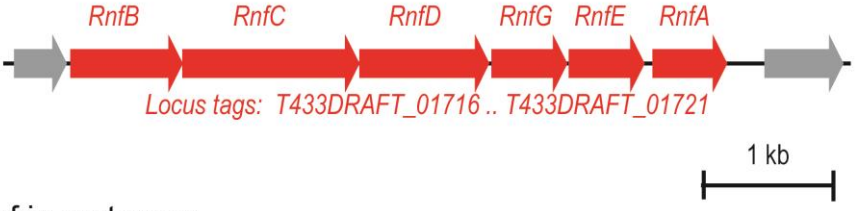

B Rnf in proteome

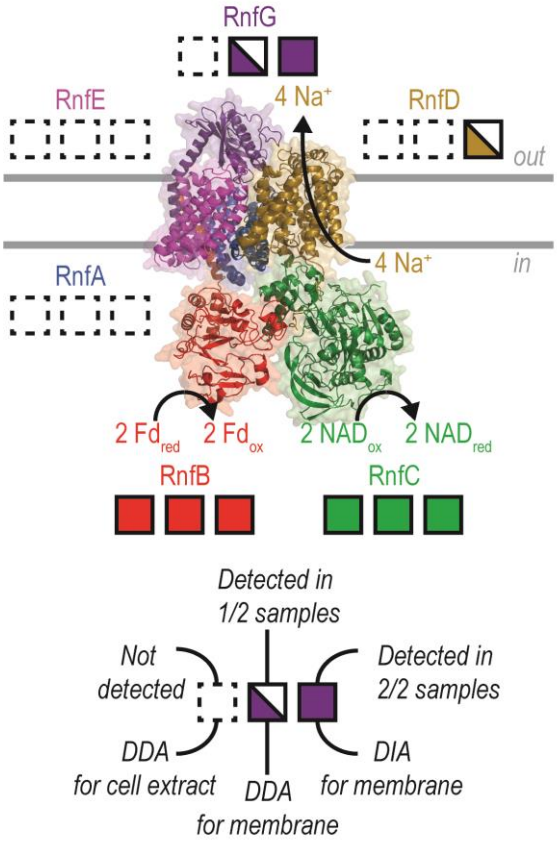

C Rnf activity

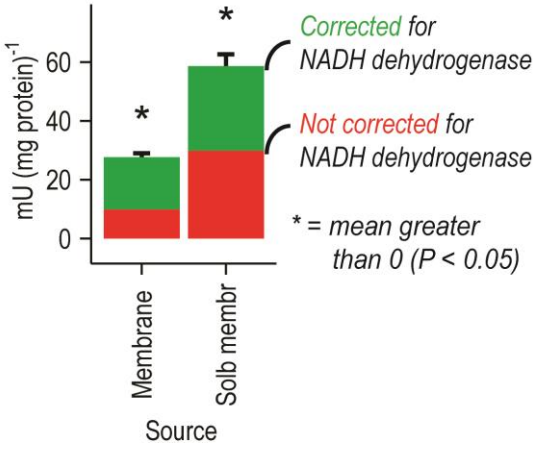

Figure 17. Rnf ion pump identified in *P. brevis* GA33. Rnf is evident in the (A) genome, (B) proteome, and (C) measurements of enzyme activity. Abbreviations: Fd_{ox}, oxidized ferredoxin; Fd_{red}, reduced ferredoxin; NAD_{ox}, oxidized NAD, NAD^+; NAD_{red}, reduced NAD, NADH; DDA, data dependent acquisition; DIA, data independent acquisition; Membrane, cell membrane sample; Solb membr, solubilized cell membrane sample.

A Rnf in genome

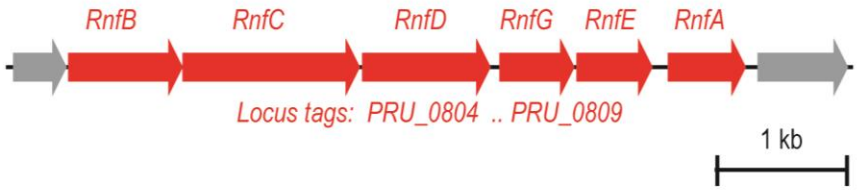

B Rnf in proteome

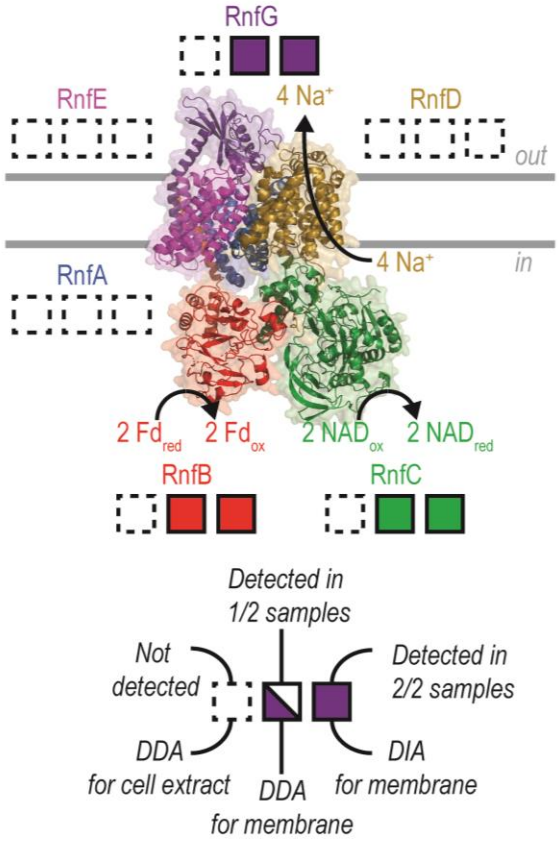

C Rnf activity

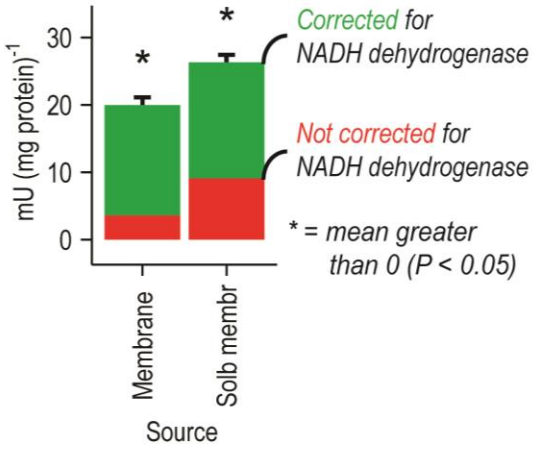

Figure 18. Rnf ion pump identified in *P. ruminicola* 23. Rnf is evident in the (A) genome, (B) proteome, and (C) measurements of enzyme activity. Abbreviations: Fd_{ox}, oxidized ferredoxin; Fd_{red}, reduced ferredoxin; NAD_{ox}, oxidized NAD, NAD^+; NAD_{red}, reduced NAD, NADH; DDA, data dependent acquisition; DIA, data independent acquisition; Membrane, cell membrane sample; Solb membr, solubilized cell membrane sample.

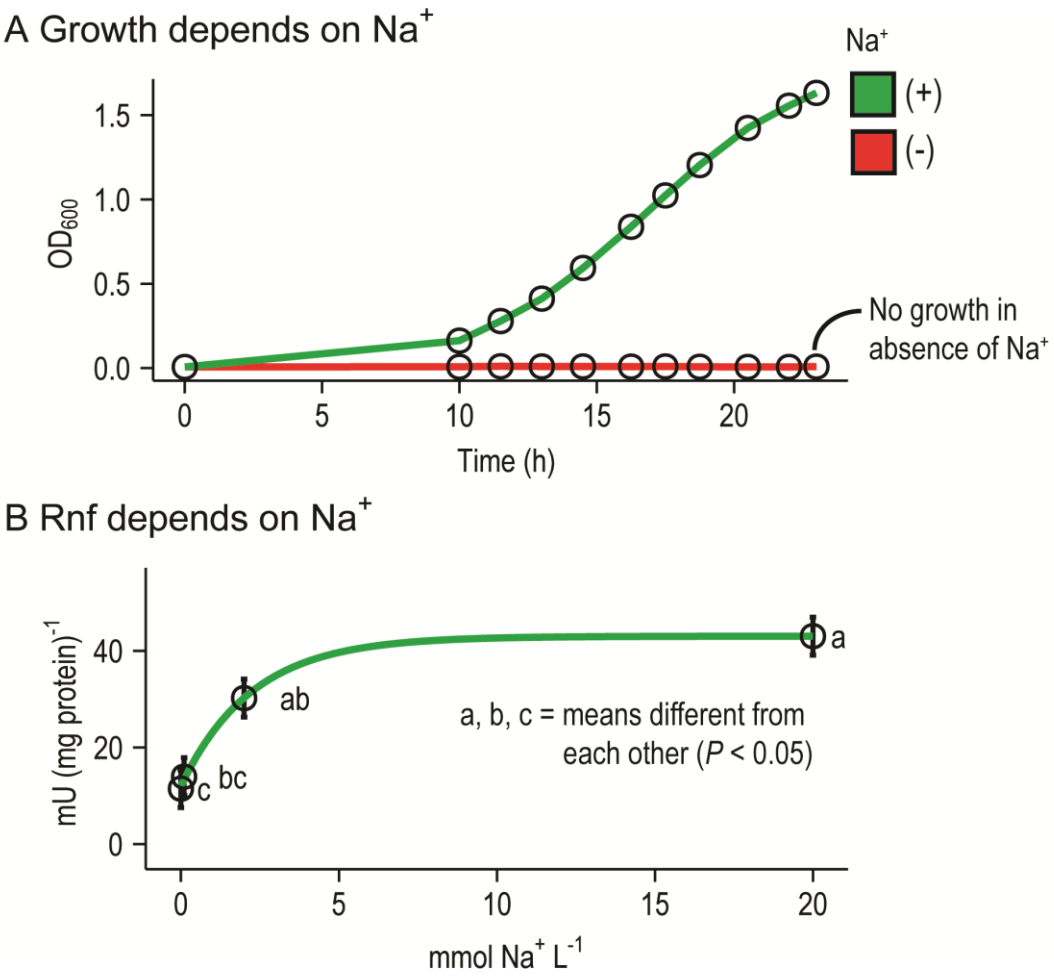

Figure 19. Na^+-dependent growth and Na^+-dependent Rnf activity. *P. brevis* GA33 depends on Na^+ for growth and for Rnf activity. The growth curve shown was one representative among two batches that were grown independently in different days.

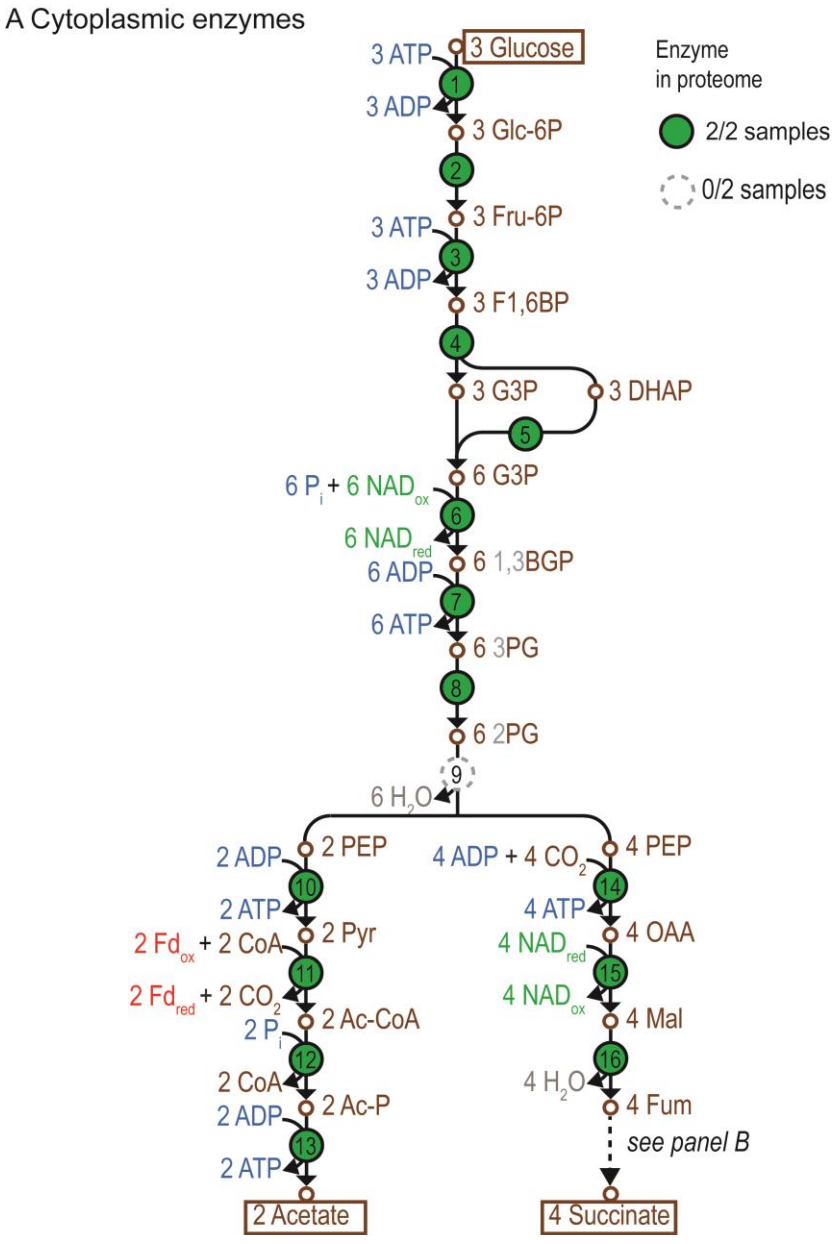
A Cytoplasmic enzymes
Enzyme in proteome
2/2 samples
0/2 samples
3 Glucose
3 ATP
3 ADP
3 Glc-6P
3 ATP
3 ADP
3 Fru-6P
3 F1,6BP
3 G3P
3 DHAP
6 G3P
6 P$_i$ + 6 NAD$_{ox}$
6 NAD$_{red}$
6 1,3BGP
6 ADP
6 ATP
6 3PG
6 2PG
6 H$_2$O
2 ADP
2 PEP
4 ADP + 4 CO$_2$
4 PEP
2 ATP
2 Pyr
4 ATP
4 OAA
2 Fd$_{ox}$ + 2 CoA
4 NAD$_{red}$
2 Fd$_{red}$ + 2 CO$_2$
2 Ac-CoA
4 NAD$_{ox}$
4 Mal
2 P$_i$
2 CoA
2 Ac-P
4 H$_2$O
4 Fum
2 ADP
see panel B
2 ATP
2 Acetate
4 Succinate

Figure 20: CONTINUED

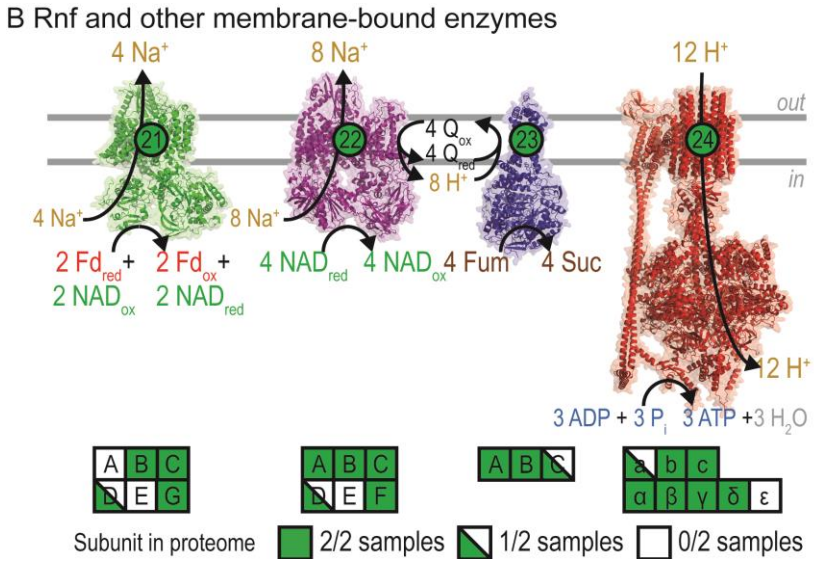

Figure 20. Enzymes identified for forming acetate and succinate/propionate in the proteome of *P. brevis* GA33. (A) Cytoplasmic enzymes. (B) Rnf and other membrane-bound enzymes. Enzymes: 1, glucokinase/hexokinase (EC 2.7.1.1, EC 2.7.1.2); 2, glucose-6-phosphate isomerase (EC 5.3.1.9); 3, 6-phosphofructokinase (EC 2.7.1.11); 4, fructose-bisphosphate aldolase (EC 4.1.2.13); 5, triose-phosphate isomerase (EC 5.3.1.1); 6, glyceraldehyde-3-phosphate dehydrogenase (phosphorylating) (EC 1.2.1.12, EC 1.2.1.59); 7, phosphoglycerate kinase (EC 2.7.2.3); 8, phosphoglycerate mutase (EC 5.4.2.11, EC 5.4.2.12); 9, phosphopyruvate hydratase (EC 4.2.1.11); 10, pyruvate kinase (EC 2.7.1.40); 11, pyruvate:ferredoxin oxidoreductase (EC 1.2.7.1, EC 1.2.7.11); 12, phosphate acetyltransferase (EC 2.3.1.8); 13, acetate kinase (EC 2.7.2.1); 14, phosphoenolpyruvate carboxykinase (ATP) (EC 4.1.1.49); 15, malate dehydrogenase (EC 1.1.1.37); 16, fumarate hydratase (EC 4.2.1.2); 21, ferredoxin-NAD^+ oxidoreductase (Na^+-transporting) (EC 7.2.1.2); 22, NADH:ubiquinone reductase (Na^+-transporting) (EC 7.2.1.1); 23, fumarate reductase/succinate dehydrogenase (EC 1.3.5.1, EC 1.3.5.4); 24, ATP synthase (EC

7.1.2.2). Abbreviations: Glc-6P, glucose-6-phosphate; Fru-6P, fructose-6-phosphate; F1,6BP, fructose-1,6-bisphophate; G3P, glyceraldehyde-3-phosphate; DHAP, dihydroxyacetone phosphate; 1,3BGP, 1,3-bisphosphoglycerate; 3PG, 3-phosphoglycerate; 2PG, 2-phosphoglycerate; PEP, phosphoenolpyruvate; Pyr, pyruvate; Ac-CoA, acetyl-CoA; Ac-P, acetyl-phosphate; OAA, oxaloacetate; Mal, malate; Fum, fumarate; Suc-CoA, succinyl-CoA; L-MM-CoA, L-methylmalonyl-CoA; D-MM-CoA, D-methylmalonyl-CoA; Pr-CoA, propionyl-CoA; Fd_{ox}, oxidized ferredoxin; Fd_{red}, reduced ferredoxin; NAD_{ox}, oxidized NAD, NAD^{+}; NAD_{red}, reduced NAD, NADH; CoA, coenzyme A; P_i, inorganic phosphate; Q_{ox}, oxidized ubiquinone; Q_{red}, reduced ubiquinone. +, enzyme present in proteome; -, enzyme not present in proteome.

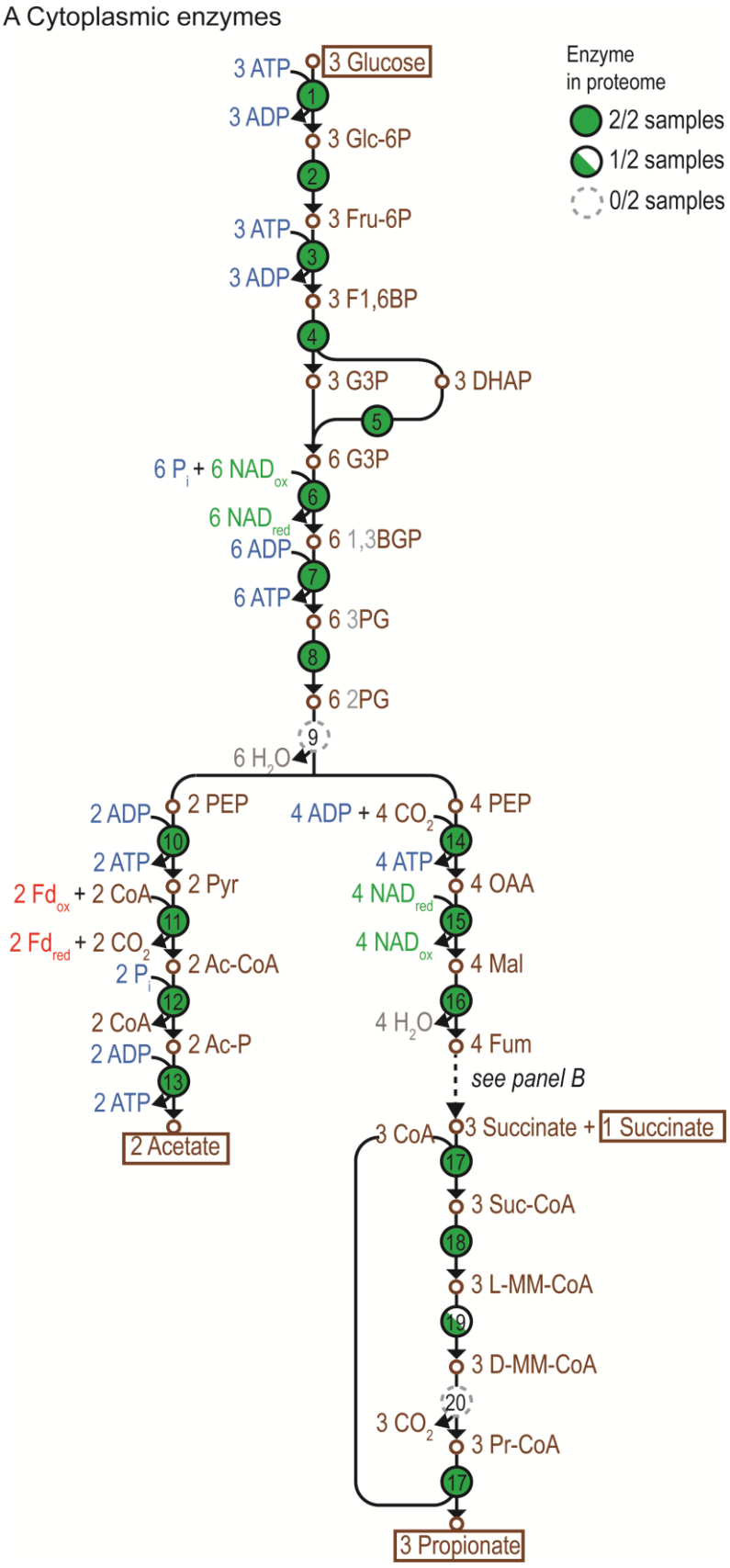
A Cytoplasmic enzymes
Enzyme in proteome
2/2 samples
1/2 samples
0/2 samples
3 ATP
3 Glucose
1
3 ADP
3 Glc-6P
2
3 ATP
3 Fru-6P
3
3 ADP
3 F1,6BP
4
3 G3P
3 DHAP
5
6 Pi + 6 NADox
6 G3P
6
6 NADred
6 1,3BGP
6 ADP
7
6 ATP
6 3PG
8
6 2PG
9
6 H2O
2 ADP
2 PEP
10
2 ATP
2 Pyr
2 Fdox + 2 CoA
11
2 Fdred + 2 CO2
2 Ac-CoA
2 Pi
12
2 CoA
2 Ac-P
2 ADP
13
2 ATP
2 Acetate
4 ADP + 4 CO2
4 PEP
14
4 ATP
4 OAA
4 NADred
15
4 NADox
4 Mal
16
4 H2O
4 Fum
see panel B
3 CoA
3 Succinate + 1 Succinate
17
3 Suc-CoA
18
3 L-MM-CoA
19
3 D-MM-CoA
20
3 CO2
3 Pr-CoA
17
3 Propionate

Figure 21: CONTINUED

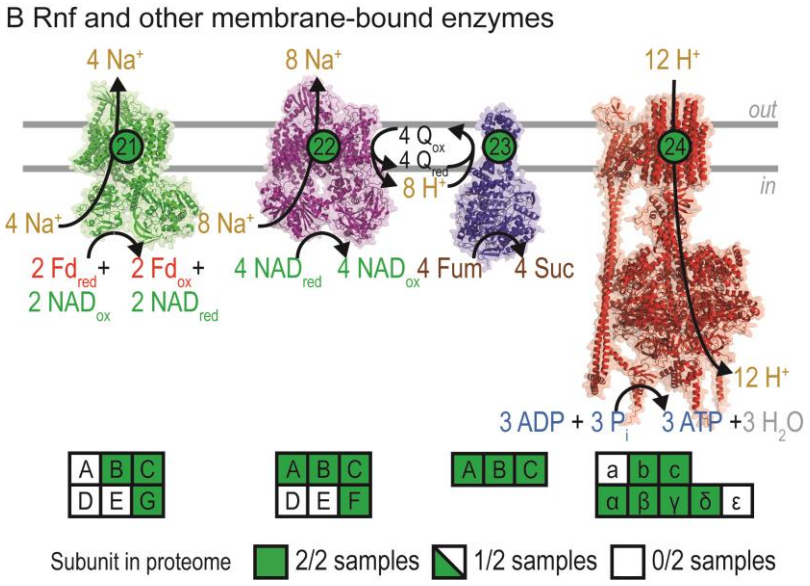

Figure 21. Enzymes identified for forming acetate and succinate/propionate in the proteome of *P. ruminicola* 23. (A) Cytoplasmic enzymes. (B) Rnf and other membrane-bound enzymes. Enzymes: 17, propionyl-CoA:succinate-CoA transferase (EC 2.8.3.27); 18, methylmalonyl-CoA mutase (EC 5.4.99.2); 19, methylmalonyl-CoA epimerase (EC 5.1.99.1); 20, methylmalonyl-CoA decarboxylase (EC 4.1.1.41). See Figure 20 for other enzyme names and abbreviations.

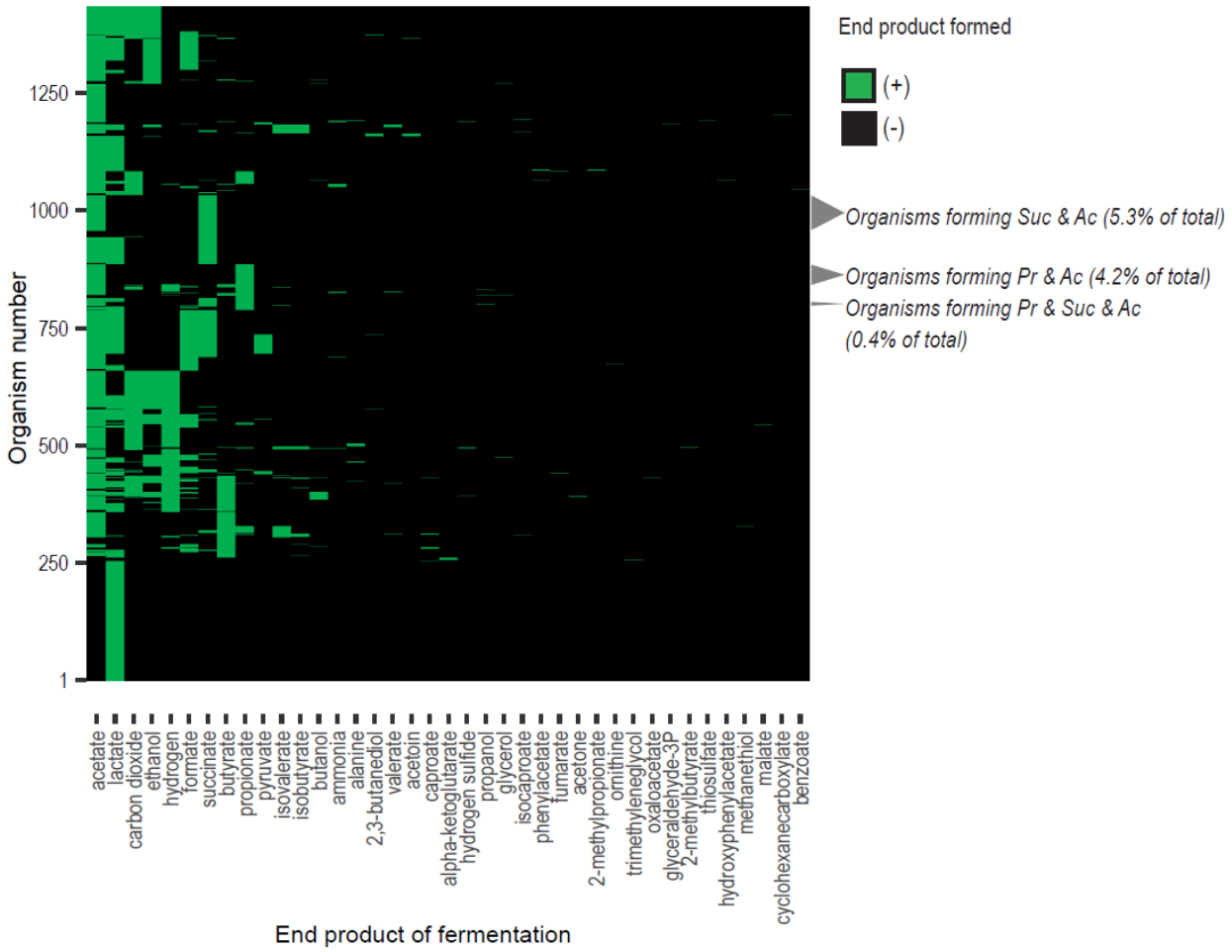

Figure 22. A heat map showing the production of end products by many fermentative organisms. Organisms (n = 1,436) and their reported end products (n = 39) are from *Bergey's Manual of Systematics of Archaea and Bacteria* (Whitman 2022). Minor (trace) end products are not included. Abbreviations: *Ac*, acetate; *Suc*, succinate; *Pr*, propionate; +, end product formed by the organism; +, end product not formed by the organism.

A Alluvial graph

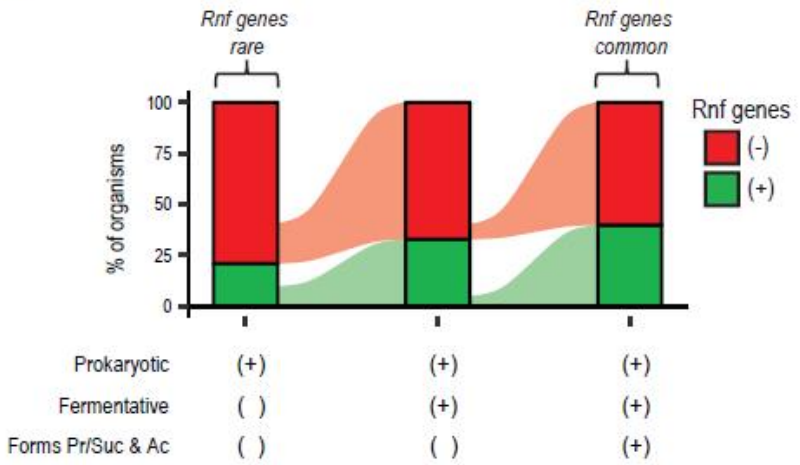

B Phylogenetic tree

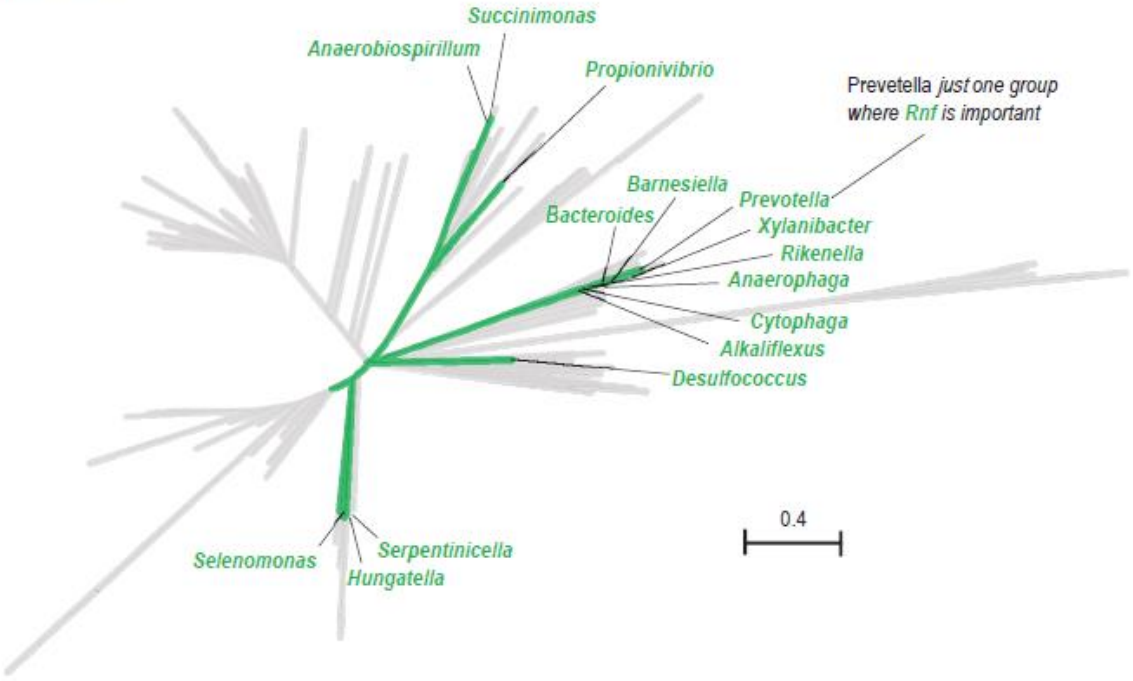

Figure 23: CONTINUED

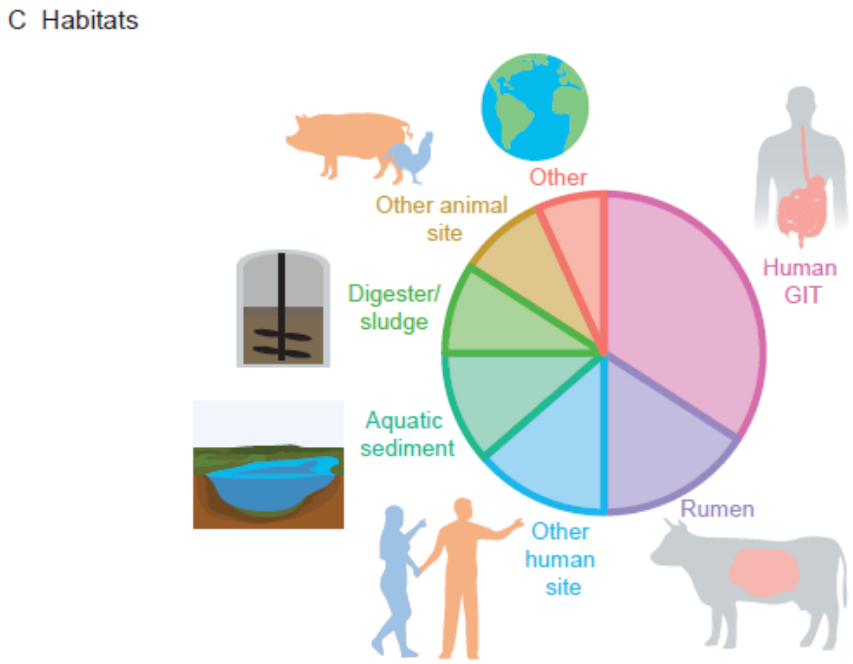

Figure 23. Distribution of Rnf in prokaryotes. (A) Alluvial graph showing percentage of prokaryotes with Rnf genes. Rnf genes are enriched in organisms that are fermentative and form acetate and succinate/propionate. (B) Phylogenetic tree of prokaryotes, highlighting those with Rnf genes and that form acetate and succinate/propionate during fermentation. (C) Habitats of prokaryotes with Rnf genes and observed to form acetate and succinate/propionate during fermentation.

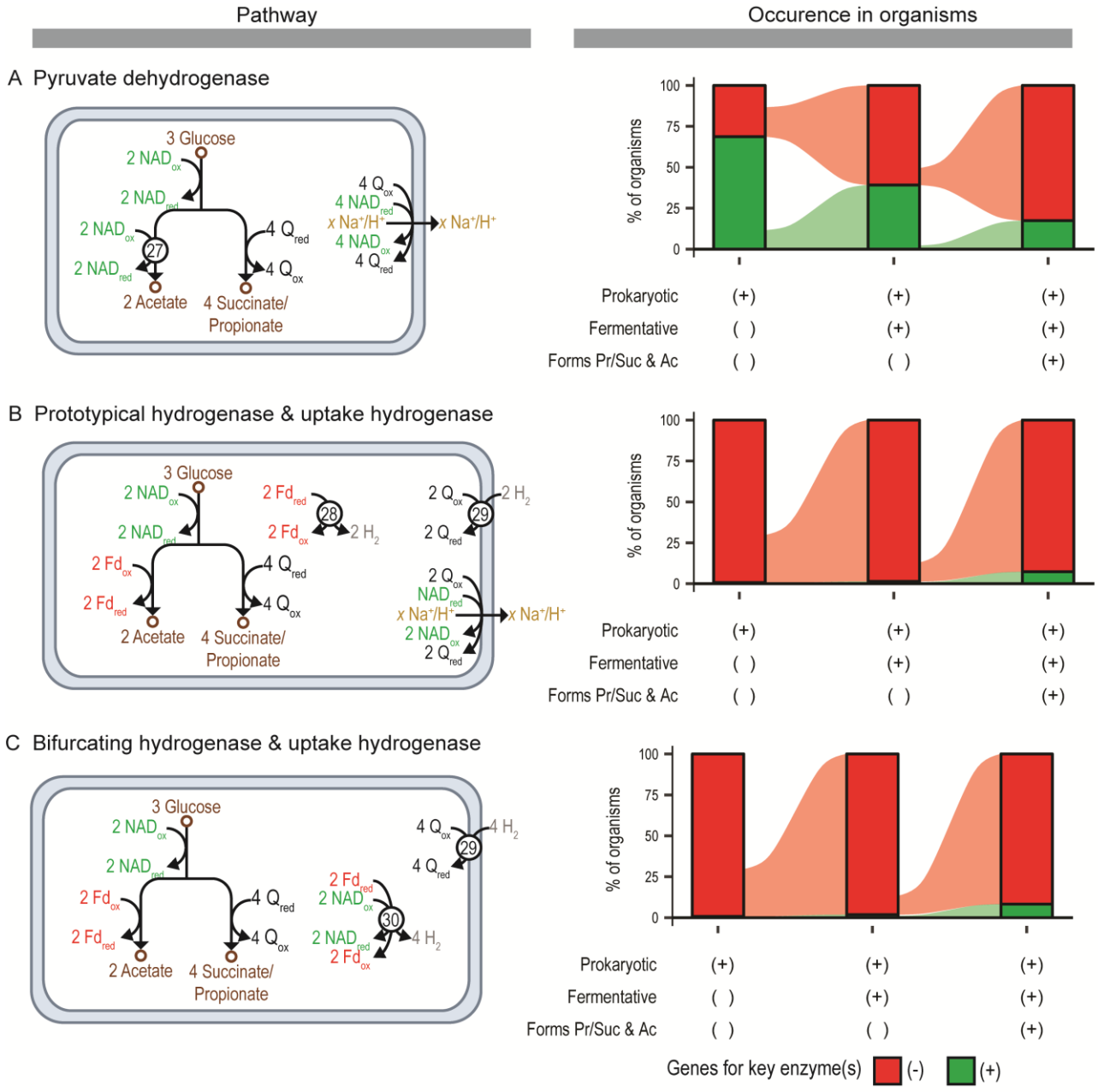
Pathway
Occurence in organisms
A Pyruvate dehydrogenase
3 Glucose
2 NAD ox
2 NAD red
2 NAD ox
2 NAD red
27
4 Q red
4 Q ox
2 Acetate
4 Succinate/
Propionate
4 Q ox
4 NAD red
x Na+/H+
4 NAD ox
4 Q red
x Na+/H+
% of organisms
100
75
50
25
0
Prokaryotic (+) (+) (+)
Fermentative ( ) (+) (+)
Forms Pr/Suc & Ac ( ) ( ) (+)
B Prototypical hydrogenase & uptake hydrogenase
3 Glucose
2 NAD ox
2 NAD red
2 Fd red
28
2 Fd ox
2 H2
2 Fd ox
2 Fd red
4 Q red
4 Q ox
2 Acetate
4 Succinate/
Propionate
2 Q ox
29
2 H2
2 Q red
2 Q ox
NAD red
x Na+/H+
2 NAD ox
2 Q red
x Na+/H+
% of organisms
100
75
50
25
0
Prokaryotic (+) (+) (+)
Fermentative ( ) (+) (+)
Forms Pr/Suc & Ac ( ) ( ) (+)
C Bifurcating hydrogenase & uptake hydrogenase
3 Glucose
2 NAD ox
2 NAD red
2 Fd ox
2 Fd red
4 Q red
4 Q ox
2 Acetate
4 Succinate/
Propionate
4 Q ox
29
4 H2
4 Q red
2 Fd red
2 NAD ox
30
2 NAD red
2 Fd ox
4 H2
% of organisms
100
75
50
25
0
Prokaryotic (+) (+) (+)
Fermentative ( ) (+) (+)
Forms Pr/Suc & Ac ( ) ( ) (+)
Genes for key enzyme(s) (-) (+)

Figure 24: CONTINUED

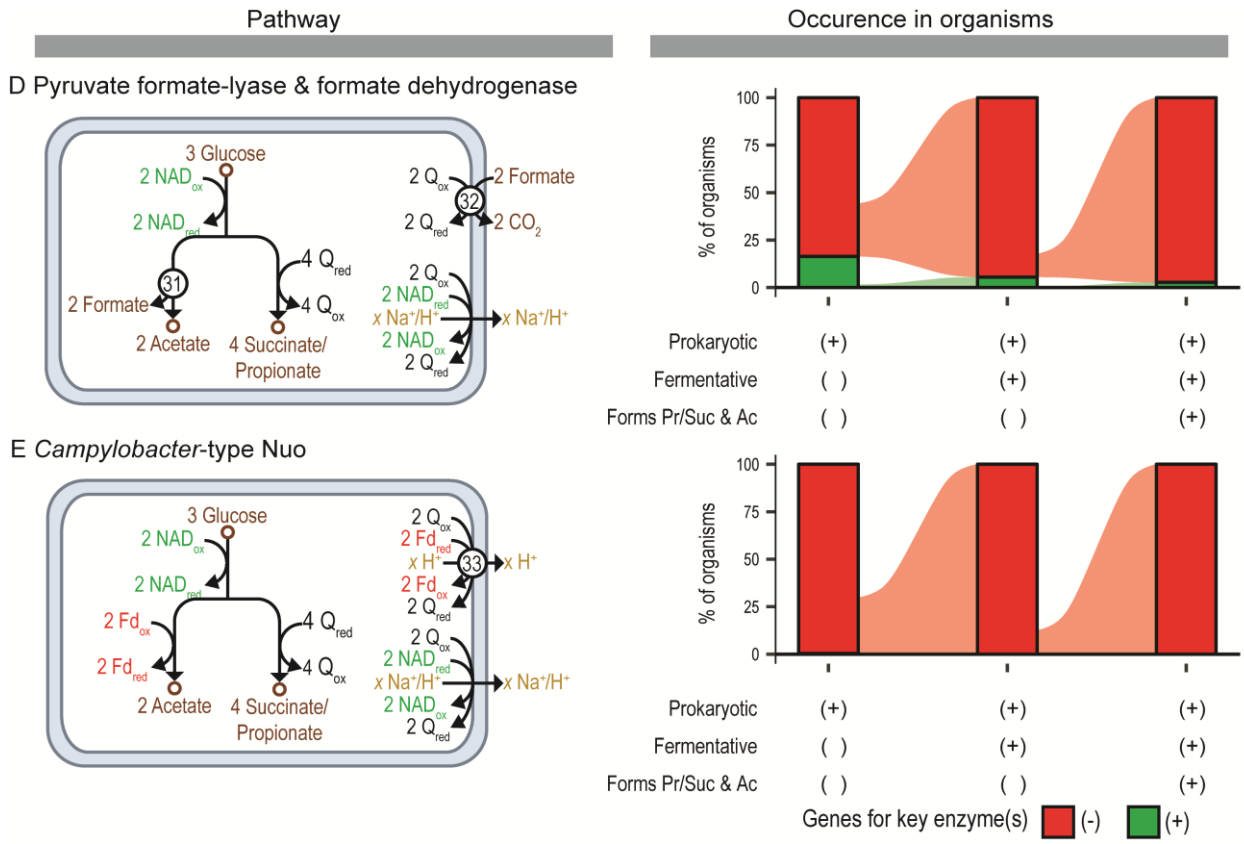

Figure 24. Alternatives to Rnf for forming acetate and propionate/succinate. Rnf is not needed in all pathways that form acetate and propionate/succinate, but these alternatives are uncommon. Alternatives to Rnf involve (A) pyruvate dehydrogenase, (B) prototypical hydrogenase and uptake hydrogenase, (C) bifurcating hydrogenase and uptake hydrogenase, (D) pyruvate formate-lyase and formate dehydrogenase, and (E) Campylobacter-type Nuo. Conversion of Q_{red} to Q_{ox} is drawn in middle of cell, but it actually occurs at membrane. Abbreviations: Fd_{ox}, oxidized ferredoxin; Fd_{red}, reduced ferredoxin; NAD_{ox}, oxidized NAD, NAD^+; NAD_{red}, reduced NAD, NADH; Q_{ox}, oxidized ubiquinone; Q_{red}, reduced ubiquinone.

Appendix 2

Dataset S6: Information for organisms in *Bergey's Manual of Systematics of Archaea and Bacteria*. Download Dataset S6 by searching https://docs.google.com/spreadsheets/d/1Ma2PTASHt03v0I4CrYhS-5Ub2dpcjLfwwCwlWBmc1c4/edit?usp=sharing

Dataset S7: Locus tags for Rnf and alternatives. Download Dataset S7 by searching https://docs.google.com/spreadsheets/d/1mP0yEmZlBvkBZEuNTr-d0Fg1qumDjPDPYUujH7QP7xs/edit?usp=sharing

Dataset S8: More information on organisms that form propionate, succinate, and acetate. Download Dataset S8 by searching https://docs.google.com/spreadsheets/d/15ccrYxJxbNA0U8MBvLw_x0Saiokvdt0HMPBz-KHOsFc/edit?usp=sharing

Chapter 4. Conclusions

Biochemical pathways for forming acetate and propionate during fermentation have been studied for several decades. Among all pathways reported to form acetate during fermentation, the SCACT/SCS pathway has not been reported in prokaryotes. Furthermore, there is step missing for regenerating redox cofactors in the pathway for propionate formation during fermentation in bacteria. The research in this dissertation employed enzymatic assays, genomic analysis, shotgun proteomics analysis, and other approaches to determine new pathways for forming fermentation acids during fermentation in bacteria.

In Chapter 2, we discovered enzymes for the SCACT/SCS pathway in the fermentative bacterium *Cutibacterium granulosum*. This pathway represents a new way for bacteria to form acetate from acetyl-CoA and synthesize ATP via substrate level phosphorylation. The pathway resembles one present in eukaryotes, but the genes encoding it are bacterial, not eukaryotic, in origin. We also found more than 30 other fermentative bacteria that encode this pathway, demonstrating that it could be common. This pathway could be targets for controlling fermentation and yields of acetate, with relevance to food, agriculture, and industry.

In Chapter 3, we showed that fermentation was apparently unbalanced and produced excess Fd_{red} and NAD_{ox} during propionate formation in *Prevotella*. The enzyme Rnf converts the excess Fd_{red} and NAD_{ox} back to Fd_{ox} and NAD_{red}. This is demonstrated by these observations: 1) genes encoding Rnf were expressed in the cell; 2) Rnf had significant ferredoxin:NAD^+ oxidoreductase activity; and 3) this activity was dependent on sodium concentration. Rnf thus fills in the missing steps of propionate-forming pathway and allows fermentation to continue. We found 44

fermentative type strains that form propionate (or its precursor, succinate) encode Rnf genes, suggesting Rnf is important to propionate formation in bacteria.

There is still much that will be learned about fermentation, including enzymes and pathways for carbon conversion, redox balance, and energy conservation during fermentation. Specifically, future work should focus on 1) identifying alternative steps to bypass enolase in *P. brevis* and many other rumen bacteria; 2) improving approaches for genetic manipulation of *Prevotella* species; and 3) determining if Rnf can contribute to extra ATP production (not just balance redox cofactors) during propionate formation. The combination of multiple omics analysis, genetic manipulation, and biochemical analysis can help elucidate fermentation pathways. This could lead to developments in the manipulation of the rumen fermentation to increase milk and meat production and to decrease methane emission.

References

Adil S, Magray SN (2012). Impact and manipulation of gut microflora in poultry: a review. *J Anim Vet Adv* **11:** 873-877.

Ahvenjarvi S, Vaga M, Vanhatalo A, Huhtanen P (2018). Ruminal metabolism of grass silage soluble nitrogen fractions. *J Dairy Sci* **101:** 279-294.

Allaker R, Greenman J, Osborne R, Gowers J (1985). Cytotoxic activity of *Propionibacterium acnes* and other skin organisms. *British Journal of Dermatology* **113:** 229-235.

Allen SH, Kellermeyer RW, Stjernholm RL, Wood HG (1964). Purification and properties of enzymes involved in the propionic acid fermentation. *J Bacteriol* **87:** 171-187.

Annison EF, Leng RA, Lindsay DB, White RR (1963). The metabolism of acetic acid, propionic acid and butyric acid in sheep. *Biochem J* **88:** 248-252.

Aramaki T, Blanc-Mathieu R, Endo H, Ohkubo K, Kanehisa M, Goto S *et al* (2020). KofamKOALA: KEGG Ortholog assignment based on profile HMM and adaptive score threshold. *Bioinformatics* **36:** 2251-2252.

Aschenbach JR, Kristensen NB, Donkin SS, Hammon HM, Penner GB (2010). Gluconeogenesis in dairy cows: the secret of making sweet milk from sour dough. *Iubmb Life* **62:** 869-877.

Atteia A, van Lis R, Gelius-Dietrich G, Adrait A, Garin J, Joyard J *et al* (2006). Pyruvate formate-lyase and a novel route of eukaryotic ATP synthesis in *Chlamydomonas* mitochondria. *J Biol Chem* **281:** 9909-9918.

Bach A, Calsamiglia S, Stern MD (2005). Nitrogen metabolism in the rumen. *J Dairy Sci* **88 Suppl 1:** E9-21.

Barker HA, Beck JV (1942). *Clostridium acidi-uridi* and *Clostridium cylindrosporum*, organisms fermenting uric acid and some other purines. *J Bacteriol* **43:** 291-304.

Bauer R, Dicks LM (2004). Control of malolactic fermentation in wine. A review. *South African Journal of Enology and Viticulture* **25:** 74-88.

Benemann JR (1973). Nitrogen fixation in termites. *Science* **181:** 164-165.

Bergman EN (1990). Energy contributions of volatile fatty acids from the gastrointestinal tract in various species. *Physiol Rev* **70:** 567-590.

Biegel E, Muller V (2010). Bacterial Na^+-translocating ferredoxin:NAD^+ oxidoreductase. *Proc Natl Acad Sci USA* **107:** 18138-18142.

Biegel E, Schmidt S, Gonzalez JM, Muller V (2011). Biochemistry, evolution and physiological function of the Rnf complex, a novel ion-motive electron transport complex in prokaryotes. *Cell Mol Life Sci* **68:** 613-634.

Bielen AA, Willquist K, Engman J, van der Oost J, van Niel EW, Kengen SW (2010). Pyrophosphate as a central energy carrier in the hydrogen-producing extremely thermophilic *Caldicellulosiruptor saccharolyticus*. *FEMS Microbiol Lett* **307:** 48-54.

Black AL, Kleiber M, Brown AM (1961). Butyrate metabolism in the lactating cow. *Journal of Biological Chemistry* **236:** 2399-2403.

Bodenhofer U, Bonatesta E, Horejs-Kainrath C, Hochreiter S (2015). msa: an R package for multiple sequence alignment. *Bioinformatics* **31:** 3997-3999.

Boiangiu CD, Jayamani E, Brugel D, Herrmann G, Kim J, Forzi L *et al* (2005). Sodium ion pumps and hydrogen production in glutamate fermenting anaerobic bacteria. *J Mol Microbiol Biotechnol* **10:** 105-119.

Bothe H, Nolteernsting U (1975). Pyruvate dehydrogenase complex, pyruvate:ferredoxin oxidoreductase and lipoic acid content in microorganisms. *Archives of Microbiology* **102:** 53-57.

Boyd DA, Cvitkovitch DG, Hamilton IR (1995). Sequence, expression, and function of the gene for the nonphosphorylating, NADP-dependent glyceraldehyde-3-phosphate dehydrogenase of *Streptococcus mutans*. *J Bacteriol* **177:** 2622-2627.

Bradford MM (1976). A rapid and sensitive method for the quantitation of microgram quantities of protein utilizing the principle of protein-dye binding. *Anal Biochem* **72:** 248-254.

Bruggemann H, Baumer S, Fricke WF, Wiezer A, Liesegang H, Decker I *et al* (2003). The genome sequence of *Clostridium tetani*, the causative agent of tetanus disease. *Proc Natl Acad Sci USA* **100:** 1316-1321.

Buckel W, Barker HA (1974). Two pathways of glutamate fermentation by anaerobic bacteria. *J Bacteriol* **117:** 1248-1260.

Buckel W (2001). Unusual enzymes involved in five pathways of glutamate fermentation. *Appl Microbiol Biotechnol* **57:** 263-273.

Buckel W, Thauer RK (2013). Energy conservation via electron bifurcating ferredoxin reduction and proton/Na^+ translocating ferredoxin oxidation. *Biochim Biophys Acta* **1827:** 94-113.

Buckel W (2021). Energy conservation in fermentations of anaerobic bacteria. *Front Microbiol* **12:** 703525.

Caspi R, Billington R, Ferrer L, Foerster H, Fulcher CA, Keseler IM *et al* (2016). The MetaCyc database of metabolic pathways and enzymes and the BioCyc collection of pathway/genome databases. *Nucleic Acids Res* **44:** D471-480.

Caspi R, Billington R, Keseler IM, Kothari A, Krummenacker M, Midford PE *et al* (2020). The MetaCyc database of metabolic pathways and enzymes - a 2019 update. *Nucleic Acids Res* **48:** D445-D453.

Castellano-Hinojosa A, Armato C, Pozo C, Gonzalez-Martinez A, Gonzalez-Lopez J (2018). New concepts in anaerobic digestion processes: recent advances and biological aspects. *Appl Microbiol Biotechnol* **102:** 5065-5076.

Chen IA, Chu K, Palaniappan K, Pillay M, Ratner A, Huang J *et al* (2019). IMG/M v.5.0: an integrated data management and comparative analysis system for microbial genomes and microbiomes. *Nucleic Acids Res* **47:** D666-D677.

Chen X, Li S, Liu L (2014). Engineering redox balance through cofactor systems. *Trends in biotechnology* **32:** 337-343.

Craig R, Beavis RC (2004). TANDEM: matching proteins with tandem mass spectra. *Bioinformatics* **20:** 1466-1467.

Deborde C, Rolin DB, Boyaval P (1999). *In vivo* ^{13}C NMR study of the bidirectional reactions of the Wood-Werkman cycle and around the pyruvate node in *Propionibacterium freudenreichii* subsp. *shermanii* and *Propionibacterium acidipropionici*. *Metabolic Engineering* **1:** 309-319.

Dehority BA (2003). *Rumen microbiology*, vol. 372. Nottingham University Press: Nottingham.

Denman SE, McSweeney CS (2006). Development of a real-time PCR assay for monitoring anaerobic fungal and cellulolytic bacterial populations within the rumen. *Fems Microbiol Ecol* **58:** 572-582.

Desai MS, Brune A (2012). *Bacteroidales* ectosymbionts of gut flagellates shape the nitrogen-fixing community in dry-wood termites. *Isme J* **6:** 1302-1313.

Dijkhuizen L, Van der Werf B, Harder W (1980). Metabolic regulation in *Pseudomonas oxalaticus* OX1. Diauxic growth on mixtures of oxalate and formate or acetate. *Archives of Microbiology* **124:** 261-268.

Dyksma S, Gallert C (2019). *Candidatus* Syntrophosphaera thermopropionivorans: a novel player in syntrophic propionate oxidation during anaerobic digestion. *Environ Microbiol Rep* **11:** 558-570.

Eddy SR (2011). Accelerated profile HMM searches. *PLoS Comput Biol* **7:** e1002195.

El-Gebali S, Mistry J, Bateman A, Eddy SR, Luciani A, Potter SC *et al* (2019). The Pfam protein families database in 2019. *Nucleic Acids Res* **47:** D427-D432.

Elia M, Cummings JH (2007). Physiological aspects of energy metabolism and gastrointestinal effects of carbohydrates. *Eur J Clin Nutr* **61 Suppl 1:** S40-74.

Elling-Staats ML, Gilbert MS, Smidt H, Kwakkel RP (2021). Caecal protein fermentation in broilers: a review. *World's Poultry Science Journal* **78:** 103-123.

Engel P, Moran NA (2013). The gut microbiota of insects - diversity in structure and function. *Fems Microbiol Rev* **37:** 699-735.

Eram MS, Ma K (2013). Decarboxylation of pyruvate to acetaldehyde for ethanol production by hyperthermophiles. *Biomolecules* **3**.

Eyer P, Worek F, Kiderlen D, Sinko G, Stuglin A, Simeon-Rudolf V *et al* (2003). Molar absorption coefficients for the reduced Ellman reagent: reassessment. *Anal Biochem* **312:** 224-227.

Falentin H, Deutsch S-M, Jan G, Loux V, Thierry A, Parayre S *et al* (2010). The complete genome of *Propionibacterium freudenreichii* CIRM-BIA1^{T}, a hardy Actinobacterium with food and probiotic applications. *PloS one* **5:** e11748.

Febel H, Fekete S (1996). Factors influencing microbial growth and the efficiency of microbial protein synthesis: a review. *Acta Vet Hung* **44:** 39-56.

Firkins JL, Yu ZT, Park T, Plank JE (2020). Extending Burk Dehority's perspectives on the role of ciliate protozoa in the rumen. *Frontiers in Microbiology* **11:** 123.

Fleck CB, Brock M (2008). Characterization of an acyl-CoA: carboxylate CoA-transferase from *Aspergillus nidulans* involved in propionyl-CoA detoxification. *Mol Microbiol* **68:** 642-656.

Fleck CB, Brock M (2009). Re-characterisation of *Saccharomyces cerevisiae* Ach1p: fungal CoA-transferases are involved in acetic acid detoxification. *Fungal Genet Biol* **46:** 473-485.

Fowler ML, Ingram-Smith CJ, Smith KS (2011). Direct detection of the acetate-forming activity of the enzyme acetate kinase. *J Vis Exp*.

Fröhlich-Wyder M-T, Bisig W, Guggisberg D, Jakob E, Turgay M, Wechsler D (2017). Cheeses with propionic acid fermentation. *Cheese*. Elsevier. pp 889-910.

Galperin MY, Makarova KS, Wolf YI, Koonin EV (2015). Expanded microbial genome coverage and improved protein family annotation in the COG database. *Nucleic Acids Res* **43:** D261-269.

Gilbert RA, Klieve, A.V. (2015). Ruminal viruses (bacteriophages, archaeaphages). In: Puniya A, Singh, R., Kamra, D. (ed). *Rumen Microbiology: From Evolution to Revolution*. Springer: New Delhi.

Glasemacher J, Bock AK, Schmid R, Schonheit P (1997). Purification and properties of acetyl-CoA synthetase (ADP-forming), an archaeal enzyme of acetate formation and ATP synthesis, from the hyperthermophile *Pyrococcus furiosus*. *Eur J Biochem* **244:** 561-567.

Gottschalk G (1986). *Bacterial metabolism*. Springer Verlag: New York, NY, USA.

Grond K, Sandercock BK, Jumpponen A, Zeglin LH (2018). The avian gut microbiota: community, physiology and function in wild birds. *J Avian Biol* **49**.

Gunsalus I, Gibbs M (1952). The heterolactic fermentation. *J biol Chem* **194:** 871-875.

Hackmann TJ, Diese LE, Firkins JL (2013a). Quantifying the responses of mixed rumen microbes to excess carbohydrate. *Appl Environ Microbiol* **79:** 3786-3795.

Hackmann TJ, Keyser BL, Firkins JL (2013b). Evaluation of methods to detect changes in reserve carbohydrate for mixed rumen microbes. *J Microbiol Methods* **93:** 284-291.

Hackmann TJ, Firkins JL (2015). Electron transport phosphorylation in rumen butyrivibrios: unprecedented ATP yield for glucose fermentation to butyrate. *Front Microbiol* **6:** 622.

Hackmann TJ, Ngugi DK, Firkins JL, Tao J (2017). Genomes of rumen bacteria encode atypical pathways for fermenting hexoses to short-chain fatty acids. *Environ Microbiol* **19:** 4670-4683.

Hackmann TJ, Zhang B (2021). Using neural networks to mine text and predict metabolic traits for thousands of microbes. *PLoS Comput Biol* **17:** e1008757.

Hackmann TJ (2022). Redefining the coenzyme A transferase superfamily with a large set of manually annotated proteins. *Protein Sci* **31:** 864-881.

Haft DH, Selengut JD, Richter RA, Harkins D, Basu MK, Beck E (2013). TIGRFAMs and genome properties in 2013. *Nucleic Acids Res* **41:** D387-395.

Hamlin L, Hungate R (1956). Culture and physiology of a starch-digesting bacterium (*Bacteroides amylophilus* n. sp.) from the bovine rumen. *Journal of bacteriology* **72:** 548-554.

Hanson R, Ballard F (1967). The relative significance of acetate and glucose as precursors for lipid synthesis in liver and adipose tissue from ruminants. *Biochemical Journal* **105:** 529-536.

Haugaard N, Cutler J, Ruggieri MR (1981). Use of N-ethylmaleimide to prevent interference by sulfhydryl reagents with the glucose oxidase assay for glucose. *Anal Bioch* **116:** 341-343.

Hegarty MP, Court RD, Christie GS, Lee CP (1976). Mimosine in *Leucaena leucocephala* is metabolized to a goitrogen in ruminants. *Aust Vet J* **52:** 490-490.

Herrmann G, Jayamani E, Mai G, Buckel W (2008). Energy conservation via electron-transferring flavoprotein in anaerobic bacteria. *J Bacteriol* **190:** 784-791.

Hess V, Schuchmann K, Muller V (2013). The ferredoxin:NAD^+ oxidoreductase (Rnf) from the acetogen *Acetobacterium woodii* requires Na^+ and is reversibly coupled to the membrane potential. *J Biol Chem* **288:** 31496-31502.

Hess V, Gallegos R, Jones JA, Barquera B, Malamy MH, Muller V (2016). Occurrence of ferredoxin:NAD^+ oxidoreductase activity and its ion specificity in several Gram-positive and Gram-negative bacteria. *Peerj* **4:** e1515.

Hetzel M, Brock M, Selmer T, Pierik AJ, Golding BT, Buckel W (2003). Acryloyl-CoA reductase from *Clostridium propionicum*. An enzyme complex of propionyl-CoA dehydrogenase and electron-transferring flavoprotein. *Eur J Biochem* **270:** 902-910.

Hilpert W, Schink B, Dimroth P (1984). Life by a new decarboxylation-dependent energy conservation mechanism with Na^+ as coupling ion. *EMBO J* **3:** 1665-1670.

Hino T, Kuroda S (1993). Presence of lactate dehydrogenase and lactate racemase in *Megasphaera elsdenii* grown on glucose or lactate. *Appl Environ Microbiol* **59:** 255-259.

Hobson PN (1997). *The Rumen Microbial Ecosystem*. Chapman & Hall: London.

Huws SA, Creevey CJ, Oyama LB, Mizrahi I, Denman SE, Popova M *et al* (2018). Addressing global ruminant agricultural challenges through understanding the rumen microbiome: Past, present, and future. *Front Microbiol* **9:** 2161.

Imkamp F, Biegel E, Jayamani E, Buckel W, Muller V (2007). Dissection of the caffeate respiratory chain in the acetogen Acetobacterium woodii: identification of an Rnf-type NADH dehydrogenase as a potential coupling site. *J Bacteriol* **189:** 8145-8153.

James KL, Rios-Hernandez LA, Wofford NQ, Mouttaki H, Sieber JR, Sheik CS *et al* (2016). Pyrophosphate-dependent ATP formation from acetyl coenzyme A in *Syntrophus aciditrophicus*, a new twist on ATP Formation. *mBio* **7:** e01208-01216.

Jouany JP (1996). Effect of rumen protozoa on nitrogen utilization by ruminants. *J Nutr* **126:** S1335-S1346.

Joyner AE, Jr., Baldwin RL (1966). Enzymatic studies of pure cultures of rumen microorganisms. *J Bacteriol* **92:** 1321-1330.

Kanehisa M, Furumichi M, Tanabe M, Sato Y, Morishima K (2017). KEGG: new perspectives on genomes, pathways, diseases and drugs. *Nucleic Acids Res* **45:** D353-D361.

Kanehisa M, Furumichi M, Sato Y, Ishiguro-Watanabe M, Tanabe M (2021). KEGG: integrating viruses and cellular organisms. *Nucleic Acids Res* **49:** D545-D551.

Karkalas J (1985). An improved enzymic method for the determination of native and modified starch. *J Sci Food Agric* **36:** 1019-1027.

Keenan SW, Elsey RM (2015). The good, the bad, and the unknown: Microbial symbioses of the american alligator. *Integr Comp Biol* **55:** 972-985.

Klieve AV, Ouwerkerk D, Turner A, Roberton R (2002). The production and storage of a fermentor-grown bacterial culture containing *Synergistes jonesii*, for protecting cattle

against mimosine and 3-hydroxy-4(1H)-pyridone toxicity from feeding on *Leucaena leucocephala*. *Aust J Agr Res* **53:** 1-5.

KNAPPE J, BLASCHKOWSKI HP, GRÖBNER P, SCHMTTT T (1974). Pyruvate formate lyase of *Escherichia coli*: the acetyl‐enzyme intermediate. *European journal of biochemistry* **50:** 253-263.

Koga S, Yoshioka I, Sakuraba H, Takahashi M, Sakasegawa S, Shimizu S *et al* (2000). Biochemical characterization, cloning, and sequencing of ADP-dependent (AMP-forming) glucokinase from two hyperthermophilic archaea, *Pyrococcus furiosus* and *Thermococcus litoralis*. *J Biochem* **128:** 1079-1085.

Kohler T, Dietrich C, Scheffrahn RH, Brune A (2012). High-resolution analysis of gut environment and bacterial microbiota reveals functional compartmentation of the gut in wood-feeding higher termites (*Nasutitermes* spp.). *Appl Environ Microbiol* **78:** 4691-4701.

Kreuzberg K, Klock G, Grobheiser D (1987). Subcellular-distribution of pyruvate-degrading enzymes in *Chlamydomonas reinhardtii* studied by an improved protoplast fractionation procedure. *Physiol Plantarum* **69:** 481-488.

Kuhns M, Trifunovic D, Huber H, Muller V (2020). The Rnf complex is a Na^+ coupled respiratory enzyme in a fermenting bacterium, *Thermotoga maritima*. *Commun Biol* **3:** 431.

Kunkee RE (1991). Some roles of malic-acid in the malolactic fermentation in wine-making. *Fems Microbiology Letters* **88:** 55-72.

Kwong WK, Zheng H, Moran NA (2017). Convergent evolution of a modified, acetate-driven TCA cycle in bacteria. *Nat Microbiol* **2:** 17067.

Lamprecht W, Trauschold I (1974). Determination with hexokinase and glucose-6-phosphate dehydrogenase. In: Bergmeyer HU (ed). *Methods of enzymatic analysis*, 2 edn. Verlag Chemie: Weinheim, DE. pp 2101-2111.

Lan W, Yang C (2019). Ruminal methane production: Associated microorganisms and the potential of applying hydrogen-utilizing bacteria for mitigation. *Sci Total Environ* **654:** 1270-1283.

Langella O, Valot B, Balliau T, Blein-Nicolas M, Bonhomme L, Zivy M (2017). X!TandemPipeline: A tool to manage sequence redundancy for protein inference and phosphosite identification. *J Proteome Res* **16:** 494-503.

Lee SY, Park JH, Jang SH, Nielsen LK, Kim J, Jung KS (2008). Fermentative butanol production by Clostridia. *Biotechnology and bioengineering* **101:** 209-228.

Lindmark DG (1976). Acetate production by *Tritrichomonas foetus*. In: Van den Bossche H (ed). *Biochemistry of parasites and host-parasite relationships*. Elsevier: Amsterdam, Netherlands pp 15–21.

Lipmann F (1939). An analysis of the pyruvic acid oxidation system. *Cold Spring Harbor Symposia on Quantitative Biology*. Cold Spring Harbor Laboratory Press. pp 248-259.

Lipmann F, Tuttle LC (1945). A specific micromethod for the determination of acyl phosphates. *J Biol Chem* **159:** 21-28.

Litsanov B, Brocker M, Bott M (2012). Toward homosuccinate fermentation: metabolic engineering of *Corynebacterium glutamicum* for anaerobic production of succinate from glucose and formate. *Appl Environ Microbiol* **78:** 3325-3337.

Lo J, Olson DG, Murphy SJ, Tian L, Hon S, Lanahan A *et al* (2017). Engineering electron metabolism to increase ethanol production in *Clostridium thermocellum*. *Metab Eng* **39:** 71-79.

Loh ZH, Ouwerkerk D, Klieve AV, Hungerford NL, Fletcher MT (2020). Toxin degradation by rumen microorganisms: A review. *Toxins* **12:** 664.

Lu S, Wang J, Chitsaz F, Derbyshire MK, Geer RC, Gonzales NR *et al* (2020). CDD/SPARCLE: the conserved domain database in 2020. *Nucleic Acids Res* **48:** D265-D268.

Luna GM, Quero GM, Kokou F, Kormas K (2022). Time to integrate biotechnological approaches into fish gut microbiome research. *Curr Opin Biotechnol* **73:** 121-127.

Mackenzie DD (1967). Production and utilization of lactic acid by the ruminant. A review. *J Dairy Sci* **50:** 1772-1786.

Magnusdottir S, Heinken A, Kutt L, Ravcheev DA, Bauer E, Noronha A *et al* (2017). Generation of genome-scale metabolic reconstructions for 773 members of the human gut microbiota. *Nat Biotechnol* **35:** 81-89.

Mahmood L (2014). The metabolic processes of folic acid and Vitamin B_{12} deficiency. *Journal of Health Research and Reviews* **1:** 5.

Mai X, Adams MW (1996). Purification and characterization of two reversible and ADP-dependent acetyl coenzyme A synthetases from the hyperthermophilic archaeon *Pyrococcus furiosus*. *J Bacteriol* **178:** 5897-5903.

Marinez DI, Ricks CA, Cook RM (1976). Utilization of volatile fatty-acids in ruminants. 8. Acetate activation in mammary tissue. *J Agr Food Chem* **24:** 927-935.

Mayfield ED, Bensadoun A, Johnson BC (1966). Acetate metabolism in ruminant tissues. *J Nutr* **89:** 189-196.

McAllister TA, Newbold CJ (2008). Redirecting rumen fermentation to reduce methanogenesis. *Aust J Exp Agr* **48:** 7-13.

McCourt C (2019). Pathways for fermenting lactate to acetate in a rumen bacterium. M.S. thesis, University of Florida.

McCubbin T, Gonzalez-Garcia RA, Palfreyman RW, Stowers C, Nielsen LK, Marcellin E (2020). A pan-genome guided metabolic network reconstruction of five *Propionibacterium* species reveals extensive metabolic diversity. *Genes (Basel)* **11**.

Mead GC (1989). Microbes of the avian cecum: types present and substrates utilized. *J Exp Zool Suppl* **3:** 48-54.

Melville SB, Michel TA, Macy JM (1988). Pathway and sites for energy conservation in the metabolism of glucose by *Selenomonas ruminantium*. *J Bacteriol* **170:** 5298-5304.

Mertens E (1991). Pyrophosphate-dependent phosphofructokinase, an anaerobic glycolytic enzyme? *Febs Lett* **285:** 1-5.

Michal G, Bergmeyer HU (1983). Coenzyme A, end-point method with phosphate acetyltransferase. In: Bergmeyer HU, Bergmeyer J, Graßl M (eds). *Methods of enzymatic analysis*. Verlag Chemie: Weinheim, DE. pp 165-169.

Michel TA, Macy JM (1990). Purification of an enzyme responsible for acetate formation from acetyl coenzyme-A in *Selenomonas ruminantium*. *Fems Microbiology Letters* **68:** 189-194.

Mirdita M, Schütze K, Moriwaki Y, Heo L, Ovchinnikov S, Steinegger M (2021). ColabFold-Making protein folding accessible to all. *bioRxiv***:** doi: https://doi.org/10.1101/2021.1108.1115.456425.

Mistry J, Chuguransky S, Williams L, Qureshi M, Salazar GA, Sonnhammer ELL *et al* (2021). Pfam: The protein families database in 2021. *Nucleic Acids Res* **49:** D412-D419.

Muller M, Mentel M, van Hellemond JJ, Henze K, Woehle C, Gould SB *et al* (2012). Biochemistry and evolution of anaerobic energy metabolism in eukaryotes. *Microbiol Mol Biol Rev* **76:** 444-495.

Mullins EA, Francois JA, Kappock TJ (2008). A specialized citric acid cycle requiring succinyl-coenzyme A (CoA):acetate CoA-transferase (AarC) confers acetic acid resistance on the acidophile *Acetobacter aceti*. *J Bacteriol* **190:** 4933-4940.

Musfeldt M, Selig M, Schonheit P (1999). Acetyl coenzyme A synthetase (ADP forming) from the hyperthermophilic Archaeon *pyrococcus furiosus*: identification, cloning, separate expression of the encoding genes, *acdAI* and *acdBI*, in *Escherichia coli*, and in vitro reconstitution of the active heterotetrameric enzyme from its recombinant subunits. *J Bacteriol* **181:** 5885-5888.

Nealson KH (1997). Sediment bacteria: who's there, what are they doing, and what's new? *Annu Rev Earth Planet Sci* **25:** 403-434.

Nelson DL, Lehninger AL, Cox MM (2008). *Lehninger principles of biochemistry*. Macmillan.

Newbold CJ, de la Fuente G, Belanche A, Ramos-Morales E, McEwan NR (2015). The role of ciliate protozoa in the rumen. *Front Microbiol* **6:** 1313.

Olson DG, Horl M, Fuhrer T, Cui J, Zhou J, Maloney MI *et al* (2017). Glycolysis without pyruvate kinase in *Clostridium thermocellum*. *Metab Eng* **39:** 169-180.

Owens F, Goetsch A, Church D (1988). The ruminant animal: digestive physiology and nutrition. *Church D C-Waveland Press Inc Illinois***:** 145-171.

Owens FN, Basalan, M. (2016). Ruminal fermentation. In: Millen D, De Beni Arrigoni, M., Lauritano Pacheco, R. (ed). *Rumenology*. Springer International Publishing: Cham, Switzerland.

Parizzi LP, Grassi MCB, Llerena LA, Carazzolle MF, Queiroz VL, Lunardi I *et al* (2012). The genome sequence of *Propionibacterium acidipropionici* provides insights into its biotechnological and industrial potential. *Bmc Genomics* **13:** 1-20.

Peters JW, Lanzilotta WN, Lemon BJ, Seefeldt LC (1998). X-ray crystal structure of the Fe-only hydrogenase (CpI) from *Clostridium pasteurianum* to 1.8 angstrom resolution. *Science* **282:** 1853-1858.

Potter SC, Luciani A, Eddy SR, Park Y, Lopez R, Finn RD (2018). HMMER web server: 2018 update. *Nucleic Acids Res* **46:** W200-W204.

Qaisrani SN, Van Krimpen MM, Kwakkel RP, Verstegen MWA, Hendriks WH (2015). Dietary factors affecting hindgut protein fermentation in broilers: a review. *World Poultry Sci J* **71:** 139-160.

Rado TA, Hoch JA (1973). Phosphotransacetylase from *Bacillus subtilis*: purification and physiological studies. *Biochim Biophys Acta* **321:** 114-125.

Rawls JF, Samuel BS, Gordon JI (2004). Gnotobiotic zebrafish reveal evolutionarily conserved responses to the gut microbiota. *Proc Natl Acad Sci USA* **101:** 4596-4601.

Reeves RE, Warren LG, Susskind B, Lo HS (1977). An energy-conserving pyruvate-to-acetate pathway in *Entamoeba histolytica*. Pyruvate synthase and a new acetate thiokinase. *J Biol Chem* **252:** 726-731.

Rehman H, Rosenkranz C, Böhm J, Zentek J (2007). Dietary inulin affects the morphology but not the sodium-dependent glucose and glutamine transport in the jejunum of broilers. *Poultry Science* **86:** 118-122.

Reichardt N, Duncan SH, Young P, Belenguer A, McWilliam Leitch C, Scott KP *et al* (2014). Phylogenetic distribution of three pathways for propionate production within the human gut microbiota. *Isme J* **8:** 1323-1335.

Reimer LC, Vetcininova A, Carbasse JS, Sohngen C, Gleim D, Ebeling C *et al* (2019). BacDive in 2019: bacterial phenotypic data for high-throughput biodiversity analysis. *Nucleic Acids Res* **47:** D631-D636.

Revell L (2012). phytools: an R package for phylogenetic comparative biology (and other things). *Methods Ecol Evol* **3:** 217-223.

Riviere L, van Weelden SW, Glass P, Vegh P, Coustou V, Biran M *et al* (2004). Acetyl:succinate CoA-transferase in procyclic *Trypanosoma brucei*. Gene identification and role in carbohydrate metabolism. *J Biol Chem* **279:** 45337-45346.

Rizzo G, Lagana AS (2020). A review of vitamin B_{12}. *Molec Nutrition***:** 105-129.

Romero J, Navarrete P (2006). 16S rDNA-based analysis of dominant bacterial populations associated with early life stages of coho salmon (*Oncorhynchus kisutch*). *Microb Ecol* **51:** 422-430.

Ronimus RS, Morgan HW (2003). Distribution and phylogenies of enzymes of the Embden-Meyerhof-Parnas pathway from archaea and hyperthermophilic bacteria support a gluconeogenic origin of metabolism. *Archaea* **1:** 199-221.

Rooks MG, Garrett WS (2016). Gut microbiota, metabolites and host immunity. *Nat Rev Immunol* **16:** 341-352.

Russell J (2002). Rumen microbiology and its role in ruminant nutrition. *Cornell University Ithaca, NY*.

Saeki K, Tokuda K, Fujiwara T, Matsubara H (1993). Nucleotide sequence and genetic analysis of the region essential for functional expression of the gene for ferredoxin I, fdxN, in *Rhodobacter capsulatus*: sharing of one upstream activator sequence in opposite directions by two operons related to nitrogen fixation. *Plant Cell Physiol* **34:** 185-199.

Sanchez LB, Galperin MY, Muller M (2000). Acetyl-CoA synthetase from the amitochondriate eukaryote *Giardia lamblia* belongs to the newly recognized superfamily of acyl-CoA synthetases (nucleoside diphosphate-forming). *J Biol Chem* **275:** 5794-5803.

Sánchez LB, Galperin MY, Müller Ms (2000). Acetyl-CoA synthetase from the amitochondriate eukaryote *Giardia lamblia* Belongs to the newly recognized superfamily of acyl-CoA synthetases (nucleoside diphosphate-forming). *Journal of Biological Chemistry* **275:** 5794-5803.

Sasikaran J, Ziemski M, Zadora PK, Fleig A, Berg IA (2014). Bacterial itaconate degradation promotes pathogenicity. *Nat Chem Biol* **10:** 371-377.

Schafer T, Schonheit P (1991). Pyruvate metabolism of the hyperthermophilic archaebacterium *Pyrococcus furiosus* - Acetate formation from acetyl-CoA and ATP synthesis are catalyzed by an acetyl-CoA synthetase (ADP forming). *Archives of Microbiology* **155:** 366-377.

Schafer T, Selig M, Schonheit P (1993). Acetyl-CoA synthetase (ADP Forming) in archaea, a novel enzyme involved in acetate formation and ATP synthesis. *Archives of Microbiology* **159:** 72-83.

Scheifinger CC, Wolin MJ (1973). Propionate formation from cellulose and soluble sugars by combined cultures of *Bacteroides succinogenes* and *Selenomonas ruminantium*. *Appl Microbiol* **26:** 789-795.

Scheifinger CC, Linehan B, Wolin MJ (1975). H_2 production by *Selenomonas ruminantium* in the absence and presence of methanogenic bacteria. *Appl Microbiol* **29:** 480-483.

Schlegel K, Welte C, Deppenmeier U, Muller V (2012). Electron transport during aceticlastic methanogenesis by *Methanosarcina acetivorans* involves a sodium-translocating Rnf complex. *Febs J* **279:** 4444-4452.

Schmehl M, Jahn A, Meyer zu Vilsendorf A, Hennecke S, Masepohl B, Schuppler M *et al* (1993). Identification of a new class of nitrogen fixation genes in *Rhodobacter capsulatus*: a putative membrane complex involved in electron transport to nitrogenase. *Mol Gen Genet* **241:** 602-615.

Schmidt M, Schonheit P (2013). Acetate formation in the photoheterotrophic bacterium *Chloroflexus aurantiacus* involves an archaeal type ADP-forming acetyl-CoA synthetase isoenzyme I. *FEMS Microbiol Lett* **349:** 171-179.

Schoelmerich MC, Katsyv A, Donig J, Hackmann TJ, Muller V (2020). Energy conservation involving 2 respiratory circuits. *Proc Natl Acad Sci USA* **117:** 1167-1173.

Scholz CF, Kilian M (2016). The natural history of cutaneous propionibacteria, and reclassification of selected species within the genus *Propionibacterium* to the proposed novel genera *Acidipropionibacterium* gen. nov., *Cutibacterium* gen. nov. and *Pseudopropionibacterium* gen. nov. *International journal of systematic and evolutionary microbiology* **66:** 4422-4432.

Schonheit P, Schafer T (1995). Metabolism of hyperthermophiles. *World J Microbiol Biotechnol* **11:** 26-57.

Schönheit P, Wäscher C, Thauer RK (1978). A rapid procedure for the purification of ferredoxin from Clostridia using polyethyleneimine. *Febs Lett* **89:** 219-222.

Schuchmann K, Muller V (2012). A bacterial electron-bifurcating hydrogenase. *J Biol Chem* **287:** 31165-31171.

Schulman M, Wood HG (1975). Succinyl-CoA: propionate CoA-transferase from *Propionibacterium shermanii*. EC 2.8.3.6 succinyl-CoA:propionate CoA-transferase. *Methods Enzymol* **35:** 235-242.

Schut GJ, Adams MW (2009). The iron-hydrogenase of *Thermotoga maritima* utilizes ferredoxin and NADH synergistically: a new perspective on anaerobic hydrogen production. *J Bacteriol* **191:** 4451-4457.

Scott KP, Martin JC, Campbell G, Mayer CD, Flint HJ (2006). Whole-genome transcription profiling reveals genes up-regulated by growth on fucose in the human gut bacterium "*Roseburia inulinivorans*". *J Bacteriol* **188:** 4340-4349.

Scott RI, Yarlett N, Hillman K, Williams TN, Williams AG, Lloyd D (1983). The presence of oxygen in rumen liquor and its effects on methanogenesis. *J Appl Bacteriol* **55:** 143-149.

Shuler M, Kargi F (2002). *Bioprocess engineering: Basic concepts*, 2nd edn. Prentice Hall: Upper Saddle River, NJ.

Siebers B, Klenk HP, Hensel R (1998). PP_i-dependent phosphofructokinase from *Thermoproteus tenax*, an archaeal descendant of an ancient line in phosphofructokinase evolution. *J Bacteriol* **180:** 2137-2143.

Sievers F, Wilm A, Dineen D, Gibson TJ, Karplus K, Li W *et al* (2011). Fast, scalable generation of high-quality protein multiple sequence alignments using Clustal Omega. *Mol Syst Biol* **7:** 539.

Sievers S (2018). Membrane proteomics in Gram-positive bacteria: Two complementary approaches to target the hydrophobic species of proteins. *Methods Mol Biol* **1841:** 21-33.

Solomon KV, Haitjema CH, Henske JK, Gilmore SP, Borges-Rivera D, Lipzen A *et al* (2016). Early-branching gut fungi possess a large, comprehensive array of biomass-degrading enzymes. *Science* **351:** 1192-1195.

Solomon R, Wein T, Levy B, Eshed S, Dror R, Reiss V *et al* (2022). Protozoa populations are ecosystem engineers that shape prokaryotic community structure and function of the rumen microbial ecosystem. *Isme J* **16:** 1187-1197.

Sondergaard D, Pedersen CN, Greening C (2016). HydDB: A web tool for hydrogenase classification and analysis. *Sci Rep* **6:** 34212.

Song SJ, Sanders JG, Delsuc F, Metcalf J, Amato K, Taylor MW *et al* (2020). Comparative analyses of vertebrate gut microbiomes reveal convergence between birds and bats. *mBio* **11**.

Stamatakis A (2014). RAxML version 8: a tool for phylogenetic analysis and post-analysis of large phylogenies. *Bioinformatics* **30:** 1312-1313.

Steinbuchel A, Muller M (1986). Anaerobic pyruvate metabolism of *Tritrichomonas fetus* and *Trichomonas vaginalis* hydrogenosomes. *Mol Biochem Parasit* **20:** 57-65.

Stettner AI, Segre D (2013). The cost of efficiency in energy metabolism. *Proc Natl Acad Sci U S A* **110:** 9629-9630.

Stewart CS, Flint HJ (1989). *Bacteroides* (*Fibrobacter*) *succinogenes*, a cellulolytic anaerobic bacterium from the gastrointestinal tract. *Appl Microbiol Biot* **30:** 433-439.

Storm E, Orskov ER, Smart R (1983). The nutritive value of rumen micro-organisms in ruminants. 2. The apparent digestibility and net utilization of microbial N for growing lambs. *Br J Nutr* **50:** 471-478.

Stouthamer AH (1973). A theoretical study on the amount of ATP required for synthesis of microbial cell material. *Antonie Van Leeuwenhoek* **39:** 545-565.

Strittmatter AW, Liesegang H, Rabus R, Decker I, Amann J, Andres S *et al* (2009). Genome sequence of *Desulfobacterium autotrophicum* HRM2, a marine sulfate reducer oxidizing organic carbon completely to carbon dioxide. *Environ Microbiol* **11:** 1038-1055.

Strobel HJ (1992). Vitamin B_{12}-dependent propionate production by the ruminal bacterium *Prevotella ruminicola* 23. *Appl Environ Microbiol* **58:** 2331-2333.

Suwannakham S, Huang Y, Yang ST (2006). Construction and characterization of ack knock-out mutants of *Propionibacterium acidipropionici* for enhanced propionic acid fermentation. *Biotechnol Bioeng* **94:** 383-395.

Svihus B, Choct M, Classen HL (2013). Function and nutritional roles of the avian caeca: a review. *World Poultry Sci J* **69:** 249-263.

Taillefer M, Sparling R (2016). Glycolysis as the central core of fermentation. *Anaerobes in Biotechnology* **156:** 55-77.

Takahashi-Iniguez T, Garcia-Hernandez E, Arreguin-Espinosa R, Flores ME (2012). Role of vitamin B_{12} on methylmalonyl-CoA mutase activity. *J Zhejiang Univ Sci B* **13:** 423-437.

Takasaki K, Shoun H, Yamaguchi M, Takeo K, Nakamura A, Hoshino T *et al* (2004). Fungal ammonia fermentation, a novel metabolic mechanism that couples the dissimilatory and

assimilatory pathways of both nitrate and ethanol. Role of acetyl CoA synthetase in anaerobic ATP synthesis. *J Biol Chem* **279:** 12414-12420.

Tang KH, Barry K, Chertkov O, Dalin E, Han CS, Hauser LJ *et al* (2011). Complete genome sequence of the filamentous anoxygenic phototrophic bacterium *Chloroflexus aurantiacus*. *Bmc Genomics* **12:** 334.

Tao J, McCourt C, Sultana H, Nelson C, Driver J, Hackmann TJ (2019). Use of a fluorescent analog of glucose (2-NBDG) To identify uncultured rumen bacteria that take up glucose. *Appl Environ Microbiol* **85**.

Tao JY, Diaz RK, Teixeira CRV, Hackmann TJ (2016). Transport of a fluorescent analogue of glucose (2-NBDG) versus radiolabeled sugars by rumen bacteria and *Escherichia coli*. *Biochemistry* **55:** 2578-2589.

Thauer RK, Jungermann K, Decker K (1977). Energy conservation in chemotrophic anaerobic bacteria. *Bacteriol Rev* **41:** 100-180.

Thauer RK (1988). Citric-acid cycle, 50 years on. Modifications and an alternative pathway in anaerobic bacteria. *Eur J Biochem* **176:** 497-508.

Tielens AG, van Grinsven KW, Henze K, van Hellemond JJ, Martin W (2010). Acetate formation in the energy metabolism of parasitic helminths and protists. *Int J Parasitol* **40:** 387-397.

Tschech A, Pfennig N (1984). Growth-yield increase linked to caffeate reduction in *Acetobacterium woodii*. *Archives of Microbiology* **137:** 163-167.

Ungerfeld EM, Hackmann TJ (2020). Factors influencing the efficiency of rumen energy metabolism. *Improving Rumen Function*. Burleigh Dodds Science Publishing. pp 421-466.

Uy D, Delaunay S, Engasser JM, Goergen JL (1999). A method for the determination of pyruvate carboxylase activity during the glutamic acid fermentation with *Corynebacterium glutamicum*. *J Microbiol Meth* **39:** 91-96.

van der Oost J, Schut G, Kengen SW, Hagen WR, Thomm M, de Vos WM (1998). The ferredoxin-dependent conversion of glyceraldehyde-3-phosphate in the hyperthermophilic archaeon *Pyrococcus furiosus* represents a novel site of glycolytic regulation. *J Biol Chem* **273:** 28149-28154.

van Grinsven KW, van Hellemond JJ, Tielens AG (2009). Acetate:succinate CoA-transferase in the anaerobic mitochondria of *Fasciola hepatica*. *Mol Biochem Parasitol* **164:** 74-79.

Van Gylswyk NO (1980). *Fusobacterium polysaccharolyticum* sp. nov., a Gram-negative rod from the rumen that produces butyrate and ferments cellulose and starch. *Microbiology* **116:** 157-163.

Van Gylswyk NO (1995). *Succiniclasticum ruminis* gen. nov., sp. nov., a ruminal bacterium converting succinate to propionate as the sole energy-yielding mechanism. *Int J Syst Bacteriol* **45:** 297-300.

Villas-Boas SG, Noel S, Lane GA, Attwood G, Cookson A (2006). Extracellular metabolomics: a metabolic footprinting approach to assess fiber degradation in complex media. *Anal Biochem* **349:** 297-305.

Wallnofer P, Baldwin RL (1967). Pathway of propionate formation in *Bacteroides ruminicola*. *J Bacteriol* **93:** 504-505.

Wang AR, Ran C, Ringo E, Zhou ZG (2018). Progress in fish gastrointestinal microbiota research. *Rev Aquacult* **10:** 626-640.

Wang FP, Zhang Y, Chen Y, He Y, Qi J, Hinrichs KU *et al* (2014). Methanotrophic archaea possessing diverging methane-oxidizing and electron-transporting pathways. *Isme J* **8:** 1069-1078.

Wang J, Lin M, Xu M, Yang S-T (2016). Anaerobic fermentation for production of carboxylic acids as bulk chemicals from renewable biomass. *Anaerobes in biotechnology*. Springer. pp 323-361.

Wang S, Huang H, Moll J, Thauer RK (2010). $NADP^+$ reduction with reduced ferredoxin and $NADP^+$ reduction with NADH are coupled via an electron-bifurcating enzyme complex in *Clostridium kluyveri*. *J Bacteriol* **192:** 5115-5123.

Wang S, Huang H, Kahnt J, Thauer RK (2013). *Clostridium acidurici* electron-bifurcating formate dehydrogenase. *Appl Environ Microbiol* **79:** 6176-6179.

Warnecke F, Luginbuhl P, Ivanova N, Ghassemian M, Richardson TH, Stege JT *et al* (2007). Metagenomic and functional analysis of hindgut microbiota of a wood-feeding higher termite. *Nature* **450:** 560-565.

Weghoff MC, Bertsch J, Muller V (2015). A novel mode of lactate metabolism in strictly anaerobic bacteria. *Environ Microbiol* **17:** 670-677.

Weimer PJ (1998). Manipulating ruminal fermentation: a microbial ecological perspective. *J Anim Sci* **76:** 3114-3122.

Wenner BA, Wagner BK, Firkins JL (2018). Using video microscopy to improve quantitative estimates of protozoal motility and cell volume. *J Dairy Sci* **101:** 1060-1073.

Westphal L, Wiechmann A, Baker J, Minton NP, Muller V (2018). The Rnf complex is an energy-coupled transhydrogenase essential to reversibly link cellular NADH and ferredoxin pools in the acetogen *Acetobacterium woodii*. *J Bacteriol* **200**.

White D, Drummond J, Fuqua C (2012). *The physiology and biochemistry of prokaryotes*. Oxford University Press: New York.

Whitman WB (ed) (2020) *Bergey's manual of systematics of archaea and bacteria*. Wiley: Oxford, United Kingdom.

Whitman WB (2022). *Bergey's manual of systematics of archaea and bacteria*. Wiley: Oxford, United Kingdom.

Wiechmann A, Trifunovic D, Klein S, Muller V (2020). Homologous production, one-step purification, and proof of Na^+ transport by the Rnf complex from *Acetobacterium woodii*, a model for acetogenic conversion of C1 substrates to biofuels. *Biotechnol Biofuels* **13:** 208.

Williams VJ, Hutchings TR, Archer KA (1968). Absorption of volatile fatty acids from the reticulo-rumen and abomasum of sheep. *Aust J Biol Sci* **21:** 89-96.

Wrighton KC, Thomas BC, Sharon I, Miller CS, Castelle CJ, VerBerkmoes NC *et al* (2012). Fermentation, hydrogen, and sulfur metabolism in multiple uncultivated bacterial phyla. *Science* **337:** 1661-1665.

Xu RZ, Fang S, Zhang L, Huang W, Shao Q, Fang F *et al* (2021). Distribution patterns of functional microbial community in anaerobic digesters under different operational circumstances: A review. *Bioresour Technol* **341:** 125823.

Yasuda K, Jojima T, Suda M, Okino S, Inui M, Yukawa H (2007). Analyses of the acetate-producing pathways in *Corynebacterium glutamicum* under oxygen-deprived conditions. *Appl Microbiol Biotechnol* **77:** 853-860.

Yu G, Smith DK, Zhu H, Guan Y, Lam TTY (2017). ggtree: an R package for visualization and annotation of phylogenetic trees with their covariates and other associated data. *J Method Ecol Evol* **8:** 28-36.

Zhang B, Lingga C, Bowman C, Hackmann TJ (2021). A new pathway for forming acetate and synthesizing ATP during fermentation in bacteria. *Appl Environ Microbiol* **87:** e0295920.

Zheng Y, Kahnt J, Kwon IH, Mackie RI, Thauer RK (2014). Hydrogen formation and its regulation in *Ruminococcus albus*: involvement of an electron-bifurcating [FeFe]-hydrogenase, of a non-electron-bifurcating [FeFe]-hydrogenase, and of a putative hydrogen-sensing [FeFe]-hydrogenase. *J Bacteriol* **196:** 3840-3852.

Zhou J, Olson DG, Argyros DA, Deng Y, van Gulik WM, van Dijken JP *et al* (2013). Atypical glycolysis in *Clostridium thermocellum*. *Appl Environ Microbiol* **79:** 3000-3008.

Zhou M, Yan B, Wong JWC, Zhang Y (2018). Enhanced volatile fatty acids production from anaerobic fermentation of food waste: A mini-review focusing on acidogenic metabolic pathways. *Bioresour Technol* **248:** 68-78.

Zhu Y, Li J, Tan M, Liu L, Jiang L, Sun J *et al* (2010). Optimization and scale-up of propionic acid production by propionic acid-tolerant *Propionibacterium acidipropionici* with glycerol as the carbon source. *Bioresource Technol* **101:** 8902-8906.